2000

Manufacture and rehabilitation of guard-rail posts using composites for superior performance

Swetha Anegunta
West Virginia University

MANUFACTURE AND REHABILITATION OF GUARD-RAIL POSTS USING COMPOSITES FOR SUPERIOR PERFORMANCE

Swetha Anegunta

Thesis submitted to the
College of Engineering and Mineral Resources
at West Virginia University
in partial fulfillment of the requirements
for the degree of

Master of Science
in
Chemical Engineering

Rakesh K. Gupta, Ph.D., Chair
Ganga Rao Hota, Ph.D.
John W. Zondlo, Ph.D.

Department of Chemical Engineering

Morgantown, West Virginia
2000

Keywords: composite, reinforcement, FRP, aging, durability, guard-rail

ABSTRACT

MANUFACTURE AND REHABILITATION OF GUARD-RAIL POSTS USING COMPOSITES FOR SUPERIOR PERFORMANCE

Swetha Anegunta

The objective of this research was to study the effectiveness of an external composite reinforcement in increasing the strength and durability of a conventional CCA treated wood post. Glass fibers (with excellent mechanical properties and low cost) in a polymer matrix were used for wrapping CCA treated wood posts. Six chemically different resins were screened, and a combination of HMR (Hydroxy Methylated Resorcinol) as primer and epoxy as adhesive was found to provide the best possible adhesion of the wrap to CCA treated wood. Wooden posts of 0.5″ OD and wrapped posts of 0.6″ OD, representing a scaled down version of the proposed posts were subjected to a 6-cycle aging procedure that involved application of vacuum and pressure under water. The wrapped posts were also subjected to freeze-thaw cycling in four different liquid media: (1) water (2) 3% salt water (3) acidic solution of pH 3 (4) alkaline solution of pH 13. The retention of flexural strength and stiffness of the wrapped posts after chemical aging was measured. Samples of dimensions 50 mm X 9 mm X 2 mm wrapped with 1mm thick wrap were also subjected to aging. The retention in strength and stiffness was measured and the service life was estimated.

Results of flexure tests show that the strength of the wrapped post reduces due to aging. Results of DMTA (Dynamic Mechanical Thermal Analysis) show that freeze-thaw cycling and 6-cycle aging increase the Tg (glass transition temperature) and widen the glass transition region. After a service life of about 20 years, the stiffness of a wrapped post is predicted to be about 1.8 times that of an unwrapped wood post of the same age. Heating and freezing in liquid media causes more damage than heating and freezing in the absence of a liquid medium. Among the liquid media, it was found that the alkaline medium damages the epoxy matrix, the epoxy/glass interface and also the wood/HMR/epoxy bond. Acid medium primarily damages the epoxy/glass interface. Water diffuses easily through the epoxy matrix and primarily damages the epoxy/glass interface. Salt water damages the wood/HMR/epoxy bond. The performance in terms of flexural strength, modulus and rigidity was reduced the most by acidic medium, and the least by saltwater medium. There was no delamination at the wood/FRP interface under any of the aging conditions. It was concluded that under unaged conditions, the flexural rigidity of wood is improved by 162% due to composite wrapping. The technique of composite wrapping also shows a promise of improving the properties of guard-rail posts under actual field conditions.

ACKNOWLEDGEMENTS

I'm greatly indebted to my research advisors, Dr. Rakesh Gupta and Dr. GangaRao Hota for their invaluable guidance throughout this research. The advice and insight provided by Dr. Gupta in all matters pertaining to this research have been extremely invaluable. I was fortunate to have him as a teacher in the classroom. Dr. Hota was extremely kind in explaining the important aspects of the research. His guidance and encouragement have made a difference. I would like to express special thanks to both of them for their generous time and kind co-operation.

I'm grateful to Dr. John Zondlo for his valuable comments and suggestions that improved the quality of the report. His suggestions during the initial stages of the research were also valuable. His kindness is very much appreciated.

I'm thankful to Sharon Santos, Sharon Chadderton and Eleanor Nevera for processing my paper work and for their extremely kind and encouraging nature. I greatly appreciate the assistance of Dave Turner, Jim Hall and Dana Humberson in machining a lot of samples and also in operating heavy equipment. The creativity of Jim Hall in building experimental accessories was of great help to me.

I sincerely thank Dr. Hemanth Thippeswamy and Dr. P. V. Vijay for clearing my doubts and for their constant support and encouragement. The support and assistance of Barry Dickson are also appreciated.

My heartfelt thanks to Rajesh Kalluri, Sanjay Palakamshetty, Uday Chamarthy, Bryan King and Krit Laosiriphong for helping me conduct the accelerated aging. I'm also thankful to Shahab Ghasemzadeh and Vimala Shekar for helping me with sample

preparation and for clearing my doubts. All of their help was very much required to complete things in the required time.

Financial support for this research was provided by the West Virginia Department of Transportation. Their support is very much appreciated.

My sincere regards and appreciation to my husband, Aravind, for supporting me through tough times and for his understanding. The love and blessings of my family were essential for the successful completion of this work. I thank them for being my loving family.

TABLE OF CONTENTS

Chapter VII

DYNAMIC MECHANICAL THERMAL ANALYSIS OF WRAPPED COMPOSITES

Chapter VIII

CONCLUSIONS AND RECOMMENDATIONS

LIST OF TABLES

LIST OF FIGURES

Chapter I

INTRODUCTION

1.1 Introduction

Guardrail posts are particularly important for highway traffic safety and are constructed of steel or wood. Steel posts are more expensive than wood posts and less forgiving in terms of damping. However, wooden posts have a larger cross-sectional area and require larger and more expensive equipment for driving them into the ground. Approximately 50,000 wood guardrail posts are sold annually to the West Virginia Department of Transportation. In comparison, approximately 200,000 steel posts are used in the same time period because of ease of field installation. Also the wooden posts that are installed are subject to deterioration by environmental attack. The higher cost of steel posts, the greater difficulty in installing wood posts plus the potential for degradation, motivate the development of a more practical and economic alternative.

Fiber reinforced composite materials technology promises superior structural performance of wood posts that are wrapped with a composite fabric. Wrapping of wooden posts with glass fabric in a polymeric resin matrix can improve the mechanical properties of a conventional wood post. This technique can be used to manufacture new posts and can be extended to rehabilitate old posts as well. Enhanced service life lowers consumption of wood and reduces the use of expensive steel.

1.2 Proposed Work

Steel posts have good mechanical properties and are easy to drive into the soil. However they are expensive. Wood is highly forgiving with excellent damping capability and is easy to find in rural areas. Wood posts also have reasonable mechanical properties and low cost but are subject to environmental decay. Treatment of wood with a variety of materials is performed but treated wood can damage the soil and plant life. It can also result in end checking and splitting of wood.

The objective of the proposed work was to develop GFW (glass fabric wrapped)-wood posts using the technique of composite wrapping. In this method, a composite consisting of glass fibers embedded in a polymeric matrix is externally wrapped around a wood post. The polymeric matrix serves as an adhesive between the fibers and the wood. It protects wood from environmental attack and also forms a moisture-resistant barrier around the post that reduces decay. Expected superior mechanical properties of a wrapped post compared to an unwrapped wood post can make it possible to achieve better structural performance with a wood post, smaller in diameter than the currently used wood posts. Such a smaller diameter post wrapped with composite requires lesser driving force than a larger diameter post. The smaller wood post is also less expensive than a regular-sized wood post being used in highway applications.

The proposed GFW wood posts are being developed as a cost-effective alternative to steel posts. Wrapping of posts could also prevent direct exposure of soil to preservative treated wood. These wrapped posts are expected to render mechanical performance that is at least equal to steel posts and preservative treated posts. To achieve this objective, appropriate experiments have been suggested (in section 1.3) on samples made using CCA treated wood, E-glass fibers and a polymeric adhesive system. Details of the choice of materials and types of samples

prepared are listed in later chapters (Chapters II through VII).

1.3 Scope of the Research

To achieve the objective of developing a GFW-wood post, a research program that has both fundamental and applied aspects was proposed. The scope of this research was divided into the following tasks:

♦ **Adhesive screening**

Six different resins were tested for adhesion with CCA treated southern pine wood. Priming of wood surface before adhesion was also done. The primer/resin combination that adheres the best to wood was determined.

♦ **Laboratory manufacturing of test samples (coupons)**

Shear coupons of wood with adhesive, primer/adhesive were prepared. Shear coupons of wood with sandwiched glass fabric were also prepared. Wood samples of circular and rectangular cross-section were wrapped with glass fibers wetted in the chosen adhesive.

♦ **Testing and evaluation of the performance of shear coupons and wrapped specimens**

All shear coupons were tested for shear strength using an Instron machine. Wrapped rectangular specimens were tested for dynamic behavior using a Rheometrics Mechanical Spectrometer, model RMS 800. Wrapped dowels were tested for stiffness and flexural modulus using the Instron machine.

♦ **Monitoring of stiffness/strength degradation of wrapped posts as a function of time**

Shear coupons and wrapped specimens were exposed to moisture and chemical solutions. Variation in shear strength, flexural properties and dynamic behavior of samples was measured after exposure for different lengths of time.

♦ **Understanding the possible reaction mechanism behind the adhesive bonding between the wrap and wood, and the reasons for changes occurring with time**

Effect of factors such as moisture, length of exposure time, curing pressure, etc. on the quality of the adhesive bond was studied. The experimental results and theoretical predictions were compared and conclusions were drawn.

Each of these tasks, their experimental procedure and the explanation of results are presented in later chapters.

Chapter II

MATERIAL SELECTION

The mechanical properties and behavior of a fiber-reinforced composite are influenced by the choice of its components. Typically a fiber-reinforced composite material consists of fibers embedded in a continuous matrix. In hybrid materials, one combines FRPs with structural materials like steel, concrete and wood. In the current investigation, the principal materials of interest are fibers, resin and wood. Different types of these raw materials were examined, and the details of their properties are presented in this section.

2.1 Fibers

Fibers are the principal constituent in a fiber-reinforced composite material. They bear the major part of the load acting on a composite structure. The properties of a composite laminate such as compressive strength and modulus, tensile strength and modulus, flexural strength and modulus, fatigue strength, electrical and thermal conductivities and cost are influenced by the nature, amount and orientation of the fibers. The most commonly used fibers in composites are glass, carbon and aramid fibers.

2.1.1 Glass Fibers

Glass fibers are the most common of all reinforcing fibers for polymer matrix composites. They have high tensile strength, chemical resistance and insulating properties and are the least expensive class of reinforcing fibers. Their disadvantages are low tensile

modulus, relatively high specific gravity, low fatigue resistance, sensitivity to abrasion with handling and high hardness. The two commonly used types of glass fibers in FRP industry are E-glass (electric grade) and S-glass (high strength). E-glass has Silicon, Aluminum, Boron, Calcium, Magnesium and Sodium oxides present in it. S-glass has only Silicon, Aluminum and Magnesium oxides present in it. E-glass has the lowest cost of all commercially available reinforcing fibers and so is most widely used in the FRP industry. S-glass originally developed for aircraft components and missile casings, has the highest tensile strength among all the fibers in use.

The internal structure of glass fibers is a three dimensional network of silicon, oxygen and other atoms like boron and aluminum arranged in a random fashion. This gives glass fibers an amorphous and isotropic nature.

2.1.2 Carbon (graphite) Fibers

Carbon fibers have an exceptionally high tensile strength to weight ratio as well as tensile modulus to weight ratio, very low linear thermal expansion and high fatigue strength. They are commercially available with a variety of tensile moduli ranging from 30 Mpsi to 150 Mpsi. In general, the low modulus fibers have lower specific gravities, lower cost, and higher tensile and compressive strengths than the high modulus fibers. The disadvantages of carbon fibers are low impact resistance and high electrical conductivity and high cost. They are used mostly in the aerospace industry where weight savings is considered more important than cost.

Carbon fibers contain a blend of amorphous carbon and graphitic carbon. The arrangement of carbon atoms in the planes, the forces between the planes and the bonds

between the atoms in a plane, all result in highly anisotropic physical and mechanical properties of the fiber.

2.1.3 Kevlar 49 (Aramid) Fibers

Kevlar 49 fibers are highly crystalline aramid or aromatic polyamide fibers that have the lowest specific gravity and the highest tensile strength-to-weight ratio among the current reinforcing fibers. They have low linear thermal expansion, which is utilized in designing low thermal expansion composite printed circuit boards. The major disadvantages of aramid fiber-reinforced composites are their low compressive strengths and difficulty in cutting or machining. They are used in marine and aerospace applications where light weight, high tensile strength and resistance to impact are important.

The repeat unit in Kevlar fiber molecules contains an amide (— $\overset{H}{\underset{|}{N}}$ —) group and an aromatic ring. The repeat unit provides a higher chain stiffness, or consequently higher modulus and also better chemical and thermal stability over other commercial organic fibers, such as nylons.

Typical mechanical properties of various fibers are presented in Table 2.1.

Table 2.1: Properties of commercial reinforcing fibers [1]

Property	E-glass	S-glass	Aramid (Kevlar 49)	Graphite (PAN)
Specific gravity (----)	2.54	2.49	1.48	1.78
Diameter (μm)	10	10	11.9	7
Young's Modulus (GPa)	72.4	85.5	131.0	241.3
Ultimate Tensile Strength (MPa)	3447	4585	3620	3447
Axial co-efficient of thermal expansion ($\mu m/m/^0C$)	5.04	5.58	-2	-1.26

2.2 Adhesives

Though the adhesive matrix carries a minor part of the tensile-load acting on a composite structure, it has a major influence on inter-laminar shear and in-plane shear properties of the composite material. These properties are important design considerations for structures under bending and torsional loads. The matrix also influences the compressive strength of the composite material by preventing the fibers from buckling under compressive load. Further, physical and thermal characteristics of

the matrix like viscosity, melting point and cure temperature influence the processability and the presence of any defects in a composite. The use of a specific resin determines which properties are strongest and the range of conditions over which the composite structure can be used. In general, the best adhesive for a particular application depends on the materials to be bonded, the service assembly conditions and the economics of the bonding operation.

For high performance composites in structural applications, thermoset polymers such as epoxies, phenolics, polyesters and vinylesters are most widely used. In the formation of thermosetting polymers, the reactants undergo chemical cross-linking and produce a three dimensional solid network. The properties of the solid depend on the nature of the reactants and the cross-linking process. The following discussion presents a description of each of the more common resins.

2.2.1 Epoxies

Epoxy resins have epoxide groups (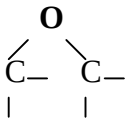) which are three membered rings containing one oxygen atom and two carbon atoms. The starting materials for the preparation of an epoxy resin are low molecular weight organic liquids. Diglycidyl ether of bisphenol A (DGEBA), shown in figure 2.1 (a) which contains an epoxide group at each end of the molecule is a common starting material for the manufacture of epoxy resins. The resins are cross-linked with catalysts or hardeners such as diethylene triamine (DETA), shown in figure 2.1(b). Starting materials may be mixed with other ingredients such as diluents (dibutyl phthalate, for example) to reduce viscosity, and flexibilizers to give impact strength of cured epoxy matrix.

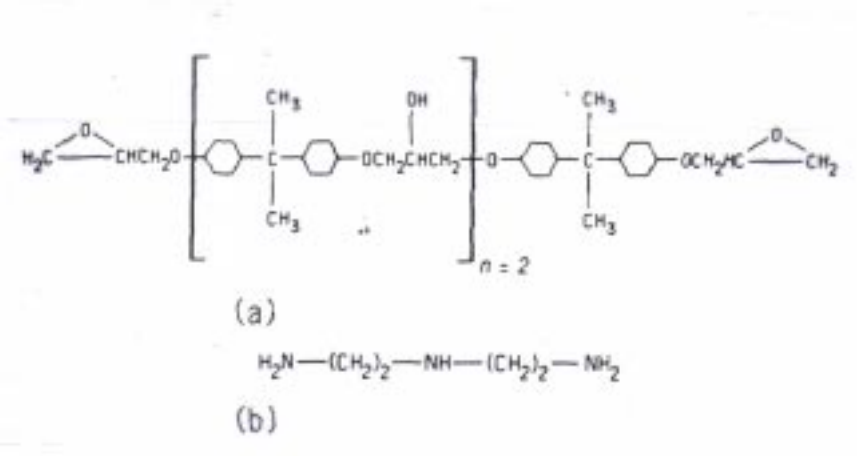

Figure 2.1 Raw materials for the preparation of epoxy resin [2]. (a) a molecule of DGEBA epoxy resin; (b) a molecule of DETA curing agent

During the cure of epoxy resin, the Hydrogen atoms of the curing agent (DETA) react with the epoxide groups of the DGEBA molecule and open the oxirane ring as shown in figure 2.2(a). With the progress of the curing reaction, the DGEBA molecules form cross-links with each other resulting in a three-dimensional structure. The resulting structure is a solid epoxy resin as shown in figure 2.2(c). The curing time and temperature of cure of the resin depend on the nature and amount of the curing agent used. The properties of a cured epoxy resin depend on the cross-link density, which depends on the chemical structure of the starting liquid resin, the functionality of the curing agent and the reaction conditions such as temperature and time.

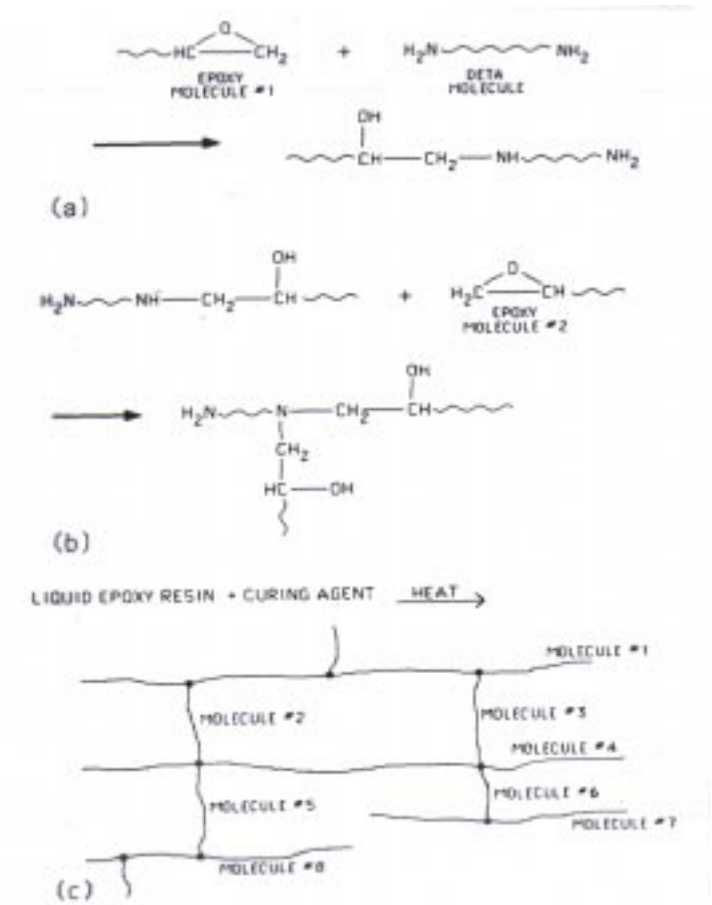

Figure 2.2 Schematic representation of a cross-linked epoxy resin [2] (a) reaction of epoxide group with DETA molecule; (b) formation of cross-links; (c) three-dimensional structure of solid epoxy resin [2]

An epoxy matrix has many advantages over other thermosetting resins:

1. it has a wide variety of properties such as tensile strength, tensile modulus, specific gravity, coefficient of thermal expansion etc. because of a large number of available starting materials, curing agents and modifiers.

2. it has low volumetric shrinkage and absence of volatile materials during cure.

3. it has excellent resistance to chemicals and solvents.

4. it has excellent adhesion to a wide variety of fillers, fibers and other substrates.

Principal disadvantages of epoxy resins are relatively high cost and long cure time. High coefficient of thermal expansion, and property changes due to moisture

absorption are other disadvantages that can affect composite performance. Epoxy resins are principally used in aerospace, aircraft and structural applications.

2.2.2 Polyesters

Unsaturated polyester resins that contain a number of C=C bonds are starting materials for the polyester matrix. Typically one reacts maleic anhydride with ethylene glycol or propylene glycol. The resulting liquid is dissolved in a reactive diluent such as styrene that reduces viscosity and acts as a cross-linking agent. An inhibitor such as hydroquinone is added in trace amounts to the liquid mix, to prevent premature polymerization during storage. Figure 2.3 shows the principal ingredients used in the preparation of a polyester resin.

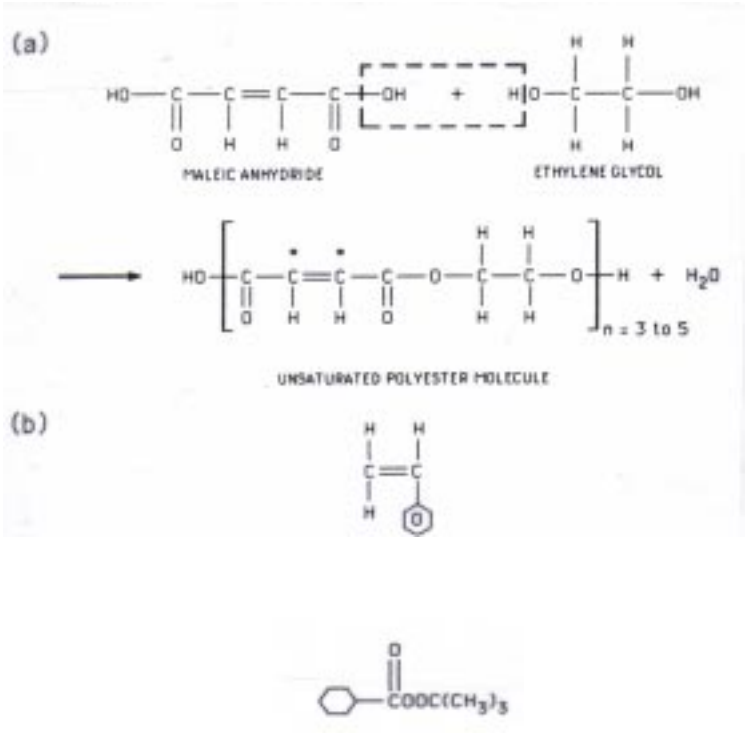

Figure 2.3: Raw materials for the preparation of a polyester resin [2]. (a) unsaturated polyester molecule; (b) styrene molecule; (c) t-butyl perbenzoate molecule (tBPB).
(The asterisk denotes reactive sites in the molecule)

The curing reaction is initiated by adding small quantities of a catalyst such as an organic peroxide. The catalyst decomposes into free radicals with the application of heat and the free radicals open the C = C bonds of styrene molecules. Styrene radicals in turn join the polyester molecules at their unsaturation points and form cross-links between them. The resulting material is a solid polyester resin. A schematic of a cross-linked polyester resin is shown in figure 2.4.

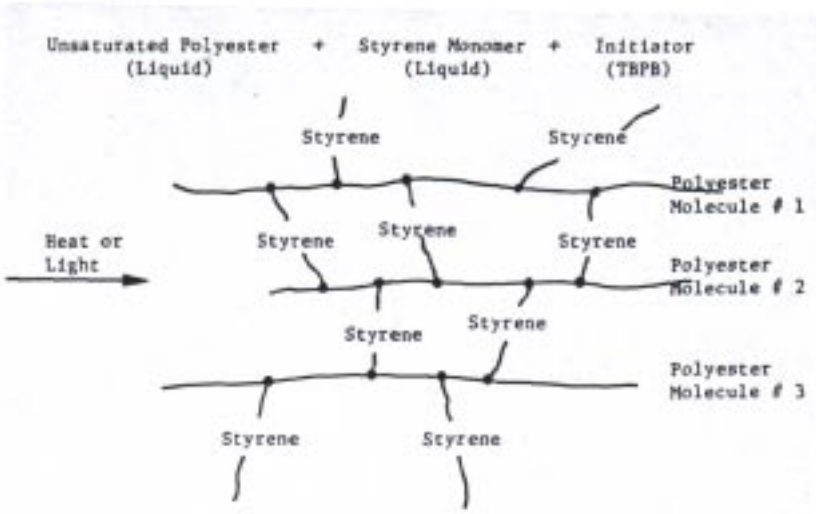

Figure 2.4: Schematic representation of a cross-linked polyester resin [2]

The curing time for polyester resin depends on the decomposition rate of the catalyst, which can be increased by the addition of small quantities of an accelerator such as cobalt naphthanate. The rate of decomposition of the catalyst can also be increased, by increasing the curing temperature upto a certain optimum. The properties of a polyester resin depend on the cross-link density, which primarily depends on the chemical nature of the raw materials, the number of unsaturation points in an unsaturated polyester molecule and the amount and nature of the diluent used.

Polyesters have excellent resistance to many mild acids and alkalis. The advantages of polyester resins are low viscosity, fast cure time, good thermal and impact

resistance, good moisture resistance and low cost. However, their properties are generally inferior to those of epoxies. The principal disadvantage of polyesters as compared to epoxies is their high volumetric shrinkage. Polyester resins are mostly used in automotive, marine, chemical and electrical applications.

2.2.3 Phenolic formaldehydes

Phenol and formaldehyde undergo a condensation reaction producing two types of phenolic resin depending on the molar ratio of the starting materials. With an excess of formaldehyde, *resole* resin is formed. It can be cross-linked (by heating etc.) without addition of other ingredients. The disadvantage of this resin is limited storage life. With an excess of phenol, *novolac* resin is produced which has indefinite shelf life because of its inability to polymerize on its own. This resin needs a source of formaldehyde as the hardener for cross-linking.

In the first stage of reaction, formaldehyde reacts with phenol forming methylolphenol as shown in figure 2.5. This stage is essentially a mixture of monomers and dimers, having a water like viscosity. The second stage is the condensation of products of the first stage and contains all sizes of molecules that are still soluble in water. The third stage is considered as one giant molecule, which is the result of chemical cross-linking of the molecules of the second stage. Figures 2.6 and 2.7 show the formation of *novolac* resin and *resole* resin respectively.

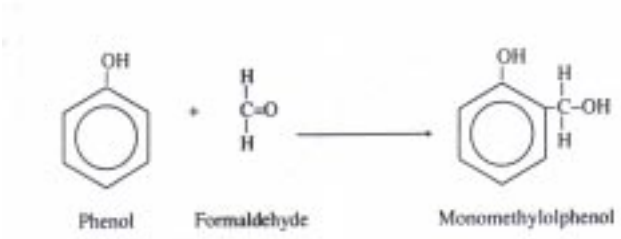

Figure 2.5: Addition of formaldehyde to phenol [3]

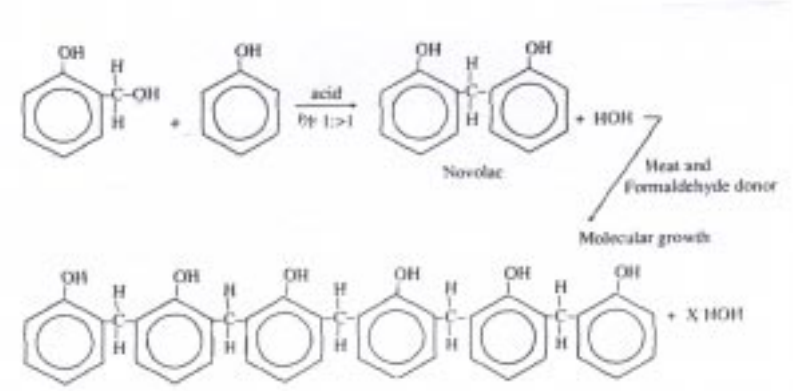

Figure 2.6: Formation of novolac resin [3]

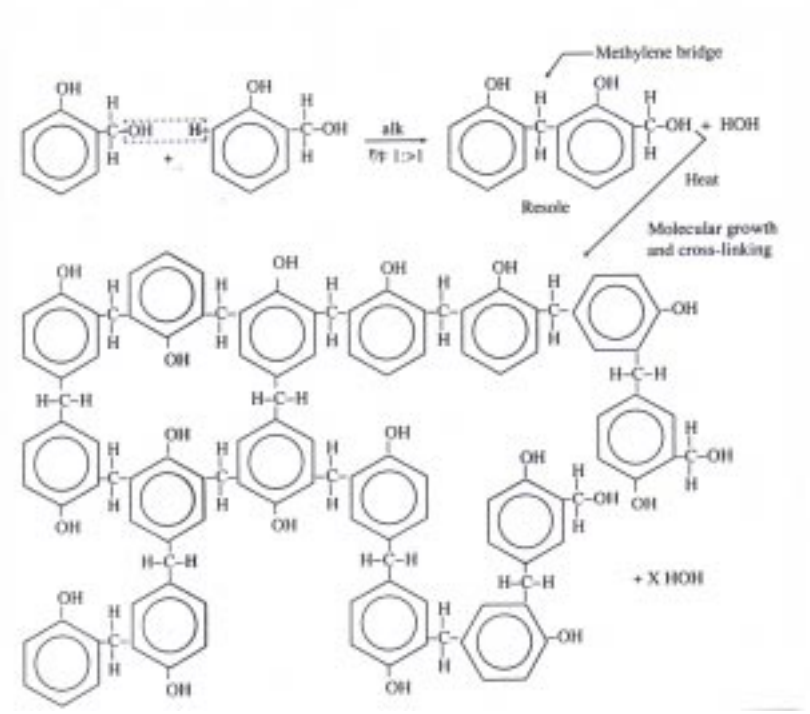

Figure 2.7: Formation of resole resin [3]

The properties of phenolic resins depend on the pH of the resin and the temperature of cure. The higher the temperature and pH, the faster is the cure. Various types of fillers and extenders such as cereal flour, wood flour, clay and lignin are also added to control the flow and penetration properties of the resin.

Cured phenolic resins provide high mechanical strength and are resistant to degradation, heat, fusion and solvation. The resistance to degradation of phenolic resins is due to the stability of the benzene ring, and C – C bonds formed during polymerization. The resistance to heat and fusion and solvation are due to their highly cross-linked structure. They are used in adhesives, coatings, laminates and binders in foundry.

2.2.4 Resorcinol-formaldehydes

Condensation reaction between resorcinol and formaldehyde produces RF (resorcinol-formaldehyde) resin that has properties similar to a phenol formaldehyde resin. The presence of a second hydroxyl group on the benzene ring (as opposed to a single hydroxyl group in the case of phenol) makes resorcinol extremely reactive to formaldehyde in forming the methylol compound and subsequently to the formation of methylene bridges in solidifying. The formation of *novolac* resin from resorcinol and formaldehyde is shown in figure 2.8.

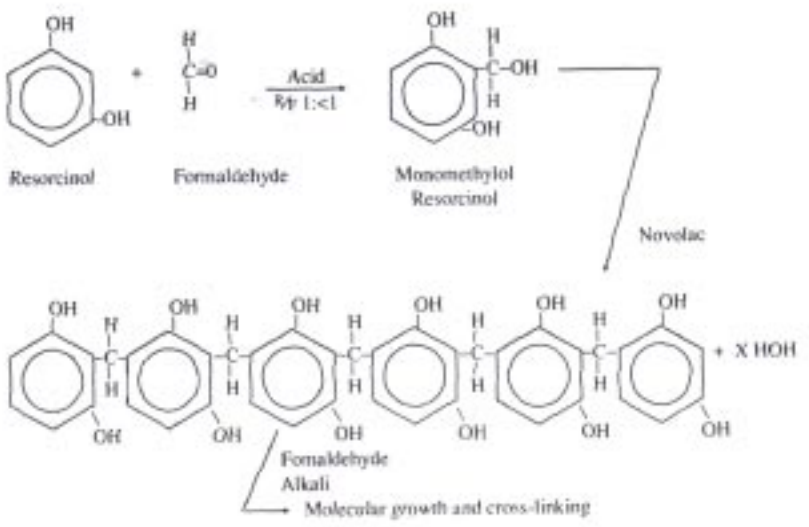

Figure 2.8: Formation of novolac from resorcinol and formaldehyde [3]

The speed of cure of resorcinolic resins depends on the pH of the resin and temperature of cure. The cure time is generally reduced by increasing the pH of the resin or by increasing the temperature. The cured state of resorcinolic resins is the same as the

highly cross-linked structure of phenolics, since resorcinol has the same three reactive hydrogens, which allow molecular growth in three directions. The durability of the RF bond depends on the extent of cure; fully cured RF is considered one of the best adhesives for bonding wood. The principal disadvantage is high cost.

Due to similarity of chemical reactions, copolymerization of resorcinol and phenolic resins is performed. The resulting phenol resorcinol formaldehyde (PRF) has lower cost due to phenolic base and room temperature cure due to resorcinol end groups. PRF resin is widely used in construction, boat building, and gluing any solid wood pieces that would be exposed to severe environmental conditions.

2.2.5 Vinyl esters

Unsaturated vinyl ester resin produced by the reaction of an unsaturated carboxylic acid and an epoxy resin is the starting material for vinyl ester resin. The resulting resin is dissolved in styrene monomer for cross-linking of C=C bonds at the ends of a molecule and also to reduce viscosity. Peroxides and accelerators are used for curing. The raw materials used and a schematic of the cross-lined vinyl ester resin are presented in Figure 2.9 and Figure 2.10 respectively.

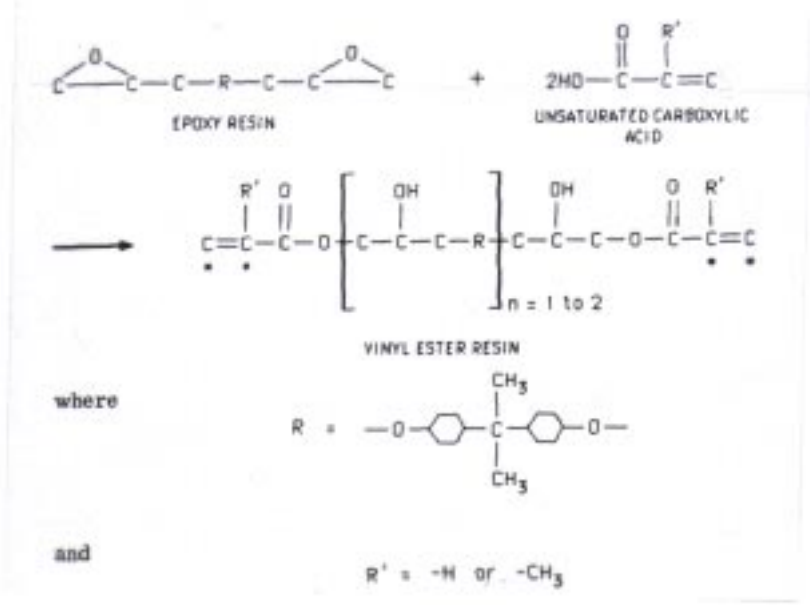

Figure 2.9: Chemistry of a vinyl ester resin [2]. (The asterisk denotes unsaturation points or reactive sites)

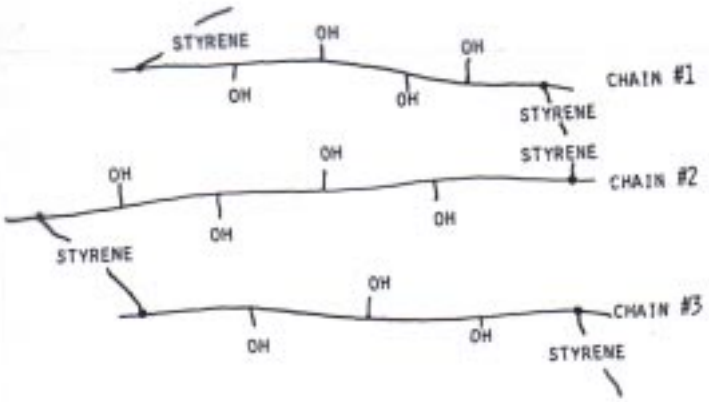

Figure 2.10 : Schematic representation of a cross-linked vinyl ester resin [2]

The curing reaction of vinyl ester resins is similar to that of polyester resins. Due to fewer cross-links, cured vinyl ester resins have greater fracture toughness than polyester resins. The hydroxyl groups along the length of a vinyl ester molecule can form hydrogen bonds with similar groups on glass fiber surface resulting in excellent fiber wet-out and good adhesion with glass fibers.

Vinyl ester resins possess excellent tensile strength and chemical resistance. They have low viscosity and low curing time. Their principal disadvantage is that they have higher volumetric shrinkage than the parent epoxy resins. They are used in corrosion resistant FRP products, aerospace industry and other exterior applications.

2.2.6 Urethanes

Polyurethanes are reaction products of isocyanate, a polyol and a curing agent like diamine. Urethanes are classified based on the polyol (generally polyethers or polyesters) used. Urethanes have excellent abrasion resistance, tear strength, shock absorption, resistance to oxygen aging, and resistance to a variety of solvents. Their life is limited under high temperature and high humidity environments.

They are widely used in flexible foams and insulation materials. Other applications are bumpers, liners of equipment handling abrasives, casting molds, high impact car panels and a variety of reaction injection molding products.

Typical properties of various adhesives are presented in Table 2.2.

Table 2.2: Properties of thermosetting resins [4]

Property	epoxy	phenolic	polyester	polyurethane
Specific gravity (----)	1.1-1.40	1.24 - 1.32	1.04 - 1.46	1.84
Water absorption (24 hr) %	0.08 - 0.15	0.1 - 0.36	0.15 - 0.6	0.2-1.5
Tensile Modulus (X 10^3 psi)	350	400-700	300-640	0-100
Tensile yield strength (psi)	-----	-----		
Thermal conductivity (10^{-4} cal-cm/sec-cm^2 ^{0}C)	4.5	3.5	-----	5
Co-efficient of linear thermal expansion (10^{-6} in/in/^{0}F)	45-65	68	55-100	100-200

2.3 Wood

Wood is a cellular, natural organic material, the porosity and surface condition of which affect its characteristics as a substrate. The bondability of the wood/adhesive system depends on many factors: species, equilibrium moisture content, physiochemical properties of wood (including the changes caused by preservative treatment or exterior exposure), adhesive properties, and the conditions under which the adhesive bond is

formed.

Northern oak, eastern cotton wood, southern pine, red maple, yellow-poplar and douglas-fir are the most commonly used types of wood for civil engineering structures.

2.3.1 Composition and structure

The components of wood are cellulose, hemicellulose and lignin. The arrangement of these components is similar to that of a fiber reinforced composite wherein, the anisotropic cellulose fibers are reinforced in isotropic lignin matrix. The partially oriented hemicelluloses are intimately connected to the other two components. The amount, organization and structure of these components influence the adhesive bonding of wood. A high cellulose content in wood leads to an increased tensile strength and a high lignin content improves compressive strength parallel to the grain.

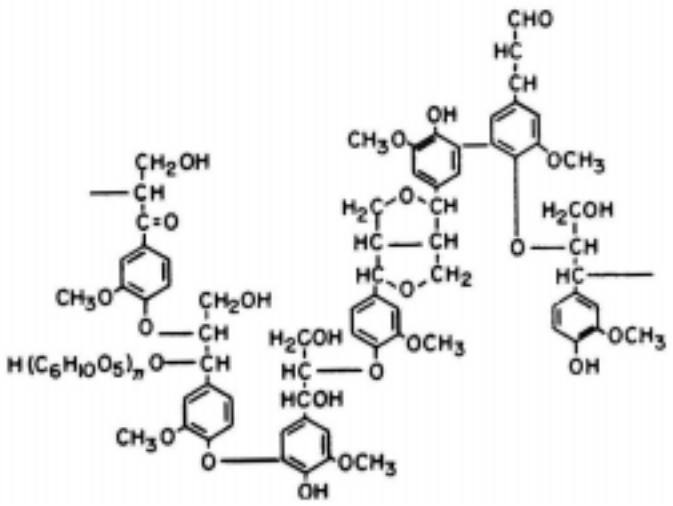

Figure 2.11 Partial structure of a lignin molecule [5]

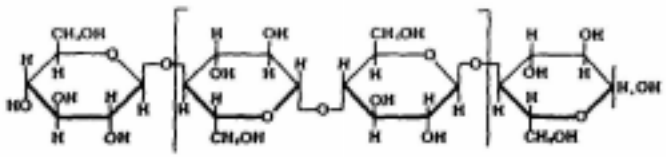

Figure 2.12 Structure of a cellulose molecule [5]

2.3.2 Preservative Treatment

Either natural or artificial weathering can produce significant changes in wettability and bondability of wood. Wood used in building construction is generally subjected to fluctuating humidity. The EMC (Equilibrium Moisture Content) is therefore constantly changing, sometimes periodically and at other times, sporadically, such as when wood is exposed to rain. Hence wood is treated with chemicals to enhance performance against fire, fungi and weather.

Chromated copper arsenate, copper naphthenate, creosote, ammoniacal preservative solutions like ammoniacal copper zinc arsenate (ACZA) and ammoniacal copper arsenate(ACA), CuDMAP {Bis-[1-(dimethylamino)-2-propanolato] copper(II)}, chromated zinc chloride etc. are some of the preservatives used for the treatment of wood.

Creosotes distilled from tars are widely used in wood preservation, and coal-tar creosote is most effective among the creosotes. High toxicity to wood destroying organisms, relative insolubility in water, low cost and ease of application to wood are the advantages of this preservative. However, the blackish-brown color renders it unsuitable where appearance is important. Also, creosote vapors are harmful to plants. Freshly

creosote-treated wood can be ignited easily and so creosote cannot be used where fire hazard is a concern.

Water based chromated copper arsenate (CCA) is the most widely used preservative. Experiments conducted at the Wood Research Institute, Michigan Technological University, indicated that wood (southern yellow pine, radiata pine and douglas-fir) thoroughly impregnated with CCA even at low retentions can be protected from damage by formosan subterranean termites, the common termites affecting wood in North America. Also, CCA treated wood is found to provide good resistance to *Limnoria* and *Teredo* marine borer attack. CCA is accepted as a very effective preservative treatment with certain wood species like pine wood and douglas-fir. Commercial CCA treatments are also known to contain wax emulsions that greatly increase the water-repellancy of the treated wood as compared to untreated wood. This is due to the higher contact angle for the CCA treated wood.

Chapter III

ADHESION FUNDAMENTALS

3.1 Adhesion

An adhesive is defined as a " substance capable of holding materials together by surface attachment" [5]. Each adhesively bonded joint is a system of two similar or dissimilar solid materials called substrates or adherends, joined by a layer of another material called the adhesive. For structural applications, the adhesive film should be considered as a material in its own right, however thin it may be.

3.1.1 Adhesive Composition

Most of the modern adhesives are composed of various components, which have their own specific function. The following components are usually present in a structural adhesive:

Base

This is the base material from which the adhesive derives its specific name, like epoxy, polyester, polyurethane resins discussed earlier under different types of matrices. It is usually a solid material that serves as the back bone of the adhesive.

Solvent

It is used to dissolve or disperse the base and additives to provide a liquid adhesive system. Solvent may not be required if the base is a liquid.

Hardener

It undergoes a chemical reaction with the base and cures the adhesive during bonding. It is usually added in stoichiometric proportions to the base.

Other additives are also added to improve adhesive properties:

Fillers are primarily added to thicken a liquid adhesive for satisfactory spreading on the adherend surface. They improve mechanical properties of polymers like hardness and modulus.

Plasticizers are high boiling point liquids or solids that are mixed with polymers to improve flexibility.

Coupling agents are chemicals used to treat the surface of fillers and they improve compatibility between filler and polymeric matrix.

Antioxidants and stabilizers are added to polymeric matrices to protect them against heat, light and oxygen.

Adhesives harden in the joint by several mechanisms such as solvent loss, melting and cooling, and chemical reaction. Thermosetting resins like phenol, resorcinol, epoxy, polyester and polyurethane used in the current experimental work, harden by an irreversible chemical reaction.

3.1.2 Adhesive Bonding Process

The adhesive bonding process begins with preparation and application of an adhesive to an adherend that has been prepared for bonding. The process continues with application of necessary curing pressure for the required time. The adhesive is usually applied to the adherend wood in a suitable pattern. The adhesive may be applied to one or both the surfaces that are to be adhered. The steps in an ideal wood adhesive bond development outlined by Marra [3] are, flow, transfer, penetration, wetting and hardening.

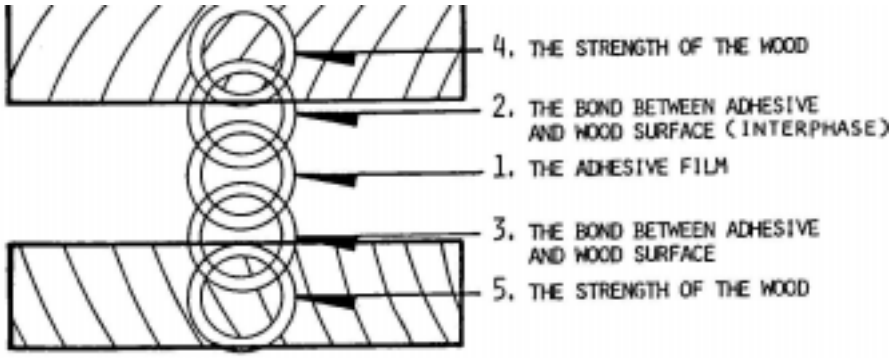

Figure 3.1: An idealized chain link concept of adhesive bond anatomy [5]

During flow, adhesive applied to the wood surface merges into a uniform wet film. When two surfaces of wood to be adhered are brought together and pressurized, the adhesive transfers to both surfaces equally. The adhesive then penetrates into the wood surfaces establishing complete contact between the adhesive and wood surfaces. During wetting, the adhesive develops an extensive and intimate molecular scale contact with the wood surface. Wetting occurs to some extent during all the previous steps. Finally during hardening, the adhesive film sets and develops cohesive strength and environmental resistance in the bond.

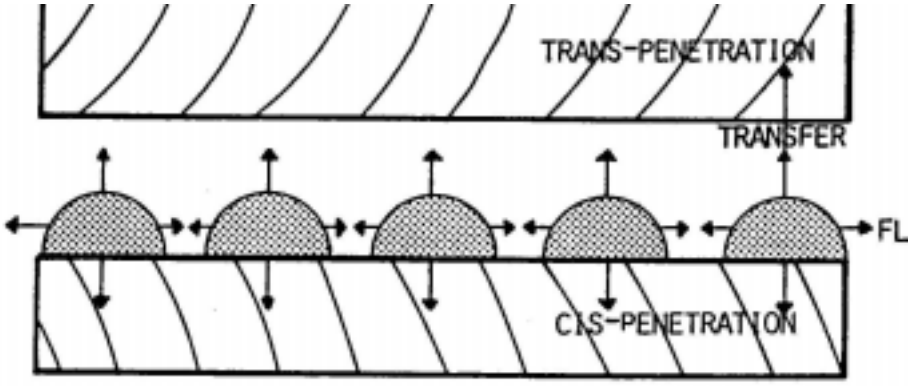

Figure 3.2: A diagrammatic sketch of flow, transfer and penetration functions in wood-adhesive bond development [5]

3.1.3 The Quality of an Adhesive Bond

The quality of an adhesive bond depends not only on the adhesive as supplied by the manufacturer, but also on the surface characteristics of wood and the conditions under which the bond is formed.

Preparation of adherend

For an adhesive to adhere effectively to the adherend, the surface should be smooth and flat so that a film of adhesive is formed. Wood adherends should be conditioned before bonding, to a moisture content that is close to that expected in service. The conditioned wood should be machined to provide a fresh, flat, smooth surface, free from any torn fibers, and it should be bonded within 24 hours of machining.

Preparation of adhesive

The components should be mixed with precision in the proportions specified by the manufacturer. Improper proportioning of curing agent, fillers, extenders or solvents can affect viscosity of the adhesive and thereby the quality of the adhesive bond.

Application of adhesive

Proper amount of the adhesive should be spread on one or both adherends rapidly and uniformly before the viscosity starts to increase. Different types of spreading equipment can be employed depending on type of adhesive, spreading speed, volume of adhesive to be spread and other factors. For small scale or laboratory operations, the adhesive can be brushed by hand or spread using a spatula. For industrial purposes,

double-roll spreaders, extruders, spraying units etc. are used.

Priming adherend surface

Priming the wood surface prior to bonding can increase compatibility of adhesives to wood surface. Based on the type of a primer, it can be used to modify different characteristics of an adhesive joint (developing tack, lengthening time between surface preparation and bonding, improving corrosion resistance of adhesive joints etc.). Primers that chemically react with the adherend surface and adhesive are known as adhesion promoters or coupling agents.

3.1.4 Factors Affecting Performance of an Adhesive

Most of the thermosetting resins used in structural applications are prepared by mixing the base resin with a curing agent that initiates the reaction within the adhesive. The optimum performance of such adhesives depend on variables such as:

- amount of hardener or curing agent that is added to or mixed in the basic resin
- open and closed assembly time of adhesion
- thickness of glueline
- pressure and temperature of curing
- conditioning after bonding such as post curing
- machining bonded specimen
- treatment given to wood

3.2 Use of Coupling Agents for Improved Adhesion

Coupling agents are used to treat the surface of adherends as well as fibers to improve interfacial properties of a complex composite. In a GFW wood post, the glass fiber/adhesive interface and wood/adhesive interface, have a major influence on the durability of the post.

The bond between glass fibers and the adhesive is improved by surface treatment of glass fibers with a variety of chemicals called sizing agents (eg: silanes). Sizing of fibers is also shown to significantly reduce the moisture attack at the interface [6]. The influence of the coupling agents, chemistry and the role of coupling agents in maintenance of surface properties after exposure to the environment is discussed by Schutte [7].

The bond between the adhesive and wood surface depends on the properties of adhesive and the surface characteristics of the wood. The surface of CCA treated wood consists of hemispherical deposits of oxides of Chromium, Copper and Arsenic [8]. The presence of these insoluble metallic oxides blocks molecular forces of attraction between the wood surface and adhesive. A 5% aqueous solution of hydroxy methylated resorcinol (HMR), when used on CCA treated wood surface has been found to increase the delamination resistance and wood failure of epoxy bonds [9]. HMR enables phenol-resorcinol-formaldehyde, isocyanate, phenol-formaldehyde and resorcinol-formaldehyde adhesives to form strong and durable bonds with CCA treated wood [10].

3.3 Performance Evaluation of Adhesive Bond

3.3.1 Introduction

Testing of bonded assemblies helps characterization of different materials based on their relative performance and determination (or prediction) of their durability. Standard methods are available to measure specific properties of adhesives, bonded assemblies and complex composites. One can use standard test methods of ASTM, AITC, etc. and measure properties like strength, stiffness, creep, etc. in different modes of applied load (shear, tension, compression, impact, bending etc.). Short-term accelerated-aging procedures that simulate long-term exposure conditions are also used to determine the durability of complex composites.

3.3.2 Test Methods

Test methods are categorized based on the materials involved, method of loading, time required for testing, equipment used, sample conditions (temperature, pressure, moisture content, and conductivity) and the required sample state after testing. Some test methods produce numerical values, some produce only qualitative results.

3.3.2.1 Destructive Testing

Destructive testing applies load on entire bonded area and evaluates the bond strength as a whole. However it destroys the bonded assembly and the specimen cannot be used further. It is used to reveal changes in strength and strain to failure of bonded assemblies.

The direction of load placed on a test specimen until failure characterizes the

destructive testing procedure. Adhesive bonded assemblies can be loaded in shear, tension, flexure, peel, cleavage or combinations of these.

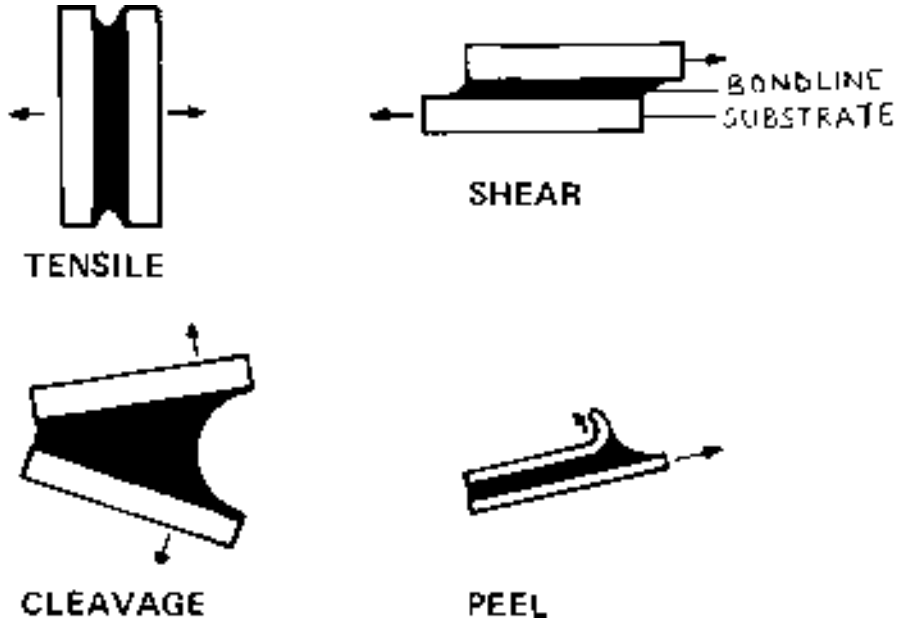

Figure 3.3: Test specimen for different types of tests [5]

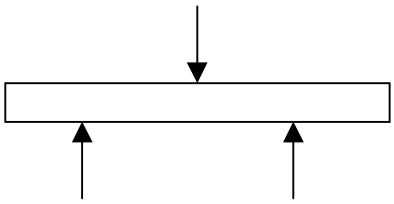

Figure 3.4: Test specimen for flexural test (three point bending)

Shear loading introduces forces parallel to the plane of the bond line. These forces slide the substrates in opposite directions, loading the entire bonded area. Bonded assemblies most often are designed to emphasize the greater efficiency of shear bonding. The shear strength of bonds is determined using ASTM D-905.

Tensile loading applies forces perpendicular to the plane of the bonded area. Tensile loading, in principle transfers the load over the entire bonded area but is difficult

to apply in a totally axial fashion. Tensile strength of a bond is the tensile load per unit cross-sectional area required to break the bond. ASTM D-897 is used to determine comparative tensile properties of adhesives.

Flexural testing applies force on a simple beam at mid-span, perpendicular to the bond line. Flexural strength of an adhesive-wood bond is the maximum breaking strength sustained by a specimen when subject to bending force. ASTM D-790 provides the typical procedure for flexural testing of complex composites.

Cleavage loading concentrates force along one end of the adhesive bond line. Cleavage strength is the tensile breaking load expressed in force per unit width of bond line. ASTM D-3433 is used to test bonds in cleavage and determine properties like fracture toughness.

Peel testing also applies force along one end of the bond line. Peel strength is a measure of the resistance to stripping of a flexible member of an assembly that is bonded to a flexible or rigid adherend. The stress distribution in a peel test is complex and the application of a constant peel force is influenced by specimen width and bond strength. 90^0 peel, 180^0 peel, and T-peel are common peel procedures in use. ASTM D-1876 and ASTM D-903 are used to determine peel testing of adhesive bonds.

Impact testing, creep testing and a variety of other tests are also used for characterizing the mechanical response of adhesive bonds. Different types of tests based on the particular type of loading are discussed in detail by Blomquist et al [5]. The mechanical properties of a few commonly used thermosetting adhesives are presented in Table 3.1.

Table 3.1: Mechanical properties of thermosetting adhesives [11]

Adhesive	Tensile yield strength (10^3 psi)	Tensile modulus (10^5 psi)	Flexural yield strength (10^3 psi)	Flexural modulus (10^5 psi)	Compressive strength (10^3 psi)	Izod impact strength (ft-lb/in)
Bisphenol A epoxy	9.5–11.5	4.5	14-18	4.5-5.4	16-24	0.2-0.5
Phenolic	6.5-7.0	8-13	9-11	11-13	22-36	0.3-0.35
Polyester	8.0	2.8	12-14	2.8-4.0	13	0.5
Polyurethane	2.5-3.0	1.1-1.6	6.0-7.0	1.2-1.7	--	7-15

3.3.2.2 Non-destructive Testing

Non-destructive testing is carried out on specimens so that they can be used even after testing. This type of testing does not damage the bond-line but the bond cannot be fully loaded. Non-destructive testing is conducted to understand the causes of strength degradation and the factors affecting it.

Scanning Electron Microscopy (SEM) is used to observe the topography of a fractured specimen and helps detect the site of failure initiation. The failure occurring at the fiber-matrix interface or wood-matrix interface can be detected. Mechanical interlocking of phenolic adhesive in CCA treated wood, for example, was studied using SEM by Vick and Kuster [8].

Dynamic Mechanical Spectrometer is used for non-destructive testing of bonded assemblies [12]. A sinusoidal strain is imposed on the sample and the resulting sinusoidal stress is measured. The dynamic mechanical spectrum of the sample is used for calculation of mechanical properties and service life.

Visual examination of bondlines can determine if uniform adhesive squeeze-out had occurred. Squeeze-out can be examined for variations in color, indicating improper mixing or curing. Scraping off the squeeze-out and examining the revealed bondline can reveal voids, cracks or delaminations.

Short pulses of ultrasonic energy can be introduced so that they can be reflected by the bond line or the far surface of the bonded assembly. A large echo or loss of back-surface echo indicates an unbonded area.

Radiographic X-ray inspection and proof loading are other techniques used for non-destructive analysis. Microscopic techniques like Rutherford Back scattering Spectroscopy (RBS), Scanning Acoustic Microscopy, Nuclear Magnetic Resonance (NMR) imaging, Transmission Microscopy and Optical Microscopy are used to observe fractured specimens.

Chapter IV

DURABILITY OF BONDED ASSEMBLIES

4.1 Introduction

The effectiveness of the proposed composite wrapping technique depends on the performance of the bond between wood and the composite wrap in the field. When installed in the field, the bond may be affected by several factors like mechanical stress, temperature, pH variation and moisture. Moisture may dissolve, soften or hydrolyze the adhesive. It can produce variations in dimensions, alter the strength of the wood and even cause decay in the wood structure. These effects are different for different species of wood. Elevated temperatures can soften, further cure or break down the adhesive film. Heat can create temporary or permanent strength loss of wood and it can change the dimensions of dry wood. Chemical attack also damages the adhesive bond, and may even damage the wood.

To ensure that the materials and manufacturing processes lead to a GFW-wood post with requisite strength and durability, testing of bonded assemblies is required. Durability of bonded assemblies can be tested by long-term exposure to atmospheric conditions or short-term exposure to harsh environments. A variety of methods are used by researchers for testing the durability of composites.

Resistance to delamination of adhesive bonds was tested by Vick [13] who employed ASTM specification D-2559-92. This method involves a vacuum soak in water, a pressure soak in water, oven drying and exposure of adhesive bonds to steam.

The resulting delamination is measured as a percentage of the total end-grain bondline length for each specimen.

Stress corrosion data for PET (polyethylene terephthalate) reinforced with glass fibers was generated by Lhymn and Schultz [14]. Loaded samples were aged in different chemical media (air, NaOH, HCl, H_2SO_4, HNO_3, NaCl) until part-through failure occurred. The time to failure under a specific initial stress was calculated for each medium.

The durability of concrete cylinders wrapped with FRP was tested by Kshirsagar et al. [15]. Wrapped cylinders were exposed to alkaline media at varying temperature for 1000 to 10,000 hours. The ultimate strength (in compression loading) and strain of aged and unaged cylinders were compared.

Devalpura et al. [16] tested GFRP (Glass Fiber Reinforced Plastic) pultruded rods in acidic and alkaline environments using an accelerated stress rupture procedure derived from ASTM D-2992 and ASTM D 3681. The percent ultimate stress versus time to failure was reported.

Standards are available for testing the durability of composites involving different materials such as concrete, wood, metal, FRPs etc. Modifications to the standards are made by researchers, depending on the expected exposure during the service life of the composite.

In the current research, accelerated aging and chemical aging were performed on bonded specimens.

4.2 Accelerated Aging

Due to changes in the atmospheric temperature, freezing and drying are expected to occur in the field. Vacuum and pressure cycles can induce interfacial stress, capillary diffusion of moisture into wood, fibers and matrix and other similar phenomena. Freezing and drying can accelerate the damage propagation. Considering these aspects, samples were subjected to a six cycle accelerated aging procedure prescribed by Chow et al. [17]. They stated that six cycles of the accelerated aging may be equivalent to more than twenty years of natural aging depending on the properties used to relate accelerated aging and natural aging. The temperature and duration of steps in each cycle were modified according to the sample size. The step of application of steam was eliminated to maintain uniformity with the aging tests being conducted at the Constructed Facilities Center (CFC). The procedure can be called a combination of ASTM D 2559-92, Chow cycle and ASTM D 1101. Each of the six cycles involved changes in temperature, pressure and moisture during which the bond-line is subjected to severe swelling and shrinkage. The following were the steps in each cycle of the accelerated aging process:

♦ vacuum soaking in water (70^0F) at 25 inches of Hg for 30 min

samples immersed in water, are placed in the vacuum/pressure cylinder and vacuum is applied to the chamber. The air inside the chamber and also the pores of wood is pulled out. During this process, the voids inside the specimens are opened and water penetrates into the samples.

♦ pressure soaking in water (70^0F) at 100 psi for 30 min

samples are immersed in water and application of pressure forces water into the specimens

♦ freezing for 4 hours

water expands on freezing causing more damage to the specimens

♦ oven drying for 6 hours at 60^0 C

drying evaporates absorbed moisture causing thaw

Four different types of samples were subjected to accelerated aging:

(1) shear coupons of CCA treated wood with adhesive film between

the samples were aged to determine the strength of wood/adhesive bond or the extent of adhesion between the wood and adhesive under long-term exposure to atmospheric conditions

(2) sandwich shear coupons of CCA treated wood with adhesive film and glass fabric in between

these samples were aged to determine the strength of wood/FRP bond or the extent to which the adhesive bonds wood and glass fibers under long-term exposure to atmospheric conditions

(3) GFRP wrapped, CCA treated wooden dowel rods (0.5″ in diameter)

these samples were aged to observe the changes in strength and modulus of GFRP wrapped posts under long-term exposure to atmospheric conditions

(4) GFRP wrapped, CCA treated rectangular wood samples (50 X 9 X 4 mm^3)

these samples were aged to predict the long-term behavior and service life of the proposed GFRP wrapped posts

4.3 Chemical Aging

Use of de-icing salt in winter, moisture changes in the atmosphere, pH changes in the soil etc., motivate the need for a long-term aging in different liquid media. In the process of chemical aging, samples were immersed in liquid media of different pH and subjected to the Cyclic Temperature and Humidity Conditioning method. This method involved the exposure of samples to alternating cycles of high and freezing temperatures. These aging conditions were adopted to observe the effect of freeze/thaw cycling in different liquid media. The aging media were, acidic solution of pH 3, alkaline solution of pH 13, water and 3% salt water. Water and salt water are the most expected conditions in the field. To observe the effect of harsher environments, pH 3 and pH 13 solutions were selected. The equipment was the Thermotron Environmental Test Chamber (4800 Controller). The temperature and humidity changes in the environmental conditioning chamber are depicted in the Figure 4.1. The humidity was 100% for the current situation because all the samples were immersed in liquid.

The samples subject to 6-cycle accelerated aging and chemical aging were tested by suitable destructive and non-destructive tests. Details of test methods, results and data analysis are discussed in Chapters V through VII.

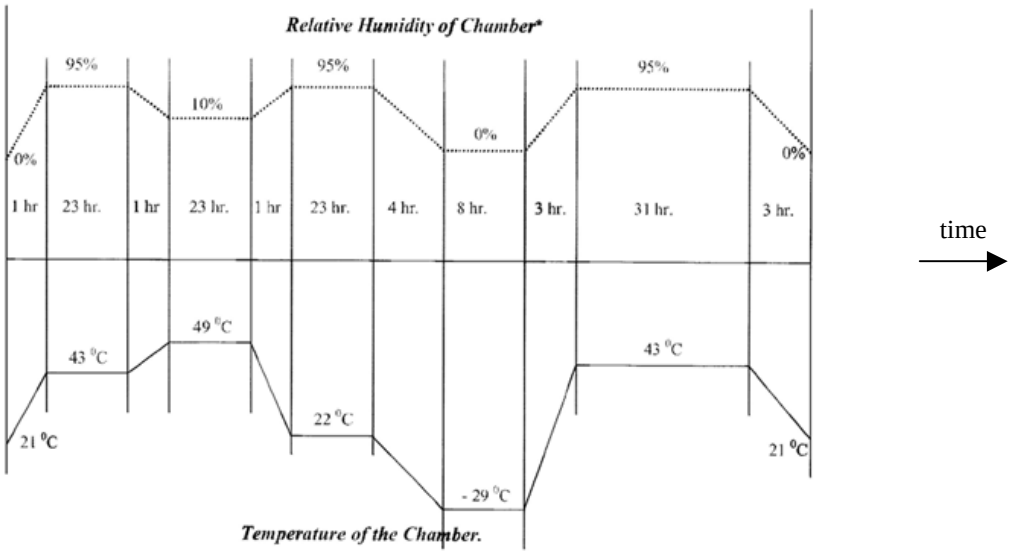

Figure 4.1: temperature and humidity variations in cyclic freeze-thaw conditioning
1 cycle = 121 hrs (5 days + 1 hour)

4.4 Summary of Test Methods Used

Test	**test type**	**Method used**	**Equipment used**
Shear loading	Destructive	Modified ASTM D-905	Instron 1011
Flexural loading	Destructive	Modified ASTM D-790	Instron 4411
Mechanical spectroscopy	Non-destructive	-----	Rheometrics Spectrometer RMS-800
6-cycle accelerated aging	Destructive	Modified Chow cycle	Pressure Cylinder
Chemical aging	Destructive	Cyclic temperature and humidity conditioning	Thermotron Environmental Test Chamber

Chapter V

ADHESIVE SCREENING

5.1 Overview

The integrity of the proposed GFW wood post depends largely on the wood/adhesive interface and adhesive/glass-fabric interface. Selection of an adhesive for wrapping glass fabric around a wood post was one of the primary tasks in this research. Six chemically different resins were screened to determine the adhesive that best adheres to CCA-treated wood and glass fibers. Adhesion to the wood surface in the presence of a primer was also investigated. This chapter presents details of sample preparation, the test procedure, different conditions of exposure and test results.

5.2 Materials Used

5.2.1 Wood

CCA treated southern-pine wood was used to prepare the experimental coupons. Southern pine is easily available and is most commonly used. Water based CCA is the most widely employed wood treatment that provides good resistance to termite attack. The wood was supplied by 84 Lumber (a local lumber company).

5.2.2 Glass Fibers

A woven fabric (0^0 /90^0), employing E-glass fibers was used in the preparation of sandwich coupons. The fabric incorporated an epoxy-compatible sizing and a phenolic-compatible sizing and was supplied by Johnston Industries. It had a density of 26 oz/sq.yd.

5.2.3 Adhesives and Primers

Table 5.1: Resins used in adhesive screening

Resin	**Trade Name**	**Supplier**
Epoxy	TYFO-S	Hexcel Fyfe
Phenol resorcinol formaldehyde (phenolic)	G-1149	BODEN Chemicals
Resorcinol formaldehyde (RF)	G-1131	BODEN Chemicals
Polyester	Polylite	Reichhold
Vinyl ester	---	Creative Pultrusions
Polyurethane	---	Reichhold
Phenol formaldehyde	G-1260	BODEN Chemicals

Table 5.1 presents the list of adhesives used in the screening process. Epoxies, polyesters, urethanes and vinyl esters are the principal categories of thermosetting adhesives. Phenol resorcinol formaldehyde and resorcinol formaldehyde, are water-based phenolic adhesives that are widely used in structural applications.

A 5% solution of HMR (hydroxy methylated resorcinol) in water, RF and G-1260 were used as primers. Most of the adhesives and primers were supplied in two

components, which were mixed in the specified proportions before bonding. HMR was prepared in the laboratory. Ten grams of a 5% HMR solution had the following composition:

water	9.043g
crystalline resorcinol	0.379g
40% formaldehyde	0.334g
sodium hydroxide	0.244g
	10.0g

These components were allowed to react for 4 hours and the primer was applied to wood surfaces 24 hours prior to adhesive bonding. RF was tested as a primer because of its low viscosity and wide use in structural applications. HMR was used as a primer because of its ability to produce moisture resistant bonds of epoxy and phenolic resins to CCA treated wood [18]. G-1260 was recommended by BODEN Chemicals, as a primer for the adhesive G-1149.

5.3 Sample Preparation

Shear block specimens were made using CCA treated wood and each of the six adhesives mentioned earlier. Two types of shear specimens were prepared. Type I (referred as shear coupons) consisted of two wood surfaces glued with an adhesive film in between. Type II (sandwich shear coupons) consisted of a resin-impregnated glass-fabric sandwiched between two wood surfaces. Two wood blocks of size 8″ X 3″ X 0.5″ were used to make about 30 shear coupons each time. These wood blocks were sliced along the tangential or flat grain direction of 12′ X 4″ X 2″ lumber pieces. The wood

blocks were air-sprayed to blow away dust particles on the surface. Primer was applied to the wood surfaces before application of adhesive according to the required specifications. For type I specimens, adhesive was prepared by mixing the components in the specified proportions and was uniformly applied to the surfaces with a metal spatula. For type II specimens, adhesive was prepared by mixing components in specified proportions. Glass fabric cut to the required size was then impregnated with the prepared adhesive and sandwiched between the wood surfaces. In both cases, the wood blocks were glued together following the open and closed assembly time recommended by the manufacturer. Pressure was then applied on the adhesive bonded assembly using a Baldwin machine. After pressure curing for the required time at room temperature, the bonded specimen was post cured in an oven at higher temperatures recommended by the manufacturer of the adhesive. The rectangular billet was cut into shear blocks of size

0.75″ X 0.5″ X 0.5″ using a band saw. Figure 5.1 shows the schematic of a rectangular billet and a shear coupon.

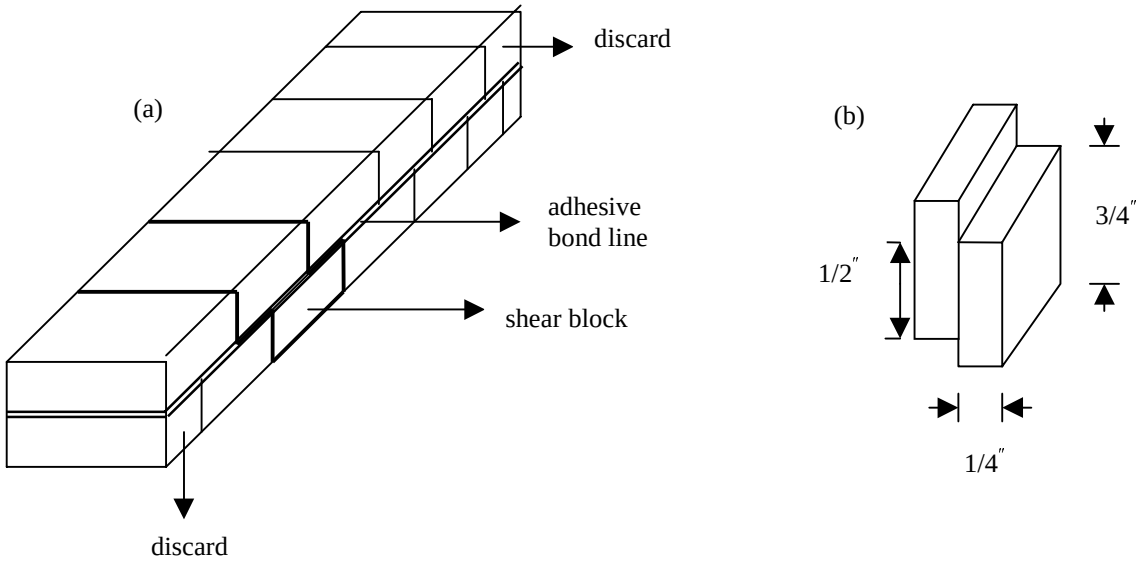

Figure 5.1: (a) rectangular billet with adhesive film in between (b) shear coupon

5.4 Description of Test Procedure

Shear loading introduces forces parallel to the plane of the bond line. These forces slide the substrates in opposite directions, loading the entire bonded area. Shear loading of an adhesive bond is therefore an effective measure of the performance of the wood/adhesive interface.

ASTM D-905 is a standard test method for evaluating the performance of wood adhesives based on the shear strength of the wood-wood bond. Therefore shear strength of adhesive bonds was determined using ASTM D-905 standard. The test results reveal the shear strength of the adhesive bond (as load per unit area of bond line in psi) and the percent wood failure (as percent of total fracture area). The failure is said to be cohesive if it is in wood or inside the adhesive film. The failure is said to be adhesive if it occurs at

the wood/adhesive interface. The desired failure mode for the effectiveness of a wood/adhesive bond is cohesive. The following are the outlines of ASTM D-905:

(1) The apparatus used has a capacity greater than or equal to 15000lbs in compression and is fitted with a shearing tool that ensures uniform distribution of the load. The specimen is loaded at a uniform rate of 5mm/min with a maximum variation of $\pm$25%.

(2) Wood blocks used for making test specimens are cut to standard size (standard size for this test method being 2″ X 0.75″ X 0.75″) to suit the dimensions of the shearing tool. These wood blocks are sanded and then air-sprayed to remove dust particles present on them.

(3) Samples are then cured based on curing time of adhesive used. The specimen is then placed in the shearing tool and loaded with a continuous motion of the movable head of the instrument at 5mm/min to failure. Shear stress at failure in pounds per square inch (psi) based on the glue-line area between laminations is calculated.

Precision of this test method is affected by (a) wood species (b) boards selected (c) grain direction (d) growth ring orientation (e) quality of bonded joint (f) condition of shear tool (g) precision of shear tool and operator. Complete details of the testing method are given in “The 1995 Book of ASTM Standards,” Vol. 15.06 [19].

In the current experimental work, an Instron machine (model 1011), with a capacity of 1000lbs was used for testing. In order to suit the capacity of the machine, sample size and cross head speed were modified. Size of shear specimens was 0.75″ X 0.5″ X 0.5″ and cross-head speed was 0.5 in/min. Figure 5.2 shows shear loading of a coupon.

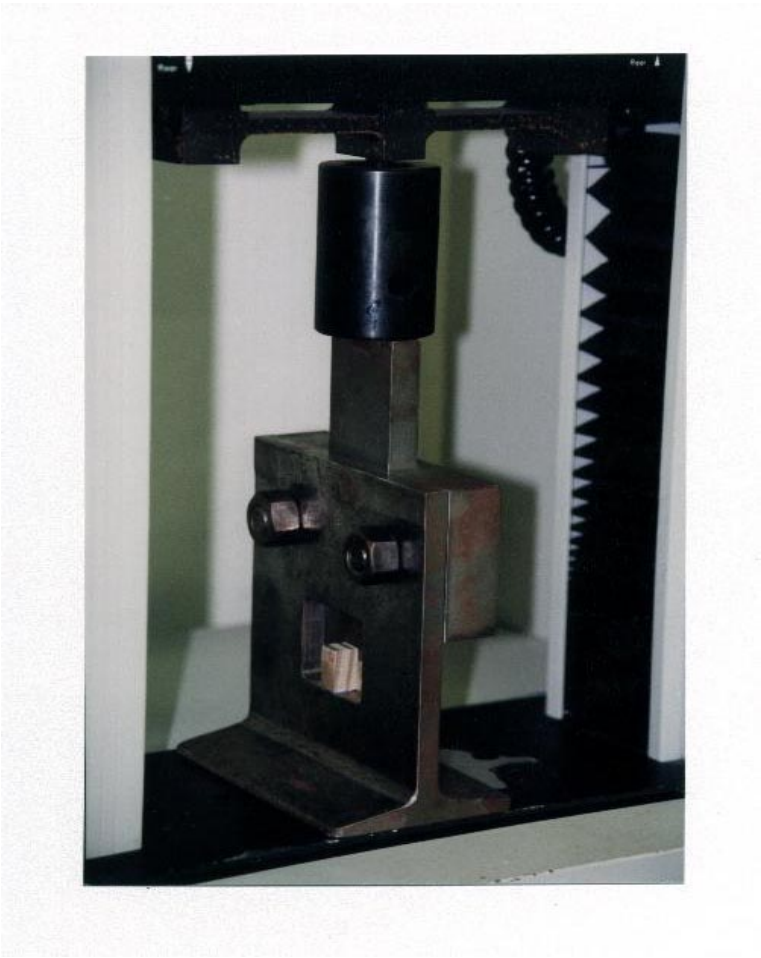

Figure 5.2: Measurement of shear strength by compressive shear loading

5.5 Sample Conditioning

Shear coupons were exposed to different conditions before testing:

(1) exposure to 6-cycle accelerated aging described in Section 4.2

(2) exposure to acidic aqueous solution of pH 3.0 for 5 days, 15 days and 25 days in atmospheric chamber (described in Chapter IV, section 4.3)

(3) exposure to alkaline aqueous solution of pH 13.0 for 5 days, 15 days and 25 days in atmospheric chamber

(4) exposure to solution of pH 7.0 for 5 days, 15 days and 25 days in atmospheric chamber

(5) exposure to 3% salt water for 5 days, 15 days and 25 days in atmospheric chamber

The reasons for the choice of these aging conditions were explained in chapter IV.

5.6 Summary of Test Results

5.6.1 Strength of Unprimed Adhesives at Different Pressures

As the first step in the process of adhesive screening, shear coupons were prepared using epoxy, phenolic, RF and polyester resins at different curing pressures ranging from 100 psi to 250 psi. At pressures beyond 250 psi, excessive squeeze out of the adhesive took place and hence 250 psi was selected as the upper limit of pressure. The optimum curing pressure of each of these resins was determined. The results are presented in Tables 5.2 through 5.6. A sample calculation of shear strength from experimental data is presented in Appendix B.1. The percent wood failure is the amount of failure in wood. For a good bond between the wood and the adhesive, the desired failure is cohesive. A wood failure value of 100% indicates that the bonded specimen fails completely in wood and there is no failure at the wood/adhesive interface. The standard error is the value by which the shear strength varies about the average value.

Table 5.2: Unaged shear strength of epoxy adhesive at varying pressure

Adhesive	Curing pressure (psi)	Cure time (hours)	No.of samples tested	Average unaged shear strength ± Standard error (psi)	Percent wood failure (%)
Epoxy	100	12	15	1265 ± 212	20
Epoxy	150	12	15	1429 ± 262	59
Epoxy	180	12	15	1401 ± 224	59
Epoxy	220	12	15	1490 ± 199	61
Epoxy	250	12	15	1897 ± 163	73

Table 5.3: Unaged shear strength of unprimed phenolic adhesive at varying pressure

Adhesive	Curing pressure (psi)	Cure time (hours)	No.of samples tested	Average unaged shear strength ± Standard error (psi)	Percent wood failure (%)
Phenolic	100	12	10	1795 ± 126	68
Phenolic	150	12	10	2098 ± 245	76
Phenolic	180	12	10	2376 ± 191	70
Phenolic	220	12	10	1795 ± 152	64
Phenolic	250	12	10	1562 ± 203	50

Table 5.4: Unaged shear strength of polyester adhesive at varying pressure

Adhesive	Curing pressure (psi)	Cure time (hours)	No.of samples tested	Average unaged shear strength ± Standard error (psi)	Percent wood failure (%)
Polyester	100	12	10	1335 + 120	6
Polyester	150	12	10	1327 ± 109	26
Polyester	180	12	10	1565 ± 114	17
Polyester	220	12	10	1581 ± 138	17
Polyester	250	12	10	1917 ± 170	32

Table 5.5: Unaged shear strength of RF adhesive at varying pressure

Adhesive	Curing pressure (psi)	Cure time (hours)	No.of samples tested	Average unaged shear strength ± Standard error (psi)	Percent wood failure (%)
RF	100	12	20	1516 ± 94	58
RF	150	12	20	1559 ± 132	56
RF	180	12	20	1513 ± 117	48
RF	220	12	20	1519 ± 110	50
RF	250	12	20	1506 ± 154	60

Table 5.6: Optimum curing pressure of adhesives (based on the average shear strength value at varying curing pressure)

Adhesive	Optimum curing pressure (psi)
Epoxy	250
Phenolic	180
RF	250
Polyester	250

5.6.2 Strength of Adhesives at Optimum Curing Pressure

In the second step, shear coupons were made using different resins at their optimum curing pressures, and tested for shear strength and extent of failure in wood. The minimum cure time for all the resins was about 12 hours. However, curing for longer time does not hurt the adhesive bond performance. Table 5.7 displays the average shear strength and percent failure in wood of different shear coupons (wood/adhesive/wood specimens).

Table 5.7: Unaged shear strength of unprimed resins

Adhesive	Curing pressure (psi)	Cure time (hours)	No.of samples tested	Average unaged shear strength ± Standard error (psi)			Percent wood failure (%)		
				Trial i	Trial ii	Trial iii	i	ii	iii
Epoxy	250	12	15	2542 ± 219	2580 ± 128	2165 ± 226	98	100	53
Phenolic	180	48	10	1757 ± 165	1517 ± 130	1450 ± 125	90	89	88
Polyester	250	24	15	1050 ± 103	1106 ± 162	1504 ± 181	40	15	68
RF	250	24	15	2677 ± 93	1498 ± 146	1457 ± 139	72	45	99
Urethane	250	48	15	1343 ± 140	----	----	92	----	----
Vinyl ester	150	96	6	156 ± 79	----	----	0	----	----

The failure of epoxy and phenolic adhered coupons was mostly in the wood. This suggests good bond formation of epoxy and phenolic resins with wood. RF and polyester adhered coupons exhibited brittle failure, which suggests a poor bond between the resins and wood. Poor bonding between polyester and wood could be due to insufficient penetration of the resin and also due to high volumetric shrinkage of polyester upon curing. Brittle failure or adhesive failure of RF bonds could also be due to poor penetration of RF into CCA treated wood. Urethane resin gave good failure in wood despite its very high viscosity. Most of the vinyl ester coupons delaminated during machining and the few that survived gave 100% adhesive failure. This eliminated the use of vinyl ester resin in further sample preparation.

5.6.3 Strength of Adhesives in Combination with Different Primers

Vick [13] showed that in the presence of HMR primer, adhesives such as epoxy, phenol-resorcinol-formaldehyde and phenolic-formaldehyde form durable bonds with CCA treated wood. Ghasemzadeh et al. [12] conducted chemical and hygrothermal aging of red oak wood-wood joints employing epoxy, polyester, polyurethane, RF and phenolic adhesives. They found the combination of epoxy as adhesive and RF as primer to be superior to all other adhesive/primer systems in terms of strength and durability.

In order to determine the effect of primer on the adhesive bond performance, epoxy, phenolic, RF and polyester resins were used in combination with different primers in preparing shear coupons. Urethane resin was not used in combination with a primer because of its very high viscosity, which would increase the thickness of the glueline, and ultimately reduce the bond strength. Tables 5.8 through 5.10 display the performance of

wood/adhesive/wood bonds in the presence of different primers under dry conditions (before aging).

Table 5.8: Unaged shear strength of adhesives using HMR primer

Adhesive	Curing pressure (psi)	Cure time (hours)	No.of samples tested	Average shear strength before aging ± Standard error (psi)			Percent wood failure (%)		
				Trial i	Trial ii	Trial iii	i	ii	iii
Epoxy	250	18	15	2885 ± 89	2022 ± 205	2143 ± 97	96	98	100
Phenolic	180	18	15	1224 ± 190	1235 ± 155	----	84	92	----
Polyester	250	18	15	2341 ± 236	975 ± 129	----	47	56	----
RF	250	18	15	2880 ± 80	2001 ± 154	1461 ± 200	73	94	86

From Tables 5.7 and 5.8 it can be seen that use of HMR primer increased the strength and cohesive failure of wood/RF/wood specimens under unaged conditions. In the presence of HMR primer, under unaged conditions, the strength of wood/phenolic/wood specimens was reduced and the percent failure in wood was not significantly affected. The effect of HMR on epoxy and polyester resins was not significant under unaged conditions.

Table 5.9: Unaged shear strength of adhesives using RF primer

Adhesive	Curing pressure (psi)	Cure time (hours)	No.of samples tested	Average shear strength before aging ± Standard error (psi)	Percent wood failure (%)
Epoxy	250	18	12	1548 ± 264	20
Phenolic	180	18	12	1500 ± 271	92
Polyester	250	18	12	485 ± 50	1

From Tables 5.7 and 5.9, it can be observed that polyester resin gave high adhesive failure and low shear strength with RF as primer. This could be due to high temperature post curing of RF and high volumetric shrinkage of polyester upon curing. Therefore this combination was eliminated from further testing. Epoxy resin showed reduced strength and reduced percent wood failure in the presence of RF primer under unaged conditions. This could be due to poor bonding between RF and epoxy, which resulted in increased adhesive failure. The effect of RF on phenolic resin under dry conditions was to increase the percent failure in wood or to increase the cohesive failure.

Table 5.10: Unaged shear strength of adhesives using G1260 primer

Adhesive	Curing pressure (psi)	Cure time (hours)	No.of samples tested	Average shear strength before aging ± Standard error (psi)	Percent wood failure (%)
Epoxy	180	18	12	1283 ± 111	11
Epoxy	180	18	12	850 ± 172	18
Phenolic	180	18	12	1290 ± 121	58

From Tables 5.7 and 5.10, it is observed that use of G-1260 primer has reduced cohesive failure of wood/epoxy/wood bond. The high adhesive failure is attributed to a

weak bond between wood and the combination of epoxy/G-1260. G-1260 is a highly viscous primer that could not have penetrated adequately into wood. Also, high viscosity of both G-1260 and epoxy could have increased the thickness of the glue-line resulting in high adhesive failure. G-1260 also reduced the strength of wood/phenolic/wood bond and gave highly brittle failures. Both the combinations, G-1260/epoxy and G-1260/phenolic were eliminated from further screening.

5.6.4 Accelerated Aged Strength of Different Combinations

After testing different primer/resin combinations and preliminary elimination, the remaining combinations were subjected to accelerated aging. During 6-cycle accelerated aging, samples were subjected to vacuum and pressure in water, followed by freezing and drying. The following table shows the unaged shear strength, aged shear strength (shear strength after 6-cycle accelerated aging) and percent decrease in strength after aging of various combinations:

Table 5.11: Unaged and aged shear strength of different primer/resin combinations

Adhesive	Primer	Average shear strength before aging ± Standard error (psi)	Percent failure in wood before aging	Average shear strength after 6-cycle aging ± Standard error (psi)	Percent failure in wood after aging	Percent decrease in shear strength after aging
Epoxy	-----	2165 ± 226	53	765 ± 147	28	65
Epoxy	-----	1897 ± 163	73	737 ± 117	14	61
Epoxy	RF	1548 ± 264	20	701 ± 306	22	55
Epoxy	HMR	1934 ± 158	100	1356 ± 137	100	30
Epoxy	HMR	2022 ± 205	98	1553 ± 199	100	23
Epoxy	HMR	1342 ± 121	85	1096 ± 159	85	18
Epoxy	HMR	1578 ± 166	100	1231 ± 167	99	22
Phenolic	-----	1884 ± 185	100	863 ± 132	100	54
Phenolic	-----	1450 ± 125	88	685 ± 73	42	53
Phenolic	RF	1500 ± 271	92	572 ± 109	88	62
Phenolic	RF	1701 ± 150	86	623 ± 89	89	63
Phenolic	HMR	1224 ± 190	84	567 ± 97	54	54
Phenolic	HMR	1235 ± 155	92	479 ± 56	98	61
RF	-----	1457 ± 139	99	819 ± 170	87	44
RF	-----	1519 ± 110	74	520 ± 99	43	66
RF	HMR	1588 ± 164	97	867 ± 104	92	45
RF	HMR	2001 ± 154	94	673 ± 95	90	66
RF	HMR	1461 ± 200	86	496 ± 73	80	66
Polyester	-----	1050 ± 103	40	554 ± 86	41	47
Polyester	-----	1106 ± 162	15	269 ± 64	20	76
Polyurethane	-----	1343 ± 140	92	711 ± 84	25	47
-----	Wood	2374 ± 88	-----	1574 ± 83	-----	34

The factors that govern the selection of an adhesive or an adhesive/primer combination are percent wood failure, percent reduction in strength upon aging and shear strength. From table 5.11 it is understood that the reduction in strength after accelerated aging is minimum for HMR/epoxy combination. This reduction in strength of HMR/epoxy combination is less than the reduction in strength of wood itself. The magnitude of shear strength after accelerated aging is also maximum for the HMR/epoxy combination. The failure of wood/HMR/epoxy/HMR/wood bond, before and after aging is highly cohesive (100% in wood). These results show that the combination of HMR as primer and epoxy as adhesive produces stronger bonds and desirable failures compared to other adhesive/primer systems.

In the case of phenolic resin, both HMR and RF primers do not significantly increase the strength retention upon aging. It seems like phenolic resin performs better without the use of a primer. The combination of RF and viscous phenolic resin increased the glueline thickness, which could have resulted in low strength and high adhesive failure. Low retention of shear strength of wood/phenolic/wood bond in presence of HMR primer, could be due to poor penetration of viscous phenolic resin into HMR primed wood.

The combination of HMR/RF shows high percent wood failure even though the reduction in strength due to accelerated aging is high. This suggests that HMR primer increases penetration of RF into CCA treated wood and produces high failure in wood. The percent failures in wood and the reduction in strength due to aging are similar for RF and phenolic resins. The similarity is found whether or not a primer is used. This can be attributed to the similar chemical nature of phenolic (phenol-resorcinol-formaldehyde)

and RF (resorcinol-formaldehyde) resins. The combination of RF and epoxy shows low failures in wood even though the aged shear strength of the combination seems comparable to the aged shear strength of RF and phenolic resins.

Unprimed urethane resin, even though shows less than 50% reduction in strength after aging, failed in adhesion (at the wood/urethane interface) after accelerated aging. Unprimed polyester resin also shows low shear strength and low failure in wood after aging.

As a result, unprimed urethane resin, unprimed polyester resin and the combination of RF/epoxy were eliminated from testing. For further investigation, epoxy, RF, phenolic resins and their combinations with HMR primer were tested for performance under water and saltwater conditions. This was done because water and salt water are the most likely conditions in the field. The coupons were immersed in water and 3% salt water and subjected to freeze-thaw cycling. During freeze-thaw cycling, the samples immersed in liquid were exposed to temperatures between -29^0 C and 50^0 C (see Section 4.3). The test results are presented in Tables 5.12 and 5.13.

Table 5.12: Strength of different primer/resin combinations exposed to freeze-thaw cycling in water and 3% saltwater

Primer	Adhesive	Average shear strength before aging ± Standard error (psi)	Aged shear strength ± Standard error (psi)							
			Water				3% salt water			
			5 days	15 days	25 days	A*	5 days	15 days	25 days	B*
----	Epoxy	1639 ±109	1042 ±198	905 ±18	877 ±274	46	1416 ±482	1205 ±152	1248 ±254	24
----	Phenolic	1884 ±185	1320 ±59	1221 ±100	1153 ±162	39	1358 ±118	1369 ±57	1313 ±138	30
----	RF	1359 ± 133	1255 ±232	948 ±144	878 ±200	35	1058 ±110	946 ±247	870 ±129	36
HMR	Epoxy	1934 ±158	1605 ±245	1447 ±114	1290 ±123	33	1604 ±100	1541 ±40	1473 ±379	24
HMR	Phenolic	1235 ±155	1139 ±84	805 ±129	1063 ±101	14	1203 ±201	1212 ±147	1192 ±146	3
HMR	RF	2001 ±154	1221 ±226	1089 ±218	645 ±291	68	1083 ±246	937 ±106	969 ±187	51

A* = % reduction in shear strength after 25 days of freeze-thaw cycling in water
B* = % reduction in shear strength after 25 days of freeze-thaw cycling in salt water

Table 5.13: Wood failure of different primer/resin combinations exposed to freeze-thaw cycling in water and 3% saltwater

Primer	Adhesive	Wood failure before aging (%)	Wood failure after aging (%)					
			Water			3% salt water		
			5 days	15 days	25 days	5 days	15 days	25 days
----	Epoxy	100	0	0	2	28	32	25
----	Phenolic	100	76	31	47	75	72	49
----	RF	76	48	95	57	66	87	35
HMR	Epoxy	100	89	96	92	75	93	89
HMR	Phenolic	92	92	75	37	91	63	44
HMR	RF	94	37	49	33	83	100	68

Under accelerated aging conditions (Table 5.11), wood/HMR/RF/HMR/wood coupons showed slightly greater cohesive failure compared to wood/RF/wood coupons. The effect of HMR on reduction of strength due to aging was not clear. From Table 5.12, it is seen that wood/RF bond performs slightly better with the use of HMR primer when it is exposed to freeze-thaw under water and salt water conditions.

Under accelerated aging conditions (Table 5.11), both wood/phenolic/wood coupons, and wood/HMR/phenolic/HMR/wood coupons showed high reduction in strength due to aging. From Table 5.12 it can be seen that HMR greatly improves the retention of strength of wood/phenolic bond when exposed to freeze-thaw under water and saltwater. However the shear strength of wood/HMR/phenolic/HMR/wood coupons is lower than the strength wood/HMR/phenolic/HMR/wood coupons. This suggests that in the absence of HMR, the penetration of phenolic resin is low even though the shear strength of the wood/phenolic bond is high. Considering retention to be more important

than the magnitude of shear strength, it is predicted that the wood/HMR/phenolic bond performs better than wood/phenolic bond under long-term aging.

Tables 5.11 and 5.12 show that wood/HMR/epoxy/HMR/wood performs better than the wood/epoxy/wood bond under accelerated aging conditions and also freeze-thaw cycling under water and saltwater conditions.

It can be observed from Table 5.13 that the combination of HMR and epoxy gave relatively high failure in wood.

5.6.5 Strength of Sandwich Samples

From the results of section 5.6.4, HMR/epoxy emerged as the best possible combination that produces strong and durable bonds to wood under accelerated aging conditions. HMR/phenolic and HMR/RF combinations displayed the next best performance. The next step was to select the primer/resin system that adheres well to glass fibers. To keep the experimental effort manageable, sandwich samples were prepared using HMR/epoxy and HMR/phenolic only. Also because phenolic and RF resins are similar in chemical nature, use of one of these resins was considered reasonable. Sandwich samples were prepared using the two combinations and subjected to 6-cycle accelerated aging.

Table 5.14 : Shear strength of sandwiches prepared with chosen combination(s)

Primer	Adhesive	Average shear strength before aging ± Standard error (psi)	Percent failure in wood before aging	Average shear strength after 6-cycle aging ± Standard error (psi)	Percent failure in wood after aging	Percent decrease in shear strength after aging
HMR	Epoxy	2222 ± 250	100	1325 ± 141	100	40
HMR	Epoxy	1726 ± 234	99	1240 ± 152	100	28
HMR	Phenolic	1268 ± 120	33	532 ± 62	20	58

Glass fabric with a density of 26 oz/sq.yd and corresponding (epoxy compatible or phenolic compatible, as appropriate) sizing was used in the preparation of sandwich samples. Table 5.13 shows that the wood/HMR/epoxy/glass/epoxy/HMR/wood bond retains greater strength compared to the wood/HMR/phenolic/glass/phenolic/HMR/wood bond under accelerated aging conditions. Also, the failure of the wood/HMR/epoxy/glass/epoxy/HMR/wood bond was completely in the wood (cohesive). The failure of the wood/HMR/phenolic /glass/phenolic/HMR/wood bond was partially inside the sandwiched fabric and partially at the wood/sandwich interface. This could be due to improper wetting of fabric by the viscous phenolic resin or poor bond between phenolic resin and glass fabric. The use of higher volume of resin for increased wetting would increase the glueline thickness. Longer assembly time for increased fabric wetting would build up the resin viscosity and reduce penetration of the resin into wood. Observation of fractured surfaces also showed that the thread used in stitching of the glass fabric prevented proper adhesion of the resin to glass fibers.

From sections 5.6.4 and 5.6.5, it was concluded that HMR/epoxy has the

advantages of high retention of shear strength after aging and high cohesive failure in wood compared to all other combinations. In other words, the combination of HMR as the primer and epoxy as the adhesive provides the best possible adhesion to glass fibers and CCA treated wood.

5.6.6 Chemical Reactions at Wood/Adhesive Interface

The quality of the wood/adhesive bond largely depends on the viscosity and chemical nature of the adhesive, curing conditions and the preservative treatment given to the wood. Wood cellulose and lignin are rich in CH_2OH and OH groups, which are capable of forming ether linkages and hydrogen bonds with the polar groups of the adhesives. During the treatment of wood with CCA, metallic oxides of Cr, Cu and As are produced on the wood surface. These non-polar deposits block the polar, hydrophilic bonding sites of cellulose and lignin present in wood. The bonded CCA reduces intermolecular forces of attraction between the wood surface and the adhesives. This is assumed to be the reason for poor adhesion of most of the thermosetting adhesives to CCA treated wood.

Vick [9] demonstrated that adhesives such as epoxy, phenol-resorcinol-formaldehyde and resorcinol-formaldehyde develop strong and durable bonds to CCA treated wood in the presence of HMR primer. Figure 5.3 shows the chemical linkages formed by epoxy resin and wood.

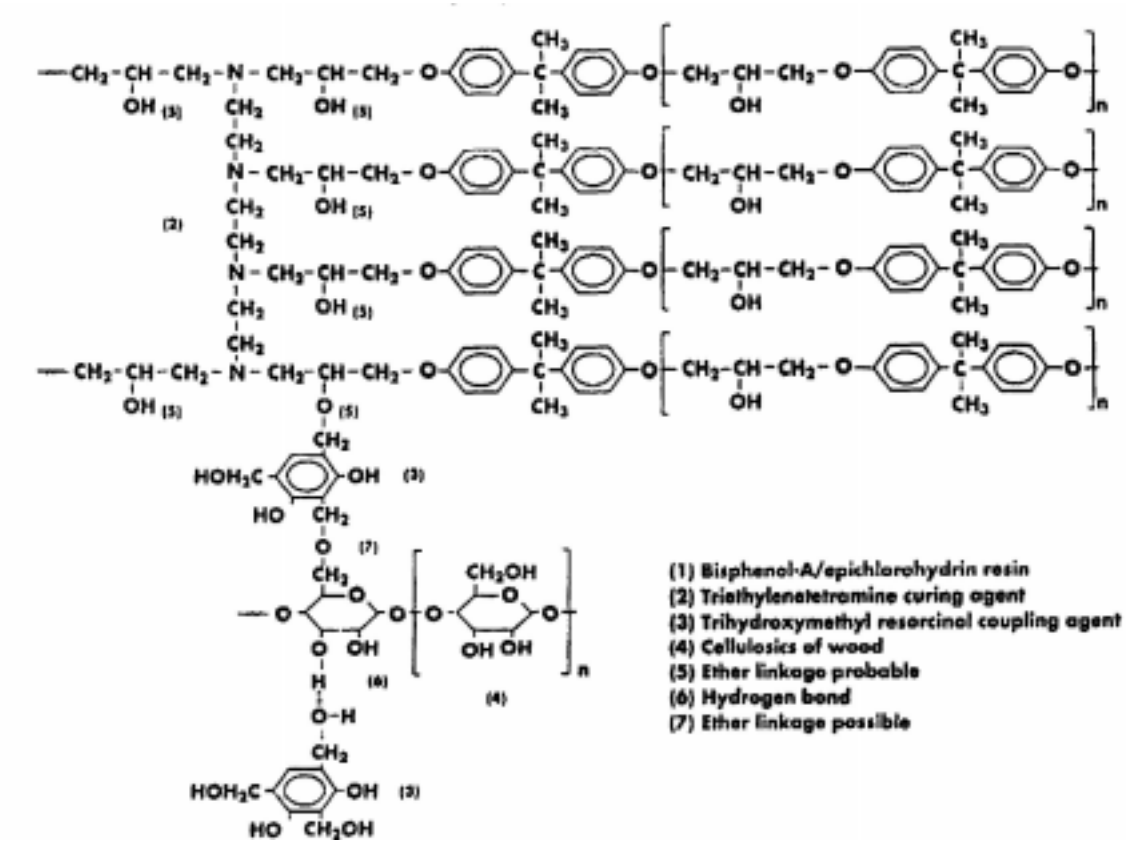

Figure 5.3: Covalent and hydrogen bonding of HMR with epoxy resin and cellulosics of wood [9]

From Figure 5.3 it can be seen that CH_2OH groups on the primer can condense with OH groups on epoxy resin and form ether linkages. CH_2OH groups on the primer can form ether linkages with CH_2OH groups and hydrogen bonds with OH groups on wood. These chemical bond forces are responsible for the high retention of shear strength of the wood/HMR/epoxy/HMR/wood specimens subjected to accelerated aging and freeze-thaw cycling.

Phenol-resorcinol-formaldehyde resin is rich in OH and CH_2OH groups and can also form similar linkages with HMR primed wood. It was observed (from Table 5.12) that the retention of shear strength of the wood/HMR/phenolic bond was higher than the

wood/phenolic bond under freeze-thaw conditions. The magnitude of strength of the wood/HMR/phenolic bond was lower than the strength of the wood/phenolic bond under freeze-thaw cycling and also accelerated aging conditions. This suggests that in the presence of HMR primer, the durability of the wood/phenolic bond is increased (moisture resistance is increased) but the strength is reduced. This could be related to the pH of HMR primed wood and the hydrophilic nature of the wood/adhesive interface.

Resorcinol-formaldehyde resin can also form ether linkages and hydrogen bonds with HMR. Though the shear strength of the wood/RF bond increased (Tables 5.11 and 5.12) with the use of HMR primer, the retention of strength did not increase. This suggests that HMR increases the strength but not the durability of wood/RF bond.

5.6.7 Performance of Chosen Combination under 6-cycle Accelerated Aging

Due to the high retention of shear strength after accelerated aging, high failure in wood and relatively high values of aged shear strength, HMR/epoxy was chosen as the primer/resin combination that would be used for composite wrapping of wood posts. To study the bond performance with progressive aging, sandwich samples prepared using HMR/epoxy combination were tested after each cycle of the 6-cycle accelerated aging.

Table 5.15: Performance of wood/HMR/epoxy/glass/epoxy/HMR/wood sandwich samples exposed to 6-cycle aging

Primer	Adhesive	Unaged shear strength ± Standard error (psi)	Aged shear strength ± Standard error (psi)					
			cycle 1	cycle 2	cycle 3	cycle 4	cycle 5	cycle 6
HMR	Epoxy	2570 ± 304	1717 ± 197	1607 ± 234	1659 ± 80	1596 ± 188	1375 ± 85	1497 ± 70
Wood failure (%)		97	97	92	96	85	93	91
Reduction in strength due to aging (%)		-----	33	38	35	38	46	42

The decrease in strength of sandwich shear samples was found to be maximum after the first cycle in the 6-cycle aging process. The strength decreased gradually from cycle 2 to cycle 5 and increased between cycle 5 and cycle 6. The increase in strength between cycle 5 and cycle 6 may be considered as erroneous data. Due to the 6-cycle accelerated aging, there was about 45% reduction in shear strength of the wood/HMR/epoxy/glass/epoxy/HMR/wood specimens. Since the 6-cycle aging simulates about 20 years of natural aging, this means that after a service life of approximately 20 years in the field, the strength of the wood/HMR/epoxy/glass bond would be half of the original strength. Flexural tests of wrapped dowels (representing a scaled down version of the guard-rail posts) reveal the change in mechanical properties due to aging. These data are presented in chapter VI.

5.6.8 Performance of Chosen Combination under Chemical Aging

The 6-cycle accelerated aging was used to predict durability. Freeze-thaw cycling in chemical solutions was conducted to observe the effect of different high and low temperature liquid media on the wood/HMR/epoxy interface and the wood/HMR/epoxy/glass interface(s). Shear coupons (sandwich and non-sandwich) prepared using HMR/epoxy combination were subjected to freeze thaw cycles in water, salt water, acidic and alkaline solutions.

Table 5.16: Shear strength of wood/HMR/epoxy/glass/epoxy/HMR/wood sandwiches exposed to different conditions

Medium	Shear strength after 5 days of aging ± Standard error (psi)	A*	Shear strength after 15 days of aging ± Standard error (psi)	B*	Shear strength after 25 days of aging ± Standard error (psi)	C*	% reduction in strength after 25 days of aging
Unaged	2222 ± 250 (100 %)						-----
Accelerated aging	1325 ± 141 (100 %)						40
pH 3	1497 ± 337	100	-----	-----	990 ± 355	100	55
pH 13	878 ± 54	100	-----	-----	654 ± 132	100	70
pH 7	1442 ± 363	100	1422 ± 319	97	1008 ± 197	100	55
3% salt water	1367 ± 232	100	1130 ± 188	100	867 ± 98	97	61

A* = % wood failure after 5 days of aging
B* = % wood failure after 15 days of aging
C* = % wood failure after 25 days of aging

Table 5.17: Shear strength of wood/HMR/epoxy/HMR/wood samples exposed to different conditions

Medium	Shear strength after 5 days of aging ± Standard error (psi)	A*	Shear strength after 15 days of aging ± Standard error (psi)	B*	Shear strength after 25 days of aging ± Standard error (psi)	C*	% reduction in strength after 25 days of aging
Unaged	1934 ± 158 (100 %)						-----
Accelerated aging	1356 ± 137 (100 %)						30
pH 3	1719 ± 199	100	1532 ± 105	100	1265 ± 304	100	34
pH 13	1107 ± 150	100	881 ± 80	100	791 ± 26	77	59
pH 7	1605 ± 245	89	1447 ± 114	96	1290 ± 123	92	33
3% salt water	1604 ± 100	75	1541 ± 40	93	1473 ± 379	89	24

Data of Tables 5.16 and 5.17 reveal the damage caused to the wood/HMR/epoxy/glass fabric bond is greater than the damage caused to the wood/HMR/epoxy bond in all aging media. This is due to the degradation of both the wood/adhesive interface and the adhesive/glass interface in the wood/HMR/epoxy/glass/epoxy/HMR/wood specimens. Based on the average shear strength value after aging, it is found that the degradation of the wood/HMR/epoxy bond strength is similar in acidic and neutral media. However, based on the standard error and wood failure values, the acidic medium seems slightly more damaging than neutral medium. The degradation was maximum in alkaline medium of pH 13. Degradation of

the wood/HMR/epoxy/glass fabric bond strength is also similar in acidic and neutral media. Maximum degradation of the wood/HMR/epoxy/glass fabric bond was in alkaline medium of pH 13 followed by salt water. Under accelerated aging conditions (from Tables 5.11 through 5.16), it is observed that the strength of the wood/HMR/epoxy/glass bond reduced by 28 - 42% while the strength of wood reduced by 34%. However, the strength of the wood/HMR/epoxy bond reduced only by 30%, suggesting that the wood/HMR/epoxy bond is at least as strong as wood itself and the wood/HMR/epoxy/glass bond is almost as strong as wood. Also the wood failure of wood/HMR/epoxy/glass/epoxy/HMR/wood samples due to freeze-thaw cycling in all aging media was 97-100% (Table 5.16). This suggests that wood is damaged more than the wood/HMR/epoxy/glass fabric bond in all the aging media. However, the wood failure of wood/HMR/epoxy/HMR/wood samples (Table 5.17) show that alkaline medium and salt water damage the wood/HMR/epoxy bond.

Lhymn and Schultz [14] studied the stress corrosion of glass/PET composites under acidic, alkaline and salt water conditions. They concluded that acids (10% HNO_3, 10% HCl, 10% H_2SO_4) attack glass fibers the most and alkali (10% NaOH) attacks the matrix the most. Maximum damage to the composite was caused by alkali (10% NaOH) and the least damage was caused by 10% NaCl solution.

Kajorncheappunngam [20] studied the aging effects of epoxy resin and glass/epoxy composites in acidic, alkaline, water and salt water media. She found that at high temperatures, minimum damage to the composite was caused by salt water and maximum damage was caused by alkaline medium. From SEM observation of aged samples she proposed that the alkaline medium primarily damages the epoxy matrix and

glass/epoxy interface.

Based on the experimental results and literature survey, the following conclusions are drawn:

In freeze-thaw cycling, samples are exposed to high temperature liquid (50 ^{0}C) and low temperature liquid (-29 ^{0}C). At low temperature, all the absorbed solutions expand and damage the wood and probably the glass/epoxy interface. The effect of all solutions is assumed to be similar during freezing. At high temperature, the damage effects are increased due to increased liquid diffusion into the specimen. The alkaline medium attacks the epoxy matrix, the wood, the wood/HMR/epoxy bond and also damages the glass/epoxy interface, producing maximum degradation of the wood/HMR/epoxy/glass/epoxy/HMR/wood specimens. H^+ions from water and acid attack the glass fiber surface and undergo ion exchange reaction with the OH groups on the glass fibers and primarily damage the glass/epoxy interface. Water also plasticizes the epoxy matrix and damages the wood/HMR/epoxy interface. Salt water damages the wood/HMR/epoxy interface.

5.7 Summary

Screening of six resins and three primers showed that the combination of HMR primer and epoxy adhesive provides the best possible adhesion to glass fibers and CCA treated wood. Under accelerated aging conditions, the wood/HMR/epoxy bond is at least as strong as wood and the wood/HMR/epoxy/glass bond is almost as strong as wood. Chemical aging showed that in acid medium, wood, glass fibers and the epoxy/glass interface are primarily damaged. In alkaline medium, the epoxy matrix, the wood, the

wood/HMR/epoxy bond and the epoxy/glass interface are damaged. In salt water, the wood/HMR/epoxy interface is damaged the most. Water damages the wood/HMR/epoxy bond, the glass fibers and the epoxy/glass interface. Maximum damage to the wood/HMR/epoxy/glass/epoxy/HMR/wood sandwich samples and the wood/HMR/epoxy/HMR/wood samples is caused by alkaline medium.

Chapter VI

STRENGTH AND STIFFNESS EVALUATION OF WRAPPED POSTS

6.1 Overview

The values of the ultimate flexural strength and modulus of a wrapped post are essential to properly establish the dynamic response of the proposed GFW guard-rail post. HMR primed wood posts wrapped with epoxy impregnated glass fabric were evaluated using flexure tests. This chapter presents the details of materials employed, sample preparation, test procedure and data analysis.

6.2 Materials Used

A CCA treated southern pine dowel of diameter 0.5″ was used as the core in the preparation of test specimens. The surface of the dowel was primed with HMR, 24 hours prior to wrapping the core with glass fabric. A woven fabric ($0^0/45^0$), employing E-glass fibers with epoxy compatible sizing was used for wrapping. The fabric was supplied by Johnston Industries and had a density of 12oz/sq.yd. Epoxy (TYFO-S) supplied by Hexcel Fyfe (now Fyfe Co) was used as the adhesive.

6.3 Sample Preparation

The set up for wrapping the posts consisted of a banding machine, glass fabric ribbon (2.5″ wide) supported on a stand and a resin bath with a fiber guide. A primed wooden dowel of diameter 0.5″ was mounted on the machine between the jaws, one of which is fixed and the other adjustable. The fabric ribbon passing through the resin bath

was wrapped on the dowel by rotating the dowel at constant speed. Figure 6.1 shows the set up for wrapping the CCA treated dowel rods.

Figure 6.1: Glass fiber wrapping of a wood post using banding machine

The wrapped dowel was mounted on a drying set up that consisted of two rotating circular discs connected to a motor. The discs were provided with adjustable screws to hold the sample. The mounted sample was rotated on this set up to prevent dripping of resin and promote uniform curing. After curing, the wrapped dowel was cut to the required length using a band saw. The finished sample was 7.5″ long. The average thickness of the GFRP wrap around the dowel was 0.0475″. The fiber volume fraction in

the composite wrap was approximately 26% (Appendix A.1). These wrapped specimens are also referred to as wood/HMR/epoxy/glass hybrids later in the chapter. A schematic of the wrapped sample is shown in the following figure:

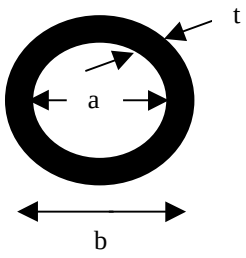

a = diameter of the inner wood core = 0.5″
b = average diameter of the wrapped wood sample = 0.595″
t = average thickness of FRP wrap around the wood core = 0.0475″

Figure 6.2: Schematic of the cross-section of a wrapped sample

6.4 Description of Test Procedure

ASTM D-790 is a standard test method used for evaluating flexural properties of high modulus composites that are in the form of sheets, plates or molded shapes. The standard is applicable to all rigid and semi-rigid materials. This standard is applicable only when the test specimen fails in the outer fibers. The standard describes two test methods, a three-point loading system and a four-point loading system. The test reveals the flexural strength and strain at failure of the composite.

To suit the small dimensions of test specimens, the three-point loading system was used for laboratory testing. All test specimens failed in the outer fibers which justified the use of the three-point loading system.

The following are the outlines of the three-point loading method of ASTM D-790:

(1) The apparatus should be properly calibrated and should be operated at constant speed of cross-head motion.

(2) The loading noses and supports should have cylindrical surfaces. To avoid stress concentration under the loading noses, the radius of the supports should be atleast 3.2mm (0.125 in) for all specimens.

(3) The specimens may be cut from sheets, plates, molded shapes or may be molded to the desired final dimensions.

(4) The width and depth of the untested specimen are measured to the nearest 0.001in. The support span-to-depth ratio is chosen such that failures occur in the outer fibers of the specimen. The machine is set to the corresponding rate of cross-head motion.

(5) The loading nose and supports are aligned so that the axes of the cylindrical surfaces are parallel and the loading nose is midway between the supports. The load is applied at the specified cross-head rate and load-deflection data are simultaneously recorded.

(6) The flexural strength and maximum strain at failure are calculated.

Complete details of the testing method are given in “The 1995 Book of ASTM Standards,” Vol. 8.01 [21].

In the current experimental work, an Instron machine (model 4411), with a capacity of 1000lbs, was used for testing. In order to represent the proposed posts, wrapped dowels were tested instead of wrapped bars. Modifications were incorporated in the calculations to account for the circular cross-section of the specimens. The length of the specimens was 7.5″ and their average outer diameter was 0.595″. Thickness of wrap was approximately 0.0475″. The support span-to-depth ratio was approximately 10:1. The rate of cross-head motion was 0.16″/min. Figure 6.2 shows the flexural loading of a GFRP wrapped specimen.

Figure 6.3: Three-point flexural loading of a wrapped specimen

6.5 Sample Conditioning

Wrapped specimens were subjected to the following conditions before testing:

(1) exposure to 6-cycle accelerated aging (described in section 4.2).

(2) exposure to freeze thaw cycles in acidic solution of pH 3.0 for 5 days, 15 days and 25 days in the atmospheric chamber (described in Chapter IV, section 4.3)

(3) exposure to freeze thaw cycles in alkaline solution of pH 13.0 for 5 days, 15 days and 25 days in the atmospheric chamber

(4) exposure to freeze thaw cycles in solution of pH 7.0 for 5 days, 15 days and 25 days in the atmospheric chamber

(5) exposure to freeze thaw cycles in 3% salt water for 5 days, 15 days and 25 days in the atmospheric chamber

6.6 Summary of Test Results

6.6.1 Accelerated Aging

The primary objective of wrapping was to improve the mechanical properties and durability of wood. To demonstrate the effectiveness of wrapping, wood and wood/HMR/epoxy/glass hybrid specimens were subjected to 6-cycle accelerated aging. As explained earlier (section 4.2), 6-cycle accelerated aging simulates approximately 20 years of natural aging conditions. The samples were tested after each cycle to observe the rate of degradation or improvement in mechanical properties with increase in the number of aging cycles. The samples were dried at room temperature for about 10 days before they were tested. Wood/epoxy/glass hybrid specimens were also tested to observe the effectiveness of HMR in improving the bond between the wood and the GFRP wrap. The test results are presented in Table 6.1. Graphical representation of these results is given in Figures 6.4 and 6.5. A set of sample calculations of flexural strength and modulus are given in Appendix B.2.

Table 6.1: Comparison of strength and modulus of wood, wood/epoxy/glass hybrid and wood/HMR/epoxy/glass hybrid specimen exposed to 6-cycle accelerated aging

Property	specimen	unaged	cycle 1	cycle 2	cycle 3	cycle 4	cycle 6
Ultimate flexural strength, σ (psi)X10^6	Wood	0.0163	0.0180	0.0201	0.0189	0.0210	0.0196
	Wood/epoxy/glass hybrid	0.0205	0.0087	0.0088	0.0092	0.0075	0.0098
	Wood/HMR/epoxy/glass hybrid	0.0169	0.0131	0.0171	0.0168	0.0133	0.0114
Flexural modulus, E (psi)X10^6	Wood	1.09	1.13	1.38	1.60	1.39	1.26
	Wood/epoxy/glass hybrid	1.79	0.72	0.89	0.72	0.52	0.69
	Wood/HMR/epoxy/glass hybrid	1.13	0.90	1.12	1.08	0.96	0.97
Flexural Rigidity, EI (lb-in^2) X 10^3	Wood	3.35	3.48	4.23	4.13	4.27	3.87
	Wood/epoxy/glass hybrid	11.47	5.98	5.46	4.01	3.35	5.38
	Wood/HMR/epoxy/glass hybrid	8.78	6.99	10.71	7.24	8.59	6.86

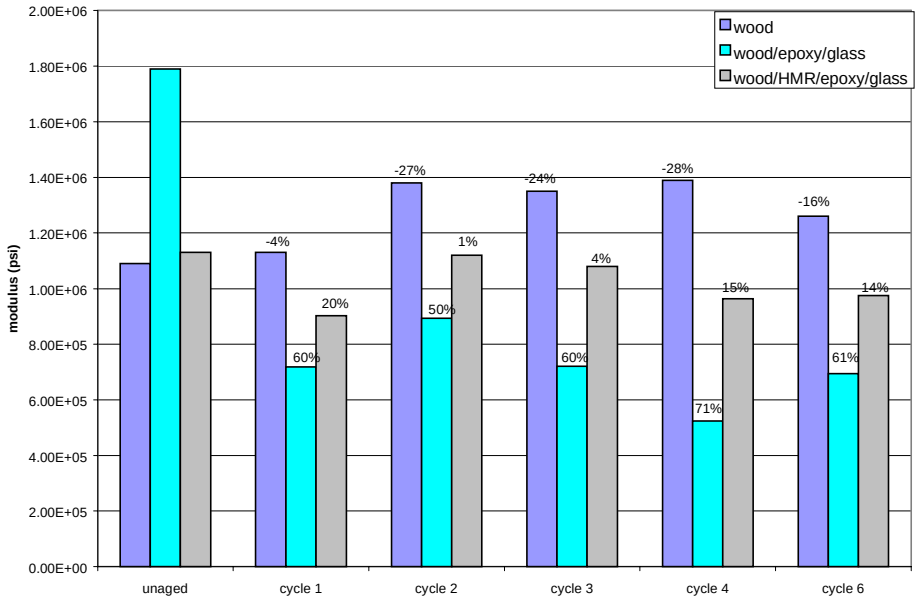

Figure 6.4: Comparison of elastic modulus (in bending) of wood, hybrid specimen after each cycle of 6-cycle aging
(% value indicates the % change in modulus compared to the unaged value. A +'ve sign indicates decrease in modulus, a –'ve sign indicates an increase in modulus)

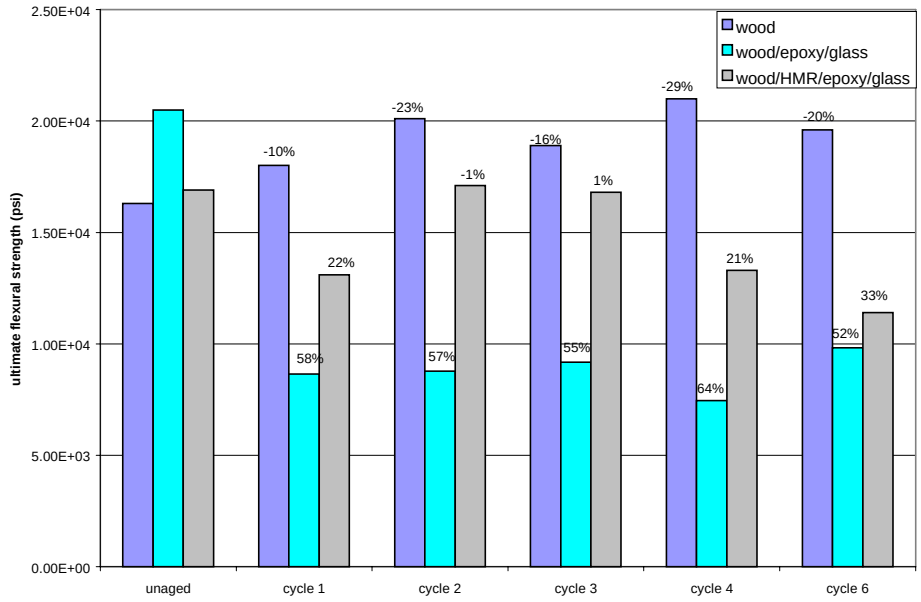

Figure 6.5: Comparison of flexural strength of wood, hybrid specimen after each cycle of 6-cycle aging
(% value indicates the % change in strength compared to the unaged value. A +'ve sign indicates decrease in strength, a –'ve sign indicates an increase in strength)

From Figures 6.4 and 6.5, it can be seen that the flexural strength and modulus of wood/epoxy/glass hybrid have decreased gradually due to the 6-cycle aging. The increase in strength and modulus between cycle 1 and cycle 2, cycle 3 and cycle 4 can be attributed to changes in moisture content, curing of epoxy resin and (or) imperfections in sample preparation. In the case of a wood/HMR/epoxy/glass specimen, the mechanical properties decreased after cycle 1 and increased to a maximum after cycle 2. The properties after cycle 2 decreased gradually. This suggests that the curing of epoxy resin in the wood/HMR/epoxy/glass specimen is nearly complete in the vicinity of cycle 2. The amount of decrease in both strength and modulus of the wood/epoxy/glass hybrid samples is greater than the decrease in the wood/HMR/epoxy/glass hybrid samples. Therefore it is concluded that priming with HMR increases the strength, modulus and retention of the wood/epoxy/glass hybrid specimens under accelerated aging conditions.

Composite wrapping of wood slightly increases the strength and modulus of the wood under unaged conditions. With the progress of aging, the mechanical properties of the wrapped hybrid decrease. An important observation from the data is that the strength and modulus of the wood increased with the progress of 6-cycle aging. The strength and modulus values of the wood are higher than those of the wrapped hybrid at the end of 6-cycle aging. All of these findings suggest that the properties of wood have not improved significantly by wrapping. However, Talakanti [22] showed that under a maximum applied strain of 4500 microstrains, after 2 million fatigue cycles, a GFRP wrapped wood specimen retains about 60% stiffness while an unwrapped wood specimen fails at 0.5 million cycles. Work currently in progress, being done by researchers at the Constructed Facilities Center (Chamarthy [23] and Laosiriphong [24]) also showed that the GFRP

wrapping increases the properties of wood upto 100%. We speculate that the unusually low values of wrapped wood compared to unwrapped wood after 6-cycle aging are due to variation of moisture content of wood in the wrapped hybrid and unwrapped wood samples.

Observation of the failed wrapped specimens under three point bending showed that the failure was entirely in the outer fibers. The samples were sliced at the region of failure and at other regions along the length of the sample. Observation of the cross-section showed that there was no delamination at the wood/FRP interface. Visual examination of the wood samples showed clearly visible longitudinal cracks in the aged wood even before testing. Most of the cracks were along the length of the samples. These cracks began to appear from cycle 3 onwards. It is therefore concluded that the cracks produced during aging from the drying of wood, result in an increase in the mechanical properties of the wood.

The wood for the sample preparation was stored at room temperature. The unwrapped wood samples were prepared about four months after the preparation of wrapped samples. Therefore it is very likely that the moisture content of wood in the wrapped samples is higher than the unwrapped ones even though they were prepared from the same log of wood. The strength of the wood varies with the moisture content of the wood. At very low moisture content (6 to10%), the strength begins to decrease. The strength is maximum at about 12% moisture content and begins to decrease gradually when the moisture content increases beyond the equilibrium level (18%).

It is therefore assumed that in the unaged wood samples, the moisture content was very low (10%) resulting in the low strength and modulus values compared to the values

in the literature [5]. During 6-cycle aging, the moisture content in the wood could have reached the 12%, which could have increased the strength and modulus. Such increases in mechanical properties due to changes in moisture content could have dominated the decrease in properties during 6-cycle aging. In short, the increases in strength and modulus of wood are due to a combination of the aging effect and the percent moisture fluctuation.

For a better understanding of the aging of wood and wood composites, flexural rigidity (EI) of the test samples was compared. Figure 6.6 shows the variation of rigidity of wood and wrapped hybrid specimens during 6-cycle aging.

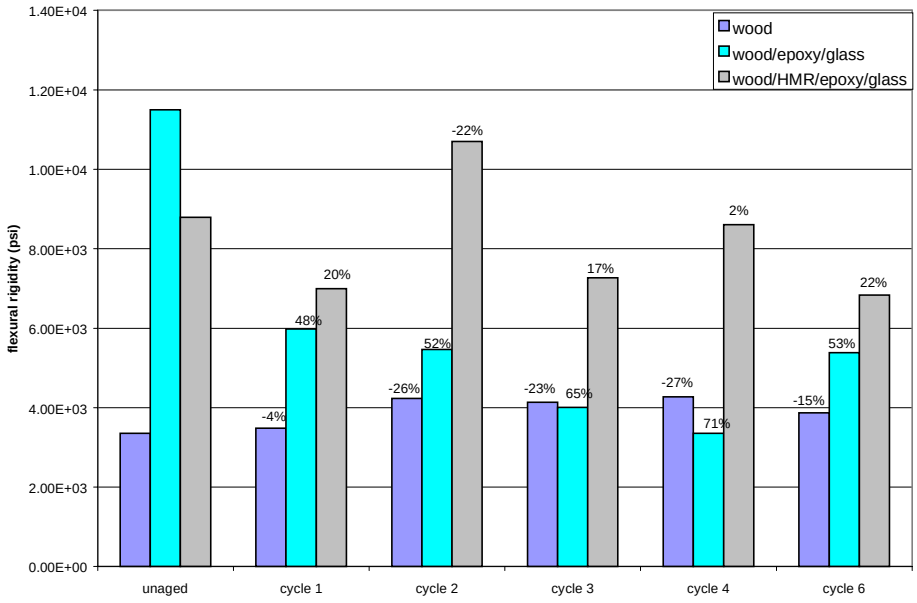

Figure 6.6: Comparison of flexural rigidity of wood, hybrid specimen after each cycle of 6-cycle aging (% value indicates the % change in flexural rigidity compared to the unaged value. A +'ve sign indicates decrease in rigidity, a –'ve sign indicates an increase in rigidity)

The following observations were made from Figure 6.6:

The rigidity of wood has increased due to composite wrapping under both unaged and 6-cycle aged conditions. The increase in rigidity due to wrapping with HMR/epoxy/glass is higher than the increase due to wrapping with epoxy/glass. From Table 6.1, the ratio of EI_{hybrid} to EI_{wood} under unaged and 6-cycle aged conditions was calculated. It was found that in the present situation, i.e. for 25% fiber volume fraction in the GFRP wrap and 0.0475″ thick wrap around a 0.5″ wood core, wrapping of wood with the HMR/epoxy/glass system improves the flexural rigidity by 2.62 times under unaged conditions and 1.77 times under 6-cycle aged conditions (from Table 6.1).

6.6.2 Prediction of Flexural Rigidity using Rule of Mixtures

Assuming a perfect bond between epoxy resin and glass fibers, wood/FRP wrap, the properties of a wood/epoxy/glass specimen can be estimated using the following rule of mixtures:

$$(EI)_{hybrid} = (EI)_{wood} + (EI)_{wrap}$$

$$= E_{wood} [I_{wood} + (E_{wrap}/E_{wood}) I_{wrap}]$$

Using this formula, the properties of a hybrid wood/epoxy/glass specimen consisting of a 0.5″ diameter wood core and a 0.0475″ epoxy/glass fiber wrap can be estimated.

Under unaged conditions,

E_{wood} = 1.31 X 10^6 psi from reference [3]

The value for a specimen as small as 0.5″ in diameter would be in the range of

2.0 X 10^6 psi to 2.4 X 10^6 psi

$E_{wrap} = E_f v_f + (1-v_f) E_m$

where v_f = fiber volume fraction

= 0.25 (for 25% volume fraction)

E_f = elastic modulus of glass fibers under unaged conditions

= 10.5 X 10^6 psi

E_m= elastic modulus of epoxy resin under accelerated aging conditions

= 0.45 X 10^6 psi

$G = E/ 2(1+ \nu)$ where G = shear modulus and ν is Poisson's ratio

G_f = 4.18 X 10^6 psi

$\nu_f = 0.26$

G_m = 0.16 X 10^6 psi

$\nu_f = 0.38$

from micro mechanics approach [25] E_{wrap} = 1.92 X 10^6 psi

$E_{wrap}/E_{wood} = 0.96$

$I_{wood} = (\pi r^4/4) = 0.0031$ in^4

$I_{wrap} = \pi[(r+t)^4 - r^4]/4 = 3.049$ X 10^{-3} in^4

Therefore

$(EI)_{hybrid}$ = 2.0 X 10^6 [0.0031 + 0.96(3.049 X 10^{-3})]

= 12.05 X 10^3 lb-in^2

Under aged conditions,

E_{wood} = 0.87 (2.0 X 10^6 psi) (assuming a 13% decrease in properties of wood as found

from DMA of 6-cycle aged wood)

$= 1.74 \times 10^6$ psi

Assuming a maximum of 10% decrease in the properties of glass fibers due to aging,

$E_f = 0.9 (10.5 \times 10^6)$ psi

$= 9.45 \times 10^6$ psi

$G_f = 0.9 (4.18 \times 10^6)$ psi

$= 3.76 \times 10^6$psi

$\nu_f = 0.26$

Kajorncheappunngam [20] plotted the master curve of epoxy resin aged in water at room temperature for 5 months under no sustained stress. Using those master curves, the properties of epoxy resin at a service life of 20 years for unaged and water aged specimen were compared. A 11% decrease in the storage modulus was observed due to aging in water at room temperature for 5 months. Assuming a 11% decrease in the properties of epoxy resin under 6-cycle aged conditions,

$E_m = 0.89 (0.45 \times 10^6)$ psi

$= 0.4 \times 10^6$ psi

$G_m = 0.89 (0.16 \times 10^6)$psi

$= 0.14 \times 10^6$ psi

$\nu_f = 0.38$

from the micro mechanics approach, [25]

$E_{wrap} = 1.73 \times 10^6$ psi

$E_{wrap}/E_{wood} = 0.865$

$I_{wood} = (\pi r^4/4) = 0.0031$ in^4 (assuming no variation in sample dimensions due to aging)

$I_{wrap} = \pi[(r+t)^4 - r^4]/4 = 3.049 \text{ X } 10^{-3}$ in^4 (assuming no variation in dimensions of the sample due to aging)

Therefore

$$(EI)_{hybrid} = 2.0 \text{ X } 10^6 [0.0031 + 0.865(3.049 \text{ X } 10^{-3})]$$

$$= 11.47 \text{ X } 10^3 \text{ lb-in}^2$$

Table 6.2: Comparison of flexural rigidity of unaged and aged wood/epoxy/glass hybrid obtained using rule of mixtures and from experiments at different values of E_{wood}

E_{wood}	$unaged_{rom}$	$aged_{rom}$	A*	$unaged_{expt}$	$aged_{expt}$	B*
$2.0 \text{ X } 10^6$	$12.05 \text{ X } 10^3$	$11.47 \text{ X } 10^3$	4.8%	$11.47\text{X } 10^3$	$5.37 \text{ X } 10^3$	53%
$2.2 \text{ X } 10^6$	$12.65 \text{ X } 10^3$	$12.12 \text{ X } 10^3$	4.2%	$11.47\text{X } 10^3$	$5.37 \text{ X } 10^3$	53%
$2.4 \text{ X } 10^6$	$13.29 \text{ X } 10^3$	$12.71 \text{ X } 10^3$	4.4%	$11.47\text{X } 10^3$	$5.37 \text{ X } 10^3$	53%

rom = value calculated using rule of mixtures
expt = experimental value
A* = percent decrease in value calculated using rule of mixtures
B* = percent decrease in value obtained from experiments

The values obtained from rule of mixtures for wood/epoxy/glass can be compared with wood/HMR/epoxy/glass to observe the effect of HMR primer in bringing the rigidity of the specimen closer to the values obtained using rule of mixtures. This is based on the assumption that according to rule of mixtures, the rigidity of wood/epoxy/glass is the same as the rigidity of wood/HMR/epoxy/glass hybrid specimens.

Table 6.3: Comparison of flexural rigidity of unaged and aged wood/HMR/epoxy/glass hybrid obtained using rule of mixtures and from experiments at different values of E_{wood}

E_{wood} (psi)	$(EI)unaged_{rom}$ ($lb\text{-}in^2$)	$(EI)aged_{rom}$	A*	$(EI)unaged_{expt}$	$(EI)aged_{expt}$	B*
2.0×10^6	12.05×10^3	11.47×10^3	4.8%	8.78×10^3	6.86×10^3	22%
2.2×10^6	12.65×10^3	12.12×10^3	4.2%	8.78×10^3	6.86×10^3	22%
2.4×10^6	13.29×10^3	12.71×10^3	4.4%	8.78×10^3	6.86×10^3	22%

From Tables 6.2 and 6.3 it is observed that the rigidity of a wood/FRP specimen decreases by 53% compared to a 4-5% decrease under perfect bonding conditions. With the use of HMR primer, the amount of decrease in rigidity is reduced from 53% to 22%. It is also observed that due to the presence of HMR primer, the performance of the wood/epoxy/glass specimen before aging is lowered. This suggests that epoxy resin bonds very well to wood but the bonds are not strong enough to withstand moisture penetration. We suspect that HMR primer reduces the affinity of the wood surface to the epoxy resin and thereby reduces the rigidity under unaged conditions. In other words, HMR primer chemically bonds to the wood surface and leaves fewer sites on wood for the epoxy resin to form bonds. Therefore, epoxy resin forms bonds mainly with HMR primer on wood. Under aged conditions, the coupling action of HMR provides moisture resistance to the wood/HMR/epoxy interface. It is concluded that the major effect of HMR primer is to improve the moisture resistance of wood/epoxy interface.

In the computation of the theoretical values of rigidity after aging, only the effect of degradation of epoxy matrix and glass fibers was considered. The effect of bond degradation at the wood/FRP interface was not included. This could be a major reason for the difference between the percent decrease in rigidity of the theoretical (4-5%) and

experimental (53% and 22%) values. If one accounts for the degradation of structural compositeness at the wood/FRP interface, the experimental values of rigidity could be much closer to the theoretical values.

6.6.3 Chemical Aging

To study the effect of different aging media, wood/HMR/epoxy/glass hybrid specimens, representing a scaled down version of the proposed GFW guard-rail posts were subjected to chemical aging. The hybrid specimens were immersed in water, salt water, acidic and alkaline media and subjected to freeze-thaw cycling. The samples were dried at room temperature for about 30 days before they were tested. Tables 6.4 through 6.6 show the performance of wood/HMR/epoxy/glass hybrid in different media.

Table 6.4: Flexural strength of wood/HMR/epoxy/glass hybrid exposed to freeze-thaw cycling in different solutions

Aging medium	Ultimate flexural strength (psi) X 10^6			A*
	After 5 days of aging	after 15 days of aging	after 25 days of aging	
Unaged	0.0169			
Acidic solution of pH 3	0.0155	0.0103	0.0096	43
Alkaline solution of pH 13	0.0172	0.0143	0.0116	31
Water	0.0133	0.0088	0.0115	32
3% salt water	0.0164	0.0143	0.0128	24

A* = percent reduction in strength after 25 days of aging

Table 6.5: Flexural modulus of wood/HMR/epoxy/glass hybrid exposed to freeze-thaw cycling in different solutions

Aging medium	Flexural modulus (psi) X 10^6			B*
	after 5 days of aging	after 15 days of aging	after 25 days of aging	
Unaged	1.13			
Acidic solution of pH 3	1.08	0.89	0.78	31
Alkaline solution of pH 13	1.18	0.89	0.89	21
Water	0.69	0.52	0.88	22
3% salt water	1.08	1.03	0.92	18

B* = percent reduction in modulus after 25 days of aging (%)

Table 6.6: Flexural rigidity of wood/HMR/epoxy/glass hybrid exposed to freeze-thaw cycling in different solutions

Aging medium	Flexural rigidity (psi) X 10^3			C*
	after 5 days of aging	After 15 days of aging	after 25 days of aging	
Unaged	8.79			
Acidic solution of pH 3	7.66	5.97	5.49	38
Alkaline solution of pH 13	8.16	5.99	6.24	29
Water	4.77	3.58	5.90	33
3% salt water	7.88	7.44	6.19	30

C* = percent reduction in rigidity after 25 days of aging (%)

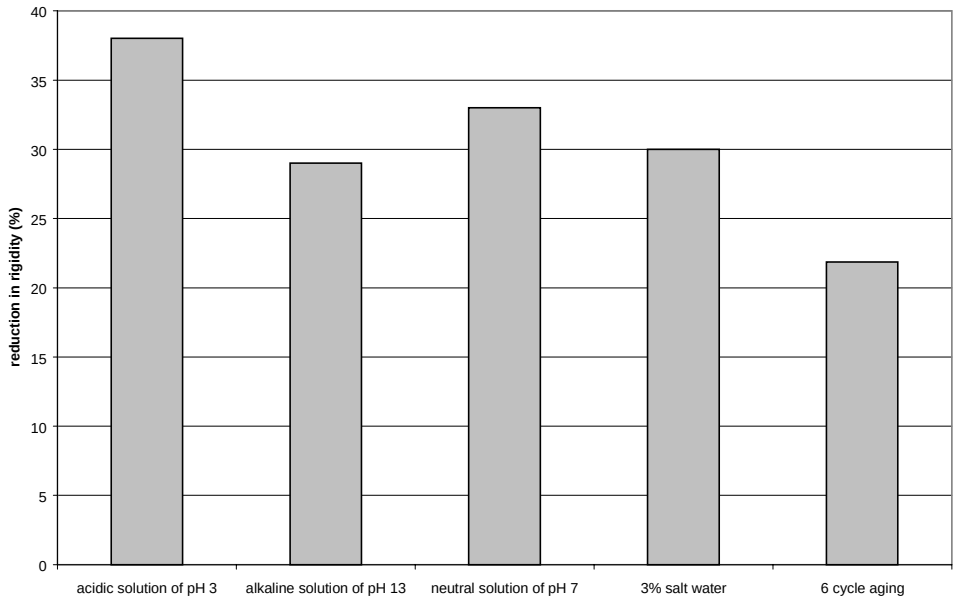

Figure 6.7: Variation of flexural rigidity of wood/HMR/epoxy/glass hybrid exposed to freeze-thaw cycling in different media for 25 days

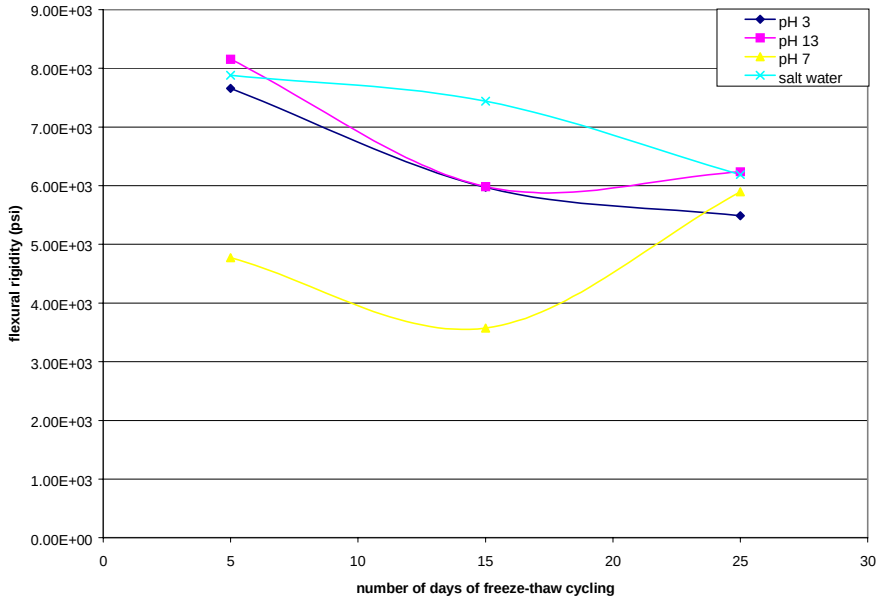

Figure 6.8: Variation of flexural rigidity of wood/HMR/epoxy/glass hybrid with time in different media

From Tables 6.4 through 6.6 and Figures 6.7 and 6.8, it can be observed that in acidic medium, flexural strength of the hybrid decreased rapidly by 39% after 15 days of aging; this value increased to 43% after 25 days of aging. Elastic modulus (in bending) and rigidity under acidic medium decreased gradually by 31% and 38% respectively after 25 days of aging. The decrease in flexural strength, modulus and rigidity, under acidic medium is maximum compared to the decrease in other aging media. From shear tests of sandwich samples (Table 5.16), a 55% decrease in wood/FRP bond strength was observed in acidic medium compared to a maximum of 70% decrease in alkaline medium of pH 13. The failure of sandwich samples in acidic medium was completely in the wood. This suggests that the wood/FRP interface is not damaged in acidic medium. Kajorncheappunngam [20] found that the Tg (glass transition temperature) of epoxy aged in 10M HCl solution for 1 month at room temperature increased from 76^0 C to 120^0 C. This increase in Tg was attributed to the progress of the curing reaction of the epoxy matrix. This suggests that the maximum decrease in mechanical properties of the wood/HMR/epoxy/glass hybrid in acidic medium could be due to the following reasons:

H^+ ions in acid form hydrogen bonds with OH groups of epoxy resin and increase the Tg of the matrix. The high temperature acid solution during freeze-thaw also aids curing of the epoxy matrix and increases the Tg. The decrease in modulus despite the increase in Tg suggests that acid causes irreversible damage to the hybrid. The low temperature acid solution causes expansion of absorbed liquid in the sample. This produces stresses at the epoxy/glass interface and also at the wood/HMR/epoxy interface. Protons in the diffused acid damage the glass fibers and the epoxy/glass interface by reacting with OH groups on the glass fibers. In short, acid diffuses through the epoxy

matrix and primarily damages the glass fibers and glass/epoxy interface.

In alkaline medium, the flexural strength decreased gradually with increase in aging cycles. The modulus again reduced initially and then did not change between 15 days and 25 days of aging. The rigidity also reduced initially and slightly increased between 15 days and 25 days of aging, suggesting that the modulus and rigidity did not change much between 15 days and 25 days of aging. Shear tests of sandwich samples (Table 5.16) show maximum decrease of 70% in the wood/FRP bond strength. Also, the wood failure of wood/HMR/epoxy/HMR/wood samples was 77%. This suggests that alkaline medium primarily damages the epoxy resin and the wood.HMR/epoxy bond. Kajorncheappunngam [20] found that in alkaline medium, the properties of the epoxy/glass interface are reduced due to damage of the epoxy matrix and also the epoxy/glass interface.

It is thought that alkali diffuses through the epoxy matrix and facilitates the curing of epoxy matrix. The Tg and modulus increase due to curing. The alkali further diffuses through the matrix and damages the HMR/epoxy interface. At longer aging periods, the modulus decreases due to increased damage of the glass/epoxy interface and the wood/FRP interface.

In neutral medium, all the properties decreased initially and later increased between 15 days and 25 days of aging. Shear tests of sandwich samples (Table 5.16) aged in water indicate a 55% reduction in wood/FRP bond strength compared to a maximum of 70% reduction in alkaline medium. The wood failure of the samples was 92%. This shows that the wood/FRP interface is not damaged as much by water. It is assumed that water diffuses into the epoxy matrix and causes plasticization. Plasticization reduces the

Tg and facilitates molecular mobility. With the progress of aging from 15 days to 25 days, the curing reaction of the epoxy matrix proceeds and forms a more cross-linked structure with increased Tg and modulus. The modulus thus increases until the matrix is completely cured. Upon prolonged aging, one can expect a further increase followed by a decrease in modulus of the wrapped composite.

In salt water, the strength and modulus of wrapped specimens reduced gradually. Saltwater medium caused minimum decrease in the properties. However, the percent of decreases in modulus and rigidity in salt water were similar to those caused by alkaline medium and water. This suggests that salt water does not highly reduce the strength of the composite but lowers the stiffness or makes the hybrid more ductile. There was a 61% decrease in shear strength of the wood/FRP bond and 24% (minimum) decrease in shear strength of the wood/HMR/epoxy bond due to aging in salt water. This suggests that the damage caused by salt water to the glass/epoxy interface is higher than the damage caused to the wood/FRP interface. Salt water is least damaging to the epoxy matrix.

Irrespective of the amount of damage caused by aging, the failure of hybrid specimens aged in all media occurred in the outer fibers. There was no delamination between the GFRP wrap and HMR primed wood surface after aging. This shows that the GFRP wrap protects wood when exposed to freeze-thaw cycles in pure water, salt water, acidic and alkaline conditions.

6.6.4 Effect of Primer

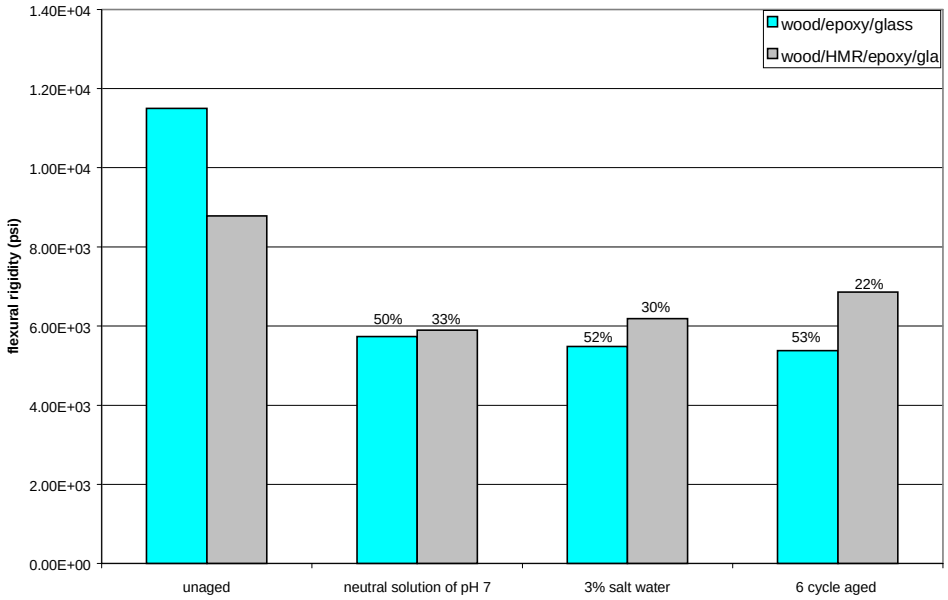

Figure 6.9: Comparison of flexural rigidity of wood/epoxy/glass hybrid and wood/HMR/epoxy/glass hybrid exposed to different conditions

Figure 6.9 compares performance of the wood/epoxy/glass bond with and without the use of HMR primer. Under unaged conditions, the rigidity of the wood/epoxy/glass is reduced by 24% with the use of HMR. However, in all aging media, the wood/epoxy/glass hybrid showed a higher percentage reduction in stiffness compared to the wood/HMR/epoxy/glass hybrid. This shows that HMR primer increases the retention of properties of wood/epoxy/glass hybrid under aged conditions. With the use of HMR primer, the rigidity of the wood/epoxy/glass hybrid specimen was increased by 3% in neutral medium, 13% in salt water and by 28% under 6-cycle accelerated aging conditions.

6.7 Cost Analysis

The following discussion presents a brief idea about the cost of a GFW wood post in comparison with the cost of an unwrapped wood post and a steel post.

From the 1999 statistics of the West Virginia Department of Transportation, the approximate cost of a W6/9 galvanized 7′ long steel guard-rail post = $25

From Southern States (a local lumber company), the approximate cost of a 5″ diameter, 7′ long pressure treated wooden guard-rail post = $7

$\rho_{wrap} = v_f \rho_f + (1-v_f) \rho_m$

where

ρ_{wrap} = density of the FRP wrap

ρ_f = density of glass fibers = 2627 kg/m^3

ρ_m = density of epoxy resin = 1160 kg/m^3

v_f = fiber volume fraction = 0.25 (for the present situation)

therefore, $\rho_{wrap} = 0.25(2627) + 0.75(1160)$

$= 1526.75$ kg/m^3

$= 95.18$ lb/ft^3

From communications with the industry, it is assumed that the thickness of an FRP wrap produced by a 40oz fabric is approximately 0.047″. Therefore the thickness of an FRP wrap produced by 2 layers of a 12oz fabric is 0.028″

Volume of the wrap = $\pi h (R^2 - r^2)$

where

h = length of the wrapped section of the CCA treated wood post

r = radius of the bare wood core

R = radius of the wrapped wood section = r + t = (2.5 + 0.028) = 2.528″

Assuming the length of the wrapped portion of a 7′ long CCA treated wood post to be 3′,

Volume of the wrap = π X 3 X $((2.528/12)^2 - (2.5/12)^2)$

= $9.21 \text{ X } 10^{-03}$ ft^3

Weight of the wrap = volume of wrap X density of wrap

= $9.21 \text{ X } 10^{-03}$ X 95.18

= 0.88 lb

From communications with the industry, the approximate cost of FRP wrap/lb (including material and labor costs) = $1.5

Cost of the wrap = weight of the wrap X cost of wrap/lb

= 0.88 X 1.5

= $ 1.32 per post.

Therefore

The cost of a 5″ diameter, 7′long unwrapped wood post = $7

The cost of 5″ diameter, 7′long wrapped post (with a 3′ long FRP wrap of thickness 0.028″) = $8.32

The cost of a W6/9 galvanized 7′ long steel guard-rail post = $ 25

As seen from the above calculations, the cost of a glass fabric wrapped CCA treated wood post is much lower than the cost of a conventional steel guard-rail post.

6.8 Summary

Composite wrapping of wood with HMR/epoxy/glass fibers (using 25% fiber volume fraction in GFRP wrap and 0.0475″ thick wrap around 0.5″ wood core) increases the flexural rigidity of wood by 2.62 times under unaged conditions and by 1.77 times under 6-cycle aging conditions (from section 6.6.1). Use of HMR primer increases the retention of mechanical properties of the wood/epoxy/glass hybrid after aging, as shown by the results of chapter V. However, the performance of the wood/epoxy/glass specimens under unaged conditions is lowered by the presence of HMR primer. Chemical aging showed that the wood/HMR/epoxy/glass hybrid is damaged the most by freeze-thaw cycling in acidic medium. In acidic medium, the glass fibers and the epoxy/glass interface are damaged the most. In alkaline medium, the epoxy/glass interface and the wood/HMR/epoxy bond, are damaged the most. In water, the glass fibers and the epoxy/glass interface are primarily damaged. In salt water, the wood/HMR/epoxy interface is damaged the most. The cost of a glass fabric wrapped CCA treated wood post is lower than the cost of a conventional steel guard-rail post (from section 6.7).

Chapter VII

DYNAMIC MECHANICAL THERMAL ANALYSIS OF WRAPPED COMPOSITES

7.1 Overview

To ensure the long-term durability of wrapped posts, accelerated aging and chemical aging were performed on coupons representing a scaled down version of the proposed glass fabric wrapped wood posts. In addition, non-destructive testing of the aged test specimens was conducted using a Rheometrics Mechanical Spectrometer (RMS 800). Dynamic spectra of aged and unaged samples were compared. Changes in the test samples due to aging and possible reasons for changes are discussed in this chapter. Details of sample preparation and test procedure are also presented, herein.

7.2 Materials Used

CCA treated southern pine strips of cross-section 10.0 mm X 2.0 mm, primed on all surfaces with HMR primer, were used as the core. Though the actual guard-rail posts to be implemented in the field are circular in cross-section, coupons used for DMTA were rectangular in cross-section. This was done to suit the requirements of the Spectrometer (RMS 800). Also, considering the size of the test coupons and the thickness of the wrap, we believe that the aging effects on circular and rectangular cross-sections would not be very different. E-glass fiber roving with epoxy compatible sizing, supplied by PPG, was used for wrapping. The diameter of glass fibers in the roving was 30 μm. Epoxy (TYFO-S) supplied by Hexcel Fyfe was used as the adhesive.

7.3 Sample Preparation

A lathe was used to prepare wrapped coupons using filament winding. The wood core was held between grips fitted to the lathe and rotated at constant speed. Fibers from a roving were allowed to pass through a resin bath and wrap around the rotating wood core. Wrapped specimens were dried using a motorized drying wheel to prevent dripping of the resin and to promote uniform curing. After curing, the wrapped specimens were cut to the required length. The edges of the specimens were sanded to fit them into the fixtures of the Spectrometer. The length of each specimen was 50mm and the length of the wrapped portion was approximately 40mm. The thickness of the wrap around the 2mm wood core was approximately 0.75mm. The fiber volume fraction of the wrap was approximately 32% (see Appendix A.2).

7.4 Description of Test Procedure

In the dynamic mechanical analysis (DMA) of a test specimen, the stress response to a sinusoidal strain is recorded. Two types of runs were conducted on the specimens:

(a) temperature sweep: a sinusoidal strain of fixed amplitude is imposed at a constant frequency and the temperature of the sample is increased at a constant rate.

(b) frequency-temperature sweep: a sinusoidal strain of fixed amplitude is imposed as a function of frequency at a series of constant temperatures

Dividing the stress amplitude in phase with the strain by the strain amplitude gives the storage modulus (G′). The storage modulus is a measure of the inherent stiffness of the wrapped specimen. Dividing the stress amplitude out of phase with the strain by the strain amplitude gives the loss modulus (G″). Typically during a temperature sweep, G′,

G″ and tanδ (or G″/ G′) are plotted as a function of temperature. These plots display changes in T_g, damping factor (G″/ G′) and modulus which may be due to structural changes that the composite has undergone during aging. During a frequency-temperature sweep, G′ as a function of frequency is plotted at various constant temperatures. These curves are superimposed onto a single curve at a chosen temperature called the reference temperature. This generates a master curve of G′ as a function of frequency at the chosen reference temperature. Comparison of master curves of the aged and unaged samples are used in identification of changes produced by aging with time. Figure 7.1 shows a wrapped coupon loaded in the RMS –800.

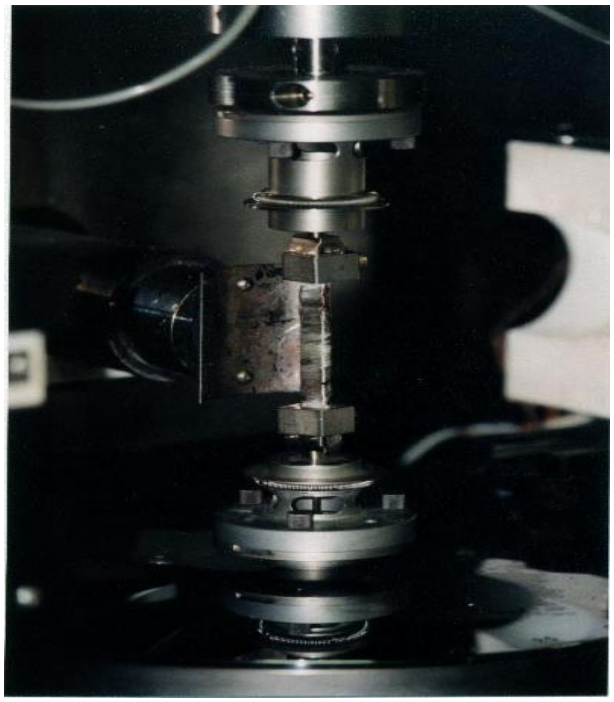

Figure 7.1: Loaded sample in the DMTA set up

7.5 Sample Conditioning

Wrapped specimens were subjected to the following conditions before testing:

(1) exposure to freeze thaw cycles in acidic solution of pH 3.0 for 5 days, 15 days and 25 days in the atmospheric chamber (described in Chapter IV, section 4.3)

(2) exposure to freeze thaw cycles in alkaline solution of pH 13.0 for 5 days, 15 days and 25 days in the atmospheric chamber

(3) exposure to freeze thaw cycles in solution of pH 7.0 for 5 days, 15 days and 25 days in the atmospheric chamber

(4) exposure to freeze thaw cycles in 3% salt water for 5 days, 15 days and 25 days in the atmospheric chamber

(5) exposure to 6-cycle accelerated aging

The duration of steps in each cycle of the 6-cycle accelerated aging was altered to suit the smaller dimensions of coupons. Each cycle of the 6-cycle accelerated aging consisted of the following steps:

(a) vacuum soaking (25 inches Hg) for 30min

(b) pressure soaking (100 psi) for 30min

(c) freezing for 3 hours at -10^0 C

(d) oven drying for 2 hours at 50^0 C

The reasons for the choice of these aging conditions are mentioned in chapter IV.

7.6 Summary of Test Results

7.6.1 Accelerated Aging of Wood and Wood/HMR/Epoxy/Glass Hybrid Specimens

In order to estimate the long-term performance, wood and wood/HMR/epoxy/glass hybrid specimens were subjected to the 6-cycle accelerated aging procedure. During accelerated aging, the samples were subjected to vacuum and pressure cycles in water, freezing and oven drying. All the samples were dried at room temperature for about 3 weeks before testing. Figures 7.2 and 7.3 show the comparison of dynamic spectra of wood and the wood/HMR/epoxy/glass hybrid under unaged and 6-cycle aged conditions.

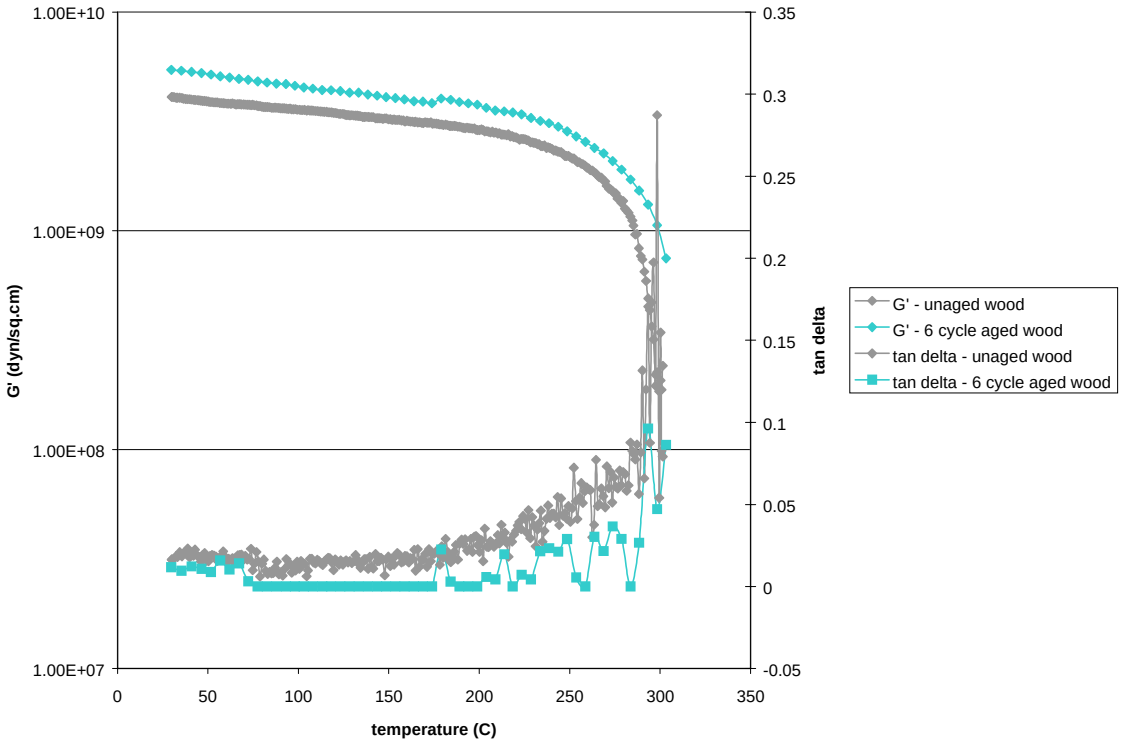

Figure 7.2: Dynamic properties of wood under unaged and 6-cycle aged conditions

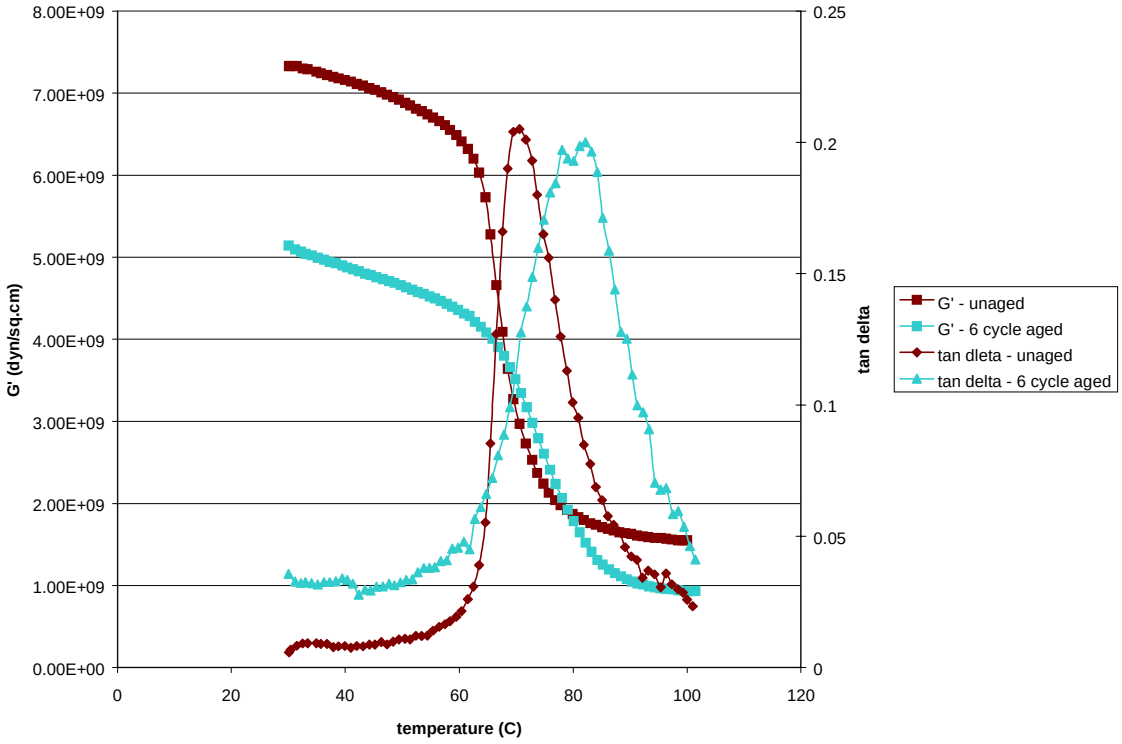

Figure 7.3: Dynamic properties of wood/HMR/epoxy/glass hybrid under unaged and 6-cycle aged conditions

Figure 7.2 shows the dynamic spectra of unaged and 6-cycle aged wood. It can be seen that the modulus of wood slightly increased due to 6-cycle accelerated aging (the G' curve of 6-cycle aged wood sample is above the G' curve of the unaged wood sample). The Tg reduced from 298^0 C to 293^0 C. Figure 7.3 shows the dynamic spectra of the unaged hybrid and the hybrid subjected to 6-cycle accelerated aging. It can be observed that due to 6-cycle aging, the Tg increased from 70.6^0 C to 82.2^0 C. This is attributed to the progress of the cross-linking reaction of epoxy matrix. The modulus decreased meaning the stiffness of the hybrid reduced due to 6-cycle aging. The decrease in modulus and the increase in Tg suggest that 6-cycle aging produces irreversible changes in the hybrid. The primary observation was that the modulus of wood was higher than the modulus of the wrapped specimen after 6-cycle aging which is in contradiction with the

expectations. This suggests that the wrap does not improve the mechanical properties of wood. The durability of wood and the wrapped specimen is yet to be compared. However, flexure tests of wrapped dowels (Section 6.6.1) showed that the flexural rigidity of bare wood has increased by about 2.6 times under unaged conditions and by 1.8 times under 6-cycle aging conditions due to wrapping. There was no delamination at the wood/wrap interface even after 6-cycle aging. Shear strength measurements also showed that the retention in strength of the wood/HMR/epoxy/glass/epoxy/HMR/wood samples is greater than or equal to the retention in strength of the solid wood samples. The failure of the wood/HMR/epoxy/glass/epoxy/HMR/wood samples was completely in the wood. In order to observe the wood/wrap interface after 6-cycle aging, the DMTA samples (wood/HMR/epoxy/glass hybrids) were sectioned using a band saw. Some of the samples showed partial delamination at the wood/wrap interface. The observations showed that the delamination occurred due to improper fiber wetting by the epoxy resin during sample preparation. Lack of confinement of the wrap to the wood core could also be due to a weak wood/HMR/epoxy/glass bond. It is assumed that the low value for the modulus of the wood/HMR/epoxy/glass specimen was primarily due to improper fiber wet out and lack of proper contact between different components of the hybrid specimen. With a good bond between HMR primed wood and the GFRP wrap, and a thorough fiber wetting, the storage modulus of a wood/HMR/epoxy/glass specimen is expected to be higher than the storage modulus of an unwrapped wood sample.

7.6.2 Chemical Aging of Wood/HMR/Epoxy/Glass Hybrid Specimen

To study the effect of different aging media, wood/HMR/epoxy/glass hybrid specimens were immersed in water, salt water, acidic and alkaline media and subjected to freeze-thaw cycling. The aged samples were analyzed by non-destructive DMTA using Rheometrics Spectrometer (RMS 800). Figures 7.3 through 7.7 show a comparison of storage modulus and tanδ curves of the wood/HMR/epoxy/glass hybrid samples aged in different liquid media. These plots were obtained during the temperature sweep of the samples.

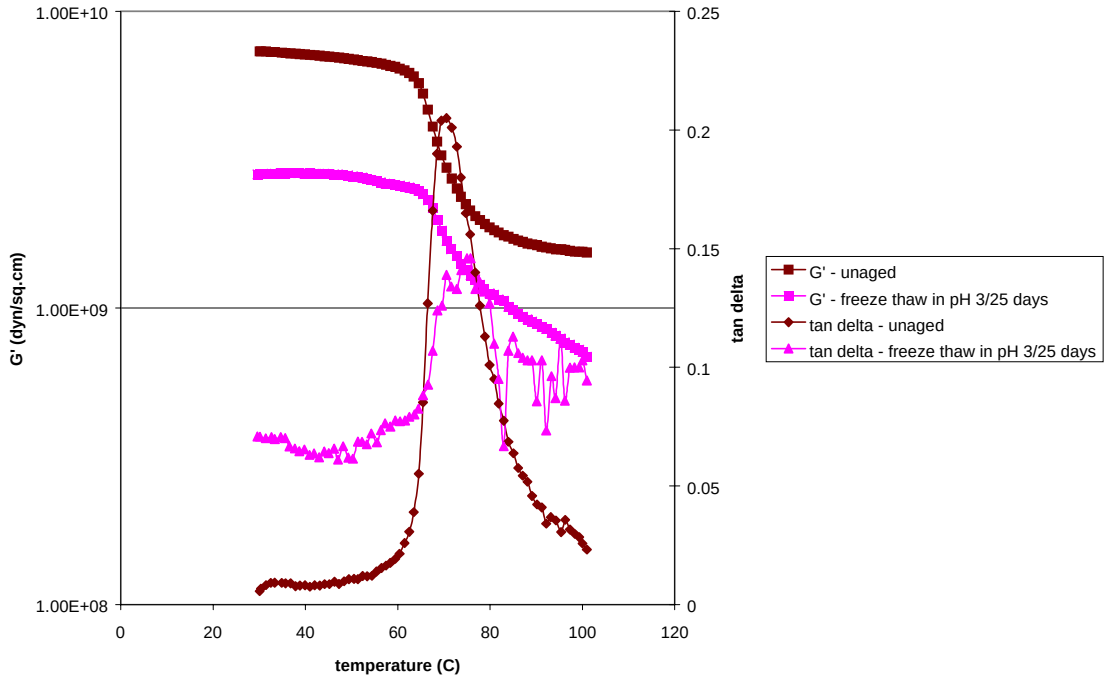

Figure 7.4: Dynamic properties of wood/HMR/epoxy/glass hybrid under unaged and acidic conditions

Figure 7.4 shows that Tg of unaged hybrid increased from 70.6^0 to 75.8^0 C due to freeze-thaw in acidic solution of pH 3 for 25 days. This is assumed to be due to enhanced

curing of the epoxy resin. The width of tan δ peak increased due to widening of the glass transition, which means the molecular weight distribution is broad in the aged hybrid. The storage modulus reduced i.e the stiffness of the hybrid reduced. An increase in Tg and reduction in modulus suggests that aging in acid medium produces some kind of irreversible damage in the hybrid. Since G′ and G″ differ by an order of magnitude (as seen from Figure C4 of Appendix C) there could be delamination at the wood/FRP interface or lack of contact between the components of the hybrid specimen.

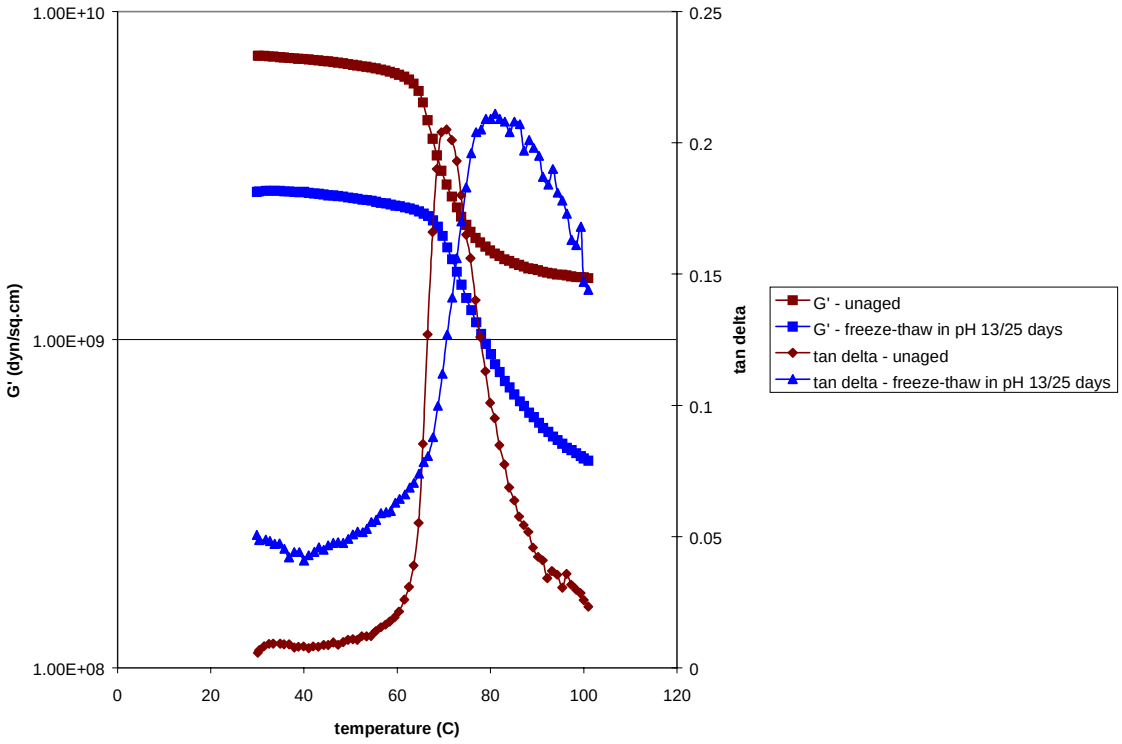

Figure 7.5: Dynamic properties of wood/HMR/epoxy/glass hybrid under unaged and alkaline conditions

From Figure 7.5 it can be observed that freeze-thaw in alkaline medium of pH 13 increased the Tg from 70.6^0 C to 81^0 C. This could be due to better curing of the

epoxy matrix. The storage modulus reduced, which means the stiffness of the hybrid reduced. The slight increase in the height of tan δ peak can be attributed to the reduced stiffness. An increase in Tg and reduction in modulus suggest that aging in alkaline medium produces irreversible damage in the hybrid.

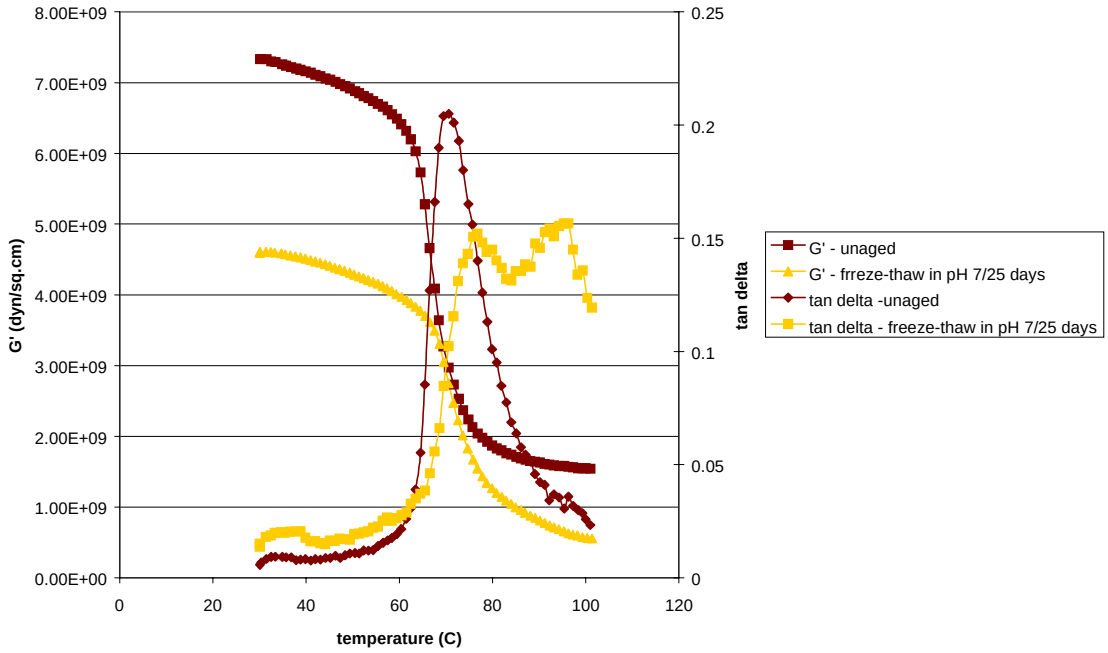

Figure 7.6: Dynamic properties of wood/HMR/epoxy/glass hybrid under unaged and neutral conditions

From Figure 7.6 it can be seen that freeze-thaw in water produced secondary glass transition peaks. The hybrid shows a wide range of glass transition (76^0C to 96^0C). This suggests the progress of cross-linking of epoxy resin and appearance of secondary phases in the matrix. The decrease in modulus or stiffness despite the increase in Tg suggests that water also damages the hybrid.

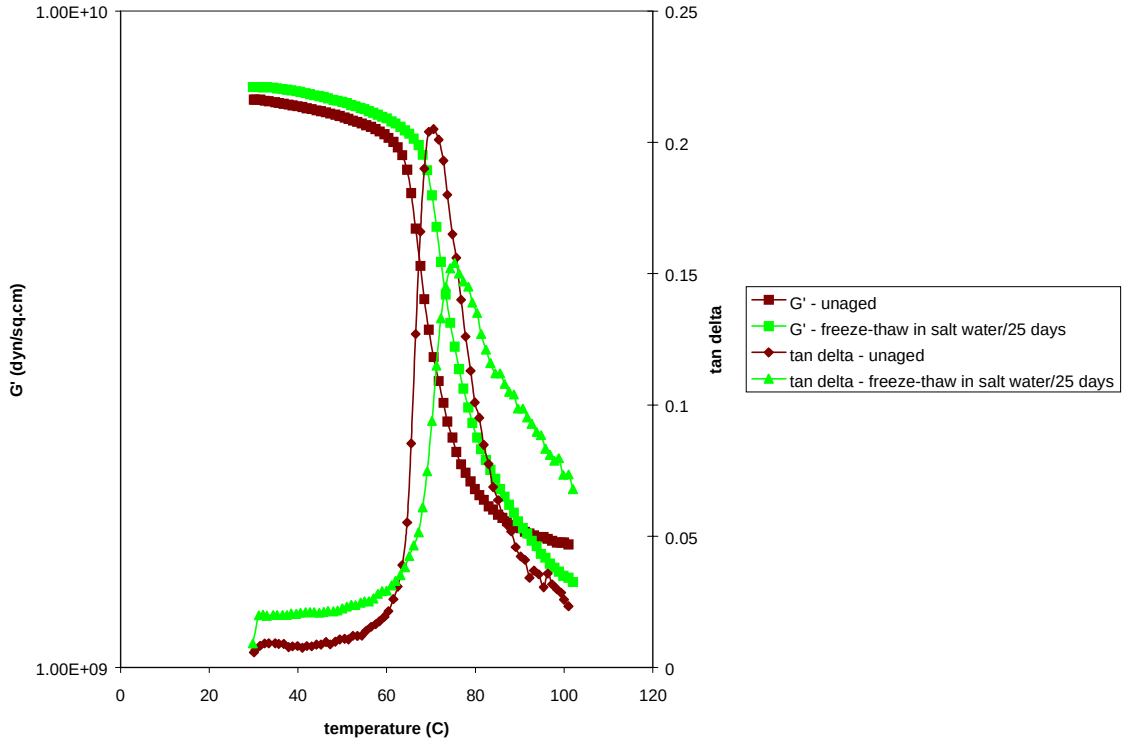

Figure 7.7: Dynamic properties of wood/HMR/epoxy/glass hybrid under unaged and salt water conditions

Figure 7.7 shows that freeze-thaw in salt water increased the Tg from 70.6^0 C to 75.3^0 C and slightly increased the modulus. This is attributed to the progress of the cross-linking reaction of the epoxy matrix. The decrease in the height of tan δ peak may also be due to the increase in modulus. A comparison of Figures 7.4 through 7.7 shows that freeze-thaw cycling in salt water does not produce irreversible changes in the hybrid sample unlike freeze-thaw cycling in water, acidic medium and alkaline medium.

Table 7.1: Variation of T_g and storage modulus of wood/HMR/epoxy/glass hybrid under different aging conditions

Condition	Glass transition temperature (^{0}C)	Percent change in storage modulus (measured at 40^{0}C)
Unaged	70.6	-----
Freeze-thaw in acidic medium	75.8	- 60
Freeze-thaw in alkaline medium	81	- 61
Freeze-thaw in water	96.3	- 37
Freeze-thaw in salt water	75.3	+ 5
6-cycle aging	82.2	- 32

The storage modulus of unaged wood/HMR/epoxy/glass hybrid was 7.16 X 10^9 dyn/sq.cm. The negative sign of percent change in modulus indicates a decrease and positive sign indicates an increase. The following is the summary of observation of Figures 7.4 through 7.7:

Freeze-thaw cycling in all the solutions widened the glass transition region and increased the Tg. It is assumed that liquid diffusion into the wrapped specimen plasticizes the epoxy matrix and facilitates molecular mobility. As a result, the cross-linking of partially cured epoxy resin occurs increasing the Tg. The maximum increase in Tg (from 70.6^0 C in dry/unaged condition to 96.3^0 C) occurred in water. This suggests that the cross-linking of the epoxy matrix progresses faster in water. The decrease in storage modulus was found to be maximum due to freeze-thaw cycling in acidic and alkaline media. Freeze-thaw cycling in water for 25 days caused as much damage as 6-cycle accelerated aging (in terms of stiffness reduction). Salt water did not seem to cause damage to the hybrid.

7.6.3 Time-Temperature Superposition

To compare the long-term behavior of wood and wood/HMR/epoxy/glass hybrid, a frequency/temperature sweep was conducted on the samples and master curves were generated. The process of generating a master curve from G' versus ω data at different isothermal temperatures is called time-temperature superposition. It is based on the assumption that the effects of changing temperature on the visco-elastic behavior of a material are equivalent to a shift in the actual time scale of measurement. A temperature range of 40^0 C to 100^0 C was used in the data collection. The frequency range was 0.1 to 100 rad/sec. The reference temperature used in the generation of master curves was 40^0 C.

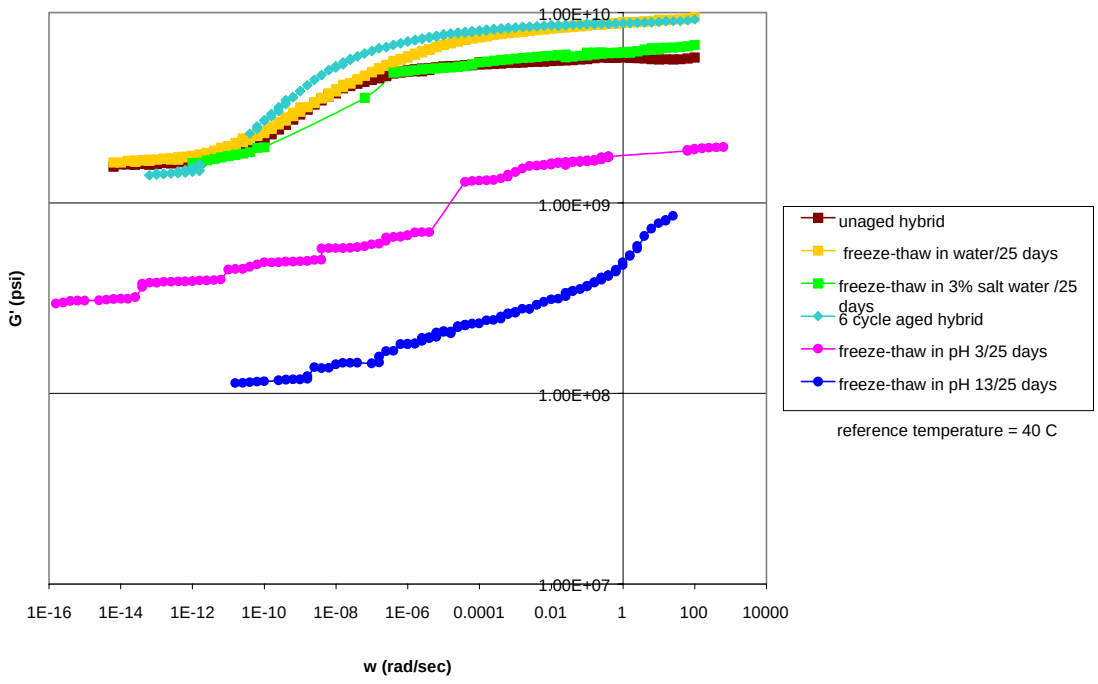

Figure 7.8: Comparison of master curves of wood/HMR/epoxy/glass hybrid aged in different media

Figure 7.8 shows the variation of storage modulus of the wood/HMR/epoxy/glass hybrid conditioned in different environments with increasing frequency or decreasing time. The degradation trend of storage modulus of the hybrid aged in water, salt water and 6-cycle aging was similar to that of the unaged hybrid. This shows that the composite wrap is able to retain its stiffness after aging in water and salt water. The modulus of the wrapped specimen was reduced the most by the alkaline medium followed by the acidic medium.

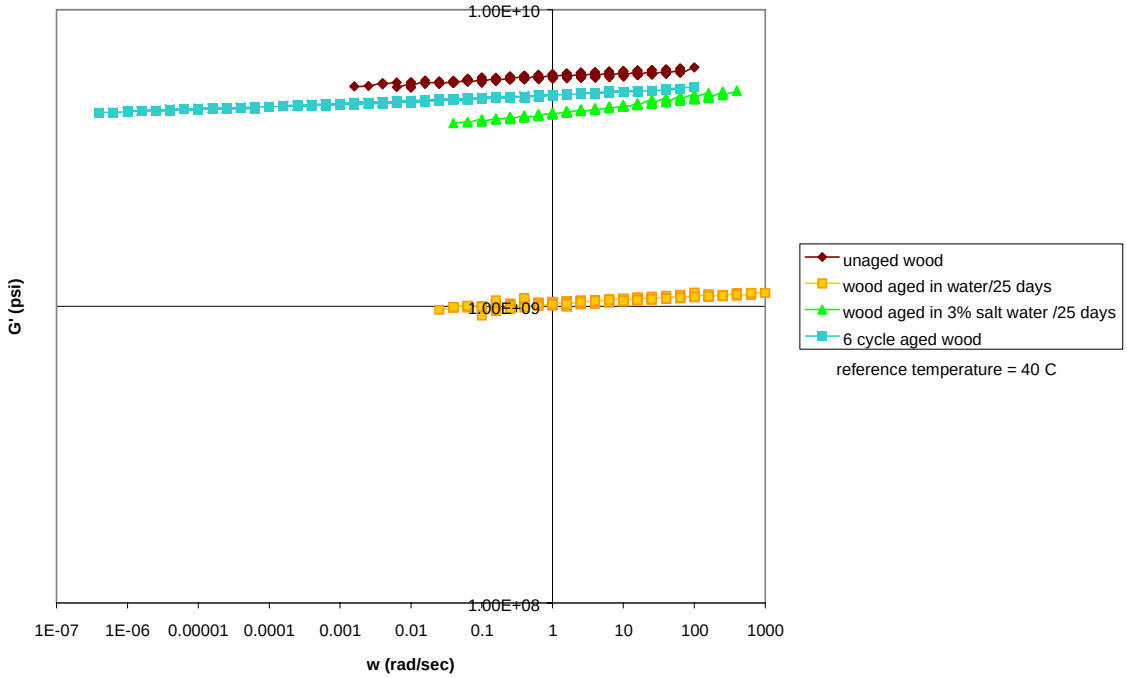

Figure 7.9: Comparison of master curves of CCA treated wood aged in different media

Figure 7.9 shows a comparison of storage modulus of unaged wood and wood exposed to freeze-thaw cycling in water and salt water. The figure shows that the stiffness of wood reduces in water and salt water and the reduction in water is higher than that in salt water. According to the research at the Forest Products Laboratory [26],

exposure to water at elevated temperatures reduces the strength of wood. This damage is irreversible at temperatures above 100^0 C. Wood is fairly resistant to many chemicals but is degraded by strong acids (pH < 2) and strong alkalies (pH > 10). Under the conditions used in this research, it was found that wood is damaged the most in an alkaline medium of pH 13 and the least by 6-cycle aging.

The master curves shown in Figures 7.8 and 7.9 were extrapolated and the moduli of wood and the hybrid were compared at a service life of 20 years. A sample calculation of the storage modulus of a hybrid specimen at a desired service life is shown in Appendix B.3. Table 7.2 shows the stiffness of wood and hybrid under different aging conditions.

Table 7.2: Storage modulus (G′) of wood and wood/HMR/epoxy/glass hybrid at a service life of 20 years

Aging condition	G′ of wood (dyn/cm^2)	G′ of wood/HMR/epoxy/glass hybrid (dyn/cm^2)
Unaged	4.55×10^9	2.94×10^9
Freeze-thaw cycling in water	0.79×10^9	3.03×10^9
Freeze-thaw cycling in 3% salt water	1.93×10^9	2.34×10^9
6-cycle aging	3.96×10^9	3.88×10^9

From Table 7.2, it can be seen that, under unaged conditions, the modulus of wood is reduced by wrapping. This contradicts the expectations as well as the results of chapter VI which show a 4% increase in modulus due to wrapping under unaged conditions. Since the modulus of the hybrid is greater than the modulus of wood under water and salt water conditions, it is assumed that the modulus of the hybrid is greater

than the modulus of wood under unaged conditions also. In water, the hybrid specimen maintained a 3.8 fold increase in the modulus in comparison with unwrapped wood specimen. In salt water, the hybrid specimen maintained a 1.2 fold increase in the storage modulus in comparison with unwrapped wood specimen. Under 6-cycle aging, the wrap does not increase the stiffness. The results of unaged specimens and 6-cycle aged specimens contradict the results of chapter V. Chapter V shows that the wood/HMR/epoxy/glass bond is atleast as strong as wood under 6-cycle aging conditions. For better judgement, the DMTA hybrid samples were sectioned and the wood/wrap interface was observed. As mentioned in section 7.6.1, there was partial delamination at the wood/wrap interface. From the observations, it appears that the delamination occurred due to improper fiber wetting by the epoxy resin during sample preparation. Rectangular cross-section of the thin wood core prevented good confinement of the wrap. Poor confinement of the wrap was primarily responsible for the low values of modulus under 6-cycle aging conditions.

7.7 Summary

From the master curves of wood/HMR/epoxy/glass hybrid, it was concluded that the performance of wrapped hybrid samples in water, salt water and under 6-cycle aging conditions is similar to the unaged hybrid samples (figure 7.8, section 7.6.3). This shows that the wrapped hybrid samples are durable under atmospheric conditions. However, wrapped hybrid samples are damaged the most in alkaline medium followed by acidic medium (figure 7.8, section 7.6.3). In both the acidic and alkaline media, a possible delamination of the wood/FRP interface might have occurred (table 7.1). Based on the

variation of T_g and the percent reduction in storage modulus (table 7.1), it is assumed that the damage caused by freeze-thaw cycling is greater than the damage caused by vacuum and pressure cycles.

The storage modulus of wood and hybrid specimens, aged in different media, were compared at a service life of 20 years. It was found that, even under saturated conditions, wood samples wrapped with HMR/epoxy/glass fibers (using 31% fiber volume fraction in GFRP wrap and a 0.75 mm thick wrap around the 10mm X 2mm wood core), maintained a 4 fold increase in the storage modulus in comparison with unwrapped, but aged wood. Under salt water conditions, the modulus of hybrid samples was found to be 1.2 times that of unwrapped wood. Under 6-cycle aging (table 7.2), the contribution of wrap in increasing the storage modulus of composite samples had diminished to an extent where no significant difference in the storage moduli of unwrapped wood and wrapped hybrid was observed. This is attributed to improper fiber wet out and poor confinement of the wrap to wood.

Results of Chapter VII are summarized in relation to the results of Chapters V and VI:

Results of chapter V show that under 6-cycle accelerated aging conditions, the failure of wood/epoxy/glass/epoxy/wood and wood/epoxy/wood samples is 100% in wood (tables 5.16 and 5.17). This means that the wood/HMR/epoxy interface(s) is durable under long-term aging conditions.

Results of chapter VI show that composite wrapping increases the flexural rigidity (EI) of wood under unaged condition as well as 6-cycle aging conditions (table 6.1). There was no delamination at the wood/FRP interface in the hybrid specimens. However,

no improvement in the flexural strength or modulus under 6-cycle aging conditions was observed due to the effect of moisture fluctuation in the unwrapped wood and hybrid samples (section 6.6.1).

The results of chapter VII show that the storage modulus of wood improved by composite wrapping, but a significant reduction in the storage modulus of wrapped hybrid specimens occurred under 6-cycle aging conditions. However, the reductions in storage modulus of wrapped wood could be attributed to possible sample preparation defects such as improper fiber wet out and poor confinement between the wrap and wood due to the rectangular geometry of the test samples.

From all these results given in Chapters V, VI and VII, it is concluded that the mechanical properties of wood have definitely improved by composite wrapping under unaged conditions. Under 6-cycle aging conditions, the wood/FRP bond is not the weakest link as indicated by the results presented in Chapters V and VI. Therefore the technique of composite wrapping is found to be promising in improving the mechanical properties under 6-cycle aging conditions. A higher fiber volume fraction in the FRP wrap would enhance the mechanical properties and thus reveal the significant strength and stiffness increases between unwrapped wood and wrapped hybrid specimens. In addition, further improvements in mechanical properties of wrapped hybrid specimens can be attained through better wrapping techniques. Testing of large-scale posts is required as being done by Chamarthy [23]. The increase in strength, modulus and stiffness of the full-size wood posts would be higher than the increase found in the present case. This is because the wood core in the full-size posts would be less perfect than the small size (0.5″ dia) posts that were used in this work.

Chapter VIII

CONCLUSIONS AND RECOMMENDATIONS

The primary objective of this research was to determine the effectiveness of composite wrapping in improving the durability and mechanical properties of CCA treated wooden guard-rail posts. The system under investigation was CCA treated wood that is externally reinforced with glass fibers. The conclusions drawn from the experimental results are listed below.

8.1 Conclusions

8.1.1 Testing of Wood/Adhesive and Wood/FRP Interface by Shear Tests

(1) Among the six resins screened, the combination of epoxy resin and HMR primer provides the best possible adhesion to CCA treated wood and glass fibers. The failure of wood/HMR/epoxy/glass bond (wood/FRP bond) under 6-cycle accelerated aging conditions is completely in the wood, i.e., wood is damaged before the wood/FRP bond under long-term aging conditions.

(2) The loss of shear strength of wood/FRP bond under accelerated aging conditions is less than or equal to the decrease in shear strength of wood, suggesting that the wood/FRP bond is atleast as durable as wood.

(3) The wood/FRP bond is damaged the most by freeze-thaw cycling in an alkaline medium. The wood/HMR/epoxy bond is damaged the most by freeze-thaw cycling in an alkaline medium followed by freeze-thaw cycling in salt water.

(4) The acidic medium does not damage the wood/HMR/epoxy bond.

8.1.2 Testing of Wood/HMR/Epoxy/Glass Hybrids by Flexure Tests

(1) GFRP wrapping of wood increases the mechanical properties of wood (flexural strength, modulus and rigidity) under unaged conditions.

(2) GFRP wrapping of wood improves the flexural rigidity of a CCA treated wood post under 6-cycle aging conditions.

(3) The strength and stiffness of a wood/HMR/epoxy/glass wrapped post is reduced the most by freeze-thaw cycling in an acidic medium. In all the aging media (water, salt water, acid, alkali), the strength is reduced more than the stiffness.

(4) The cost of a full-size glass fabric wrapped wood post is lower than the cost of a conventional steel guard-rail post.

8.1.3 Testing of Wood/HMR/Epoxy/Glass Hybrids by DMTA

(1) Composite wrapping of wood with HMR/epoxy/glass fibers increases the stiffness in water and salt water media.

(2) The strength and stiffness of wood/HMR/epoxy/glass hybrid is reduced the most under alkaline and acidic conditions.

8.1.4 Effect of Aging Media

(1) Freeze-thaw cycling helps the curing of uncured epoxy resin and increases the Tg in all aging media. The glass transition of the composite is widened due to aging. Maximum curing of the epoxy matrix occurs in water.

(2) Freeze-thaw cycling is more damaging to wood than vacuum and pressure cycling. Wood is damaged the most by freeze-thaw cycling in water. Damage caused by

saltwater to wood is less compared to the damage caused by water.

(3) Protons in acid attack the glass fiber surface and primarily damage the glass fibers and the epoxy/glass interface. Acidic medium also damages the wood. Alkaline medium damages the epoxy matrix, the wood/HMR/epoxy interface and the epoxy/glass interface the most. Salt water damages the wood/HMR/epoxy bond the most. Water damages the glass fibers, the epoxy/glass interface and the wood. No significant damage is caused by water to the wood/HMR/epoxy interface. Of all the aging media, alkaline medium and acidic medium are the most damaging to the wood/HMR/epoxy/glass hybrid.

8.2 Recommendations

(1) Testing of large-scale posts is required for better understanding of the magnitude of difference in strength and modulus of wood produced by composite wrapping.

(2) Since the epoxy/glass interface is damaged in all aging media except in salt water, the morphological and chemical changes that take place at the interface need to be investigated.

(3) Monitoring the curing of the epoxy matrix during aging can help understand the specific reasons for damage at the interface(s). This can be done by using less damaging techniques such as ultrasonics.

(4) Coating the wrapped post with epoxy resin itself or any moisture resistant materials can be experimented if the process is not expensive.

(5) Standard methods of prediction of long-term performance should be developed.

BIBLIOGRAPHY

1. A. K. Kaw, Mechanics of Composite Materials, CRC Press, Boca Raton, Florida, 1997, p 6-25.
2. P. K. Mallick, Fiber Reinforced Composites, Marcel Dekker, New York, Second edition, 1993, p 15-184.
3. A. A. Marra, Technology of Wood Bonding, Van Nostrand Reinhold, New York, 1993, Chapters 3-6 and 8-10.
4. C. A. Harper, Handbook of Plastics, Elastomers and Composites, Mc Graw-Hill, New York, Third edition, 1996, p C.1- C.62.
5. R. F. Blomquist, A. W. Christiansen, R. H. Gillespie and G. E. Myers, Adhesive Bonding of Wood and Structural Materials, Educational Modules for Materials Science and Engineering, University Park, Pennsylvania, Volume 3, 1985, Chapters 1-3.
6. K. Liao, C. R. Schultheisz, D. L. Hunston and L. C. Brinson, "Long-term Durability of Fiber-Reinforced Polymer-Matrix Composite Materials for Infrastructure Applications: A Review," NIST, Gaithersburg, Maryland, p 23-27.
7. C. L. Schutte, "Environmental Durability of Glass-Fiber Composites," Materials Science and Engineering, November 15, 1994, p 256-323.
8. C. B. Vick and T. A. Kuster, " Mechanical Interlocking of Adhesive Bonds to CCA- Treated Southern Pine – A Scanning Electron Microscopic Study," Wood and Fiber Science, Vol24, January 1992, p 36-46.

9. C. B. Vick, “More Durable Epoxy Bonds to Wood with Hydroxymethylated Resorcinol,” Adhesives Age, Vol 40, July 1997, p 24-29.

10. C. B. Vick, K. H. Ritcher and B. H. River “Hydroxymethylated Resorcinol Coupling Agent and Method for Bonding Wood,” United States Patent Number - 5,543,487, Aug 1996.

11. C. T. Lynch, Practical Handbook of Materials Science, CRC Press, Boca Raton, Florida, 1989, p 22-37 and 50-64.

12. S. Ghasemzadeh, S. Kajorncheappunngam, R. K. Gupta and H. V. S. GangaRao, “Durability of Glass-Epoxy-Wood Hybrid Composites for Rehabilitation of Railroad Crossties,” Durability of Fiber-Reinforced Polymer (FRP) Composites for Construction: Proceedings of the First International Conference (CDCC ′98), Sherbrooke, Canada, Aug 1998, p 81-93,1998.

13. C. B.Vick, “ Coupling Agent Improves Durability of PRF Bonds to CCA-Treated Southern Pine” Forest Products Journal, Vol45, March 1995, p 78- 84.

14. C.Lhyman and J.M.Schultz, “ Environmental Testing of Glass-Fiber Reinforced Thermoplastics” Polym. Engg. and Sci., September 1984, Vol24, p 1064-1070.

15. S. Kshirsagar, R. Lopez-Anido and R. K. Gupta, “Durability of Fiber Reinforced Composite Wrapping for the Rehabilitation of Concrete Piers,” Durability of Fiber Reinforced Polymer (FRP) Composites for Construction: Proceedings of the First International Conference (CDCC ′98), Sherbrooke, Canada, Aug 1998, p 117-126.

16. R. K. Devalpura, M. E. Greenwood, J. V. Ganchel and T. J. Humphry, “Evaluation of GFRP Performance Using Accelerated Test Methods,” Durability

of Fiber Reinforced Polymer (FRP) Composites for Construction: Proceedings of the First International Conference (CDCC ′98), Sherbrooke, Canada, Aug 1998, p 107-116.

17. P. Chow, S. L. Lewis, A. J. Reinschmidt and E. J. Barenberg, " Effects of Natural and Accelerated Aging on Oak Crossties," Proceedings of the American Wood Preservers Association, Toronto, Canada, May 1987, p 308-329.

18. C. B.Vick, " Hydroxy Methylated Resorcinol Coupling Agent for Enhanced Adhesion of Epoxy and Other Thermosetting Adhesives to Wood," Proceedings of the 1996 Symposium Sponsored by USDA, Portland, Oregon, June 1995, p 47-55.

19. ASTM D 905-94, "Test Method for Strength Properties of Adhesive Bonds in Shear by Compression Loading," The 1995 Annual Book of ASTM Standards, Vol 15.06, p 21-24.

20. S. Kajorncheappunngam, "The Effects of Environmental Aging on the Durability of Glass/Epoxy Composites," PhD. Dissertation, Dept. of Chemical Engg, West Virginia University, 1999, p 71-196.

21. ASTM D 790-92, "Test Method for Flexural Properties of Unreinforced and Reinforced Plastics and Electrical Insulating Materials," The 1995 Annual Book of ASTM Standards, Vol 8.01, p 155-164.

22. D. R. Talakanti, "Testing and Evaluation of Wood-GFRC Adhesive Interface Integrity Under Accelerated Aging and Mechanical Fatigue," M.S. Thesis, Dept. of Mechanical Engg, West Virginia University, 1997, p 57-59.

23. U. Chamarthy, Manufacture and Rehabilitation of Guard-rail Posts Using Composites for Superior Performance, M.S. Thesis, Dept. of Mechanical Engg, West Virginia University, in progress.

24. K. Laosiriphong, Development and Evaluation of Glass Fiber Reinforced Composite/Wood Railroad Cross-ties, M.S. Thesis, Dept. of Civil Engg, West Virginia University, in progress.

25. E. J. Barbero, Introduction to Composite Materials Design, Taylor and Francis, Philadelphia, Pennsylvania, 1998, Chapters 2-4.

26. http://www.fpl.fs.fed.us

APPENDIX A

A.1 Calculation of Fiber Volume Fraction of Flexure Test Samples

A.2 Calculation of Fiber Volume Fraction of DMTA Samples

Appendix A.1

Calculation of Fiber Volume Fraction of Wrapped Samples Tested by 3 Point Bending

The samples consisted of a wood core of diameter 0.5″ with an FRP wrap of 0.048″ thickness around the wood core.

Weight of the fabric used = 12 oz/yd^2

= 12/9 oz/ft^2

Weight of 1 sq ft. of a 1.3 oz/ft^2 fabric = 1.3 oz

= 1.3 /16 lbs

= 0.0813 lbs

for 50% over lap, weight of fabric = 0.0813 X 2

= 0.1626 lbs

Density of glass fibers = 0.094 lb/in^3

Volume of fibers = weight /density

= 0.1626/0.094 in^3

= 1.73 in ^{3}

Volume of the wrap = 1 sq.ft X thickness of wrap

= 12″ X 12″ X 0.0475″

= 6.84 in^3

Fiber volume fraction = volume of fibers /volume of wrap

= 1.73/6.84

= 25.3 %

Appendix A.2

Calculation of Fiber Volume Fraction of Wrapped Samples Tested by Mechanical Spectrometer

Average weight of resin in a wood/HMR/epoxy/glass hybrid = 0.553 g

Average weight of glass fibers in a wood/HMR/epoxy/glass hybrid = 0.572 g

Density of epoxy = 1.16×10^3 kg/m^3

Density of glass fibers = 2627 kg/m^3

Average volume of epoxy in a sample = 0.476×10^{-6} m^3

Average volume of glass fibers in a sample = 0.218×10^{-6} m^3

Fiber volume fraction = volume of fibers/ volume of fibers + volume of resin

= 31.4 %

APPENDIX B

B.1 Sample Calculation of Shear Strength from Shear Test Data

B.2 Sample Calculations of Mechanical Properties from Flexure Test Data

B.3 Sample Calculations for the Generation of a Master Curve from Mechanical Spectroscopy Data

Appendix B.1

Sample Calculation of Shear Strength from Shear Test Data

The following is the typical data obtained by testing 15 shear samples (of wood/epoxy/wood):

max. load in lbs	**% wood failure**
780	10
420	8
190	50
300	25
345	30
342	20
260	30
280	10
261	8
776	40
480	15
277	30
40	50
133	25
412	5

The maximum load value is read from the machine and the percent failure is obtained by visual examination.

The average load taken by wood/epoxy/wood specimen = 316.25 lbs.

The shear area or the area on which the load was applied = 0.5″ X 0.5″

= 0.25 sq.in.

The average shear strength of wood/epoxy/wood bond = average load/area

= 316.25/0.25

= 1265 psi

Average wood failure = 20%

Appendix B.2

Sample Calculations of Mechanical Properties from Flexure Test Data

For a 3 point bending test and cylindrical geometry of the sample,

L = loading span

P = maximum load taken by the sample before failure

M = maximum applied bending moment = PL/4

I = moment of inertia

for the present case of wood core of radius (r) and wrap of thickness 't' around the core,

$I_{hybrid} = I_{wood} + E_{wrap}/E_{wood} (I_{wrap})$

$I_{wood} = \pi r^4/4$ where 'r' is the radius of the wood core

E_{wrap}/E_{wood} = approximately 1.25 for a fiber volume fraction of 25%

$I_{wrap} = \pi[(r+t)^4 - r^4]/4$

c = distance between the axis of the specimen and point of application of load = (r+t)

σ = ultimate flexural strength = Mc/I

$= PL(r+t)/4I_{hybrid}$

δ = deflection at the mid span = $PL^3/48EI_{hybrid}$

E = Modulus of Elasticity = $(P/\delta) L^3/48I_{hybrid}$

EI = flexural rigidity or bending stiffness = $(P/\delta) L^3/48$

The load versus deflection data of a wood/HMR/epoxy/glass hybrid sample obtained during a 3 point bending test is given below:

point #	deflection (in)	load (lbs)
1	0	0.02685
2	0.00007	0.02685
3	0.00034	0.02685
4	0.00061	0.08054
5	0.00087	0.16108
6	0.00114	0.16108
7	0.00141	0.16108
8	0.00168	0.18792
9	0.00194	0.16108
10	0.00221	0.16108
11	0.00247	0.16108
12	0.00274	0.16108
13	0.00301	0.18792
14	0.00327	0.16108
15	0.00354	0.16108
16	0.00381	0.16108
17	0.00407	0.16108
18	0.00434	0.16108
19	0.00461	0.16108
20	0.00487	0.16108
21	0.00514	0.16108
22	0.00541	0.16108
23	0.00568	0.18792
24	0.00594	0.18792
25	0.00621	0.16108
26	0.00647	0.18792
27	0.00674	0.18792
28	0.00701	0.18792
29	0.00727	0.18792
30	0.00754	0.18792
31	0.00781	0.18792
32	0.00807	0.16108
33	0.00834	0.18792
34	0.00861	0.18792
35	0.00887	0.16108
36	0.00914	0.18792
37	0.00941	0.16108
38	0.00968	0.16108
39	0.00994	0.16108
40	0.01021	0.16108
41	0.01047	0.16108
42	0.01074	0.16108
43	0.01101	0.16108
44	0.01127	0.16108
45	0.01154	0.16108
46	0.01181	0.16108
47	0.01208	0.16108
48	0.01234	0.16108
49	0.01261	0.16108
50	0.01287	0.18792
51	0.01314	0.16108
52	0.01341	0.16108
53	0.01367	0.16108
54	0.01394	0.16108
55	0.01421	0.16108
56	0.01447	0.16108
57	0.01474	0.16108
58	0.01501	0.16108
59	0.01527	0.16108
60	0.01554	0.18792
61	0.01581	0.18792
62	0.01608	0.48323
63	0.01634	0.72484
64	0.01661	0.91275
65	0.01687	0.99329
66	0.01714	1.0201
67	0.01741	1.1544
68	0.01767	1.3691
69	0.01794	1.4228
70	0.01821	1.5034
71	0.01848	1.4228
72	0.01874	1.1275
73	0.01901	0.91275
74	0.01927	0.67114
75	0.01954	0.77853
76	0.01981	1.047
77	0.02008	1.3423
78	0.02034	1.6644
79	0.02061	2.0403
80	0.02087	2.3893
81	0.02114	2.7651
82	0.02141	3.1678
83	0.02167	3.5436
84	0.02194	3.9463
85	0.02221	4.349
86	0.02248	4.7785
87	0.02274	5.1812
88	0.02301	5.5839
89	0.02327	6.0134
90	0.02354	6.3892
91	0.02381	6.7919
92	0.02408	7.1678
93	0.02434	7.5973
94	0.02461	7.9731
95	0.02487	8.4027
96	0.02514	8.7785
97	0.02541	9.208
98	0.02567	9.5302
99	0.02594	9.9329
100	0.02621	10.282

point #	deflection (in)	load (lbs)
101	0.02648	10.685
102	0.02674	11.06
103	0.02701	11.49
104	0.02727	11.866
105	0.02754	12.295
106	0.02781	12.671
107	0.02807	13.127
108	0.02834	13.53
109	0.02861	13.933
110	0.02888	14.174
111	0.02914	14.416
112	0.02941	14.738
113	0.02967	14.846
114	0.02994	14.899
115	0.03021	14.98
116	0.03048	14.98
117	0.03074	15.034
118	0.03101	15.114
119	0.03127	15.168
120	0.03154	15.221
121	0.03181	15.302
122	0.03207	15.383
123	0.03234	15.463
124	0.03261	15.517
125	0.03288	15.517
126	0.03314	15.597
127	0.03341	15.624
128	0.03367	15.624
129	0.03394	15.651
130	0.03421	15.678
131	0.03448	15.732
132	0.03474	15.758
133	0.03501	15.785
134	0.03528	15.812
135	0.03554	15.893
136	0.03581	15.946
137	0.03607	15.973
138	0.03634	16.054
139	0.03661	16.107
140	0.03688	16.134
141	0.03714	16.215
142	0.03741	16.268
143	0.03767	16.322
144	0.03794	16.483
145	0.03821	16.51
146	0.03848	16.591
147	0.03874	16.698
148	0.03901	17.02
149	0.03928	17.235
150	0.03954	17.342

point #	deflection (in)	load (lbs)
151	0.03981	17.476
152	0.04007	17.557
153	0.04034	17.745
154	0.04061	17.825
155	0.04088	18.04
156	0.04114	18.174
157	0.04141	18.443
158	0.04167	18.685
159	0.04194	19.034
160	0.04221	19.383
161	0.04247	19.731
162	0.04274	20.08
163	0.04301	20.403
164	0.04328	20.805
165	0.04354	21.235
166	0.04381	21.664
167	0.04407	22.094
168	0.04434	22.523
169	0.04461	22.98
170	0.04488	23.436
171	0.04514	23.893
172	0.04541	24.295
173	0.04568	24.778
174	0.04594	25.154
175	0.04621	25.611
176	0.04647	26.013
177	0.04674	26.443
178	0.04701	26.846
179	0.04728	27.275
180	0.04754	27.678
181	0.04781	28.107
182	0.04807	28.51
183	0.04834	28.966
184	0.04861	29.342
185	0.04888	29.799
186	0.04914	30.201
187	0.04941	30.658
188	0.04968	31.033
189	0.04994	31.49
190	0.05021	31.866
191	0.05047	32.295
192	0.05074	32.671
193	0.05101	33.101
194	0.05128	33.45
195	0.05154	33.879
196	0.05181	34.255
197	0.05208	34.658
198	0.05234	35.06
199	0.05261	35.49
200	0.05288	35.866

point #	deflection (in)	load (lbs)
201	0.05314	36.268
202	0.05341	36.671
203	0.05368	37.047
204	0.05394	37.423
205	0.05421	37.799
206	0.05447	38.174
207	0.05474	38.577
208	0.05501	38.953
209	0.05528	39.302
210	0.05554	39.731
211	0.05581	40.107
212	0.05608	40.483
213	0.05634	40.859
214	0.05661	41.235
215	0.05687	41.584
216	0.05714	41.96
217	0.05741	42.309
218	0.05768	42.711
219	0.05794	43.06
220	0.05821	43.463
221	0.05847	43.812
222	0.05874	44.215
223	0.05901	44.564
224	0.05928	44.966
225	0.05954	45.315
226	0.05981	45.718
227	0.06008	46.121
228	0.06034	46.55
229	0.06061	46.926
230	0.06087	47.382
231	0.06114	47.758
232	0.06141	48.215
233	0.06168	48.59
234	0.06194	49.047
235	0.06221	49.423
236	0.06248	49.852
237	0.06274	50.228
238	0.06301	50.684
239	0.06328	51.114
240	0.06354	51.57
241	0.06381	51.946
242	0.06408	52.403
243	0.06434	52.859
244	0.06461	53.288
245	0.06487	53.691
246	0.06514	54.094
247	0.06541	54.523
248	0.06568	54.98
249	0.06594	55.409
250	0.06621	55.866

point #	deflection (in)	load (lbs)
251	0.06648	56.322
252	0.06674	56.752
253	0.06701	57.208
254	0.06728	57.637
255	0.06754	58.067
256	0.06781	58.47
257	0.06808	58.926
258	0.06834	59.329
259	0.06861	59.812
260	0.06888	60.215
261	0.06914	60.698
262	0.06941	61.101
263	0.06968	61.584
264	0.06994	61.986
265	0.07021	62.416
266	0.07048	62.819
267	0.07074	63.275
268	0.07101	63.678
269	0.07127	64.134
270	0.07154	64.537
271	0.07181	65.02
272	0.07208	65.44901
273	0.07234	65.90601
274	0.07261	66.30901
275	0.07288	66.792
276	0.07314	67.194
277	0.07341	67.678
278	0.07368	68.08
279	0.07394	68.59
280	0.07421	69.02
281	0.07448	69.50301
282	0.07474	69.93301
283	0.07501	70.416
284	0.07527	70.872
285	0.07554	71.356
286	0.07581	71.785
287	0.07608	72.215
288	0.07634	72.67101
289	0.07661	73.12701
290	0.07688	73.58401
291	0.07714	74.067
292	0.07741	74.523
293	0.07768	75.007
294	0.07794	75.46301
295	0.07821	75.89201
296	0.07848	76.34901
297	0.07874	76.778
298	0.07901	77.262
299	0.07928	77.691
300	0.07954	78.147

point #	deflection (in)	load (lbs)
301	0.07981	78.577
302	0.08008	79.06001
303	0.08034	79.49001
304	0.08061	79.97301
305	0.08088	80.402
306	0.08114	80.859
307	0.08141	81.262
308	0.08168	81.718
309	0.08194	82.121
310	0.08221	82.604
311	0.08248	83.006
312	0.08274	83.49001
313	0.08301	83.89201
314	0.08328	84.37601
315	0.08354	84.75101
316	0.08488	86.899
317	0.08621	89.02
318	0.08754	91.11401
319	0.08888	93.20801
320	0.09021	95.16801
321	0.09154	97.23501
322	0.09288	99.11401
323	0.09421	101.15
324	0.09554	102.98
325	0.09688	105.02
326	0.09821	106.95
327	0.09954	108.99
328	0.10088	110.87
329	0.10221	112.86
330	0.10354	114.79
331	0.10488	116.72
332	0.10621	118.66
333	0.10754	120.59
334	0.10888	122.58
335	0.11021	124.46
336	0.11154	126.39
337	0.11288	128.27
338	0.11421	130.15
339	0.11554	132.08
340	0.11688	133.96
341	0.11821	135.84
342	0.11954	137.72
343	0.12088	139.54
344	0.12221	141.37
345	0.12354	143.14
346	0.12488	144.97
347	0.12621	146.68
348	0.12754	148.51
349	0.12888	150.23
350	0.13021	152
351	0.13154	153.66
352	0.13288	155.44
353	0.13421	157.1
354	0.13554	158.82
355	0.13688	160.43
356	0.13821	162.09
357	0.13954	163.76
358	0.14088	165.42
359	0.14221	167.09
360	0.14355	168.75
361	0.14488	170.31
362	0.14621	171.92
363	0.14755	173.42
364	0.14888	175.03
365	0.15021	176.48
366	0.15155	178.04
367	0.15288	179.54
368	0.15421	181.05
369	0.15554	182.44
370	0.15688	183.89
371	0.15821	185.23
372	0.15954	186.63
373	0.16088	188.08
374	0.16221	189.42
375	0.16354	190.87
376	0.16488	192.21
377	0.16621	193.56
378	0.16754	194.9
379	0.16888	196.11
380	0.17021	197.31
381	0.17154	198.52
382	0.17288	199.6
383	0.17421	200.67
384	0.17554	201.88
385	0.17688	202.95
386	0.17821	204.03
387	0.17954	204.97
388	0.18088	206.17
389	0.18221	207.38
390	0.18354	208.46
391	0.18488	209.66
392	0.18621	210.87
393	0.18755	212.08
394	0.18888	213.15
395	0.19021	214.36
396	0.19154	215.57
397	0.19288	216.64
398	0.19421	217.72
399	0.19555	218.66
400	0.19687	219.19

point #	deflection (in)	load (lbs)
401	0.19821	219.73
402	0.19954	220.27
403	0.20088	220.94
404	0.20221	221.74
405	0.20355	222.55
406	0.20488	223.36
407	0.20621	224.16
408	0.20754	223.76
409	0.20888	224.16
410	0.21021	224.56
411	0.21155	225.23
412	0.21288	225.91
413	0.21421	226.58
414	0.21554	227.25
415	0.21688	228.05
416	0.21821	228.72
417	0.21955	229.4
418	0.22088	230.2
419	0.22221	230.74
420	0.22354	231.54
421	0.22488	232.21
422	0.22621	233.02
423	0.22754	233.69
424	0.22888	234.36
425	0.23021	235.03
426	0.23155	235.7
427	0.23288	236.24
428	0.23421	236.91
429	0.23554	237.58
430	0.23688	238.39
431	0.23821	238.93
432	0.23955	239.73
433	0.24088	240.4
434	0.24221	241.21
435	0.24354	241.74
436	0.24488	242.55
437	0.24621	243.22
438	0.24755	243.89
439	0.24888	244.43
440	0.25021	245.1
441	0.25154	245.64
442	0.25288	246.17
443	0.25421	246.58
444	0.25555	246.98
445	0.25688	247.38
446	0.25821	247.78
447	0.25954	248.19
448	0.26088	248.72
449	0.26221	249.13
450	0.26355	249.53

point #	deflection (in)	load (lbs)
451	0.26488	249.93
452	0.26621	250.2
453	0.26754	250.6
454	0.26888	251.01
455	0.27021	251.27
456	0.27155	251.68
457	0.27288	251.95
458	0.27421	252.21
459	0.27555	252.35
460	0.27688	252.62
461	0.27821	252.89
462	0.27955	253.02
463	0.28088	253.42
464	0.28221	253.69
465	0.28355	253.82
466	0.28488	254.09
467	0.28621	254.5
468	0.28755	254.76
469	0.28888	255.03
470	0.29021	255.44
471	0.29155	255.7
472	0.29288	255.97
473	0.29421	256.38
474	0.29554	256.64
475	0.29688	256.78
476	0.29821	256.91
477	0.29955	257.05
478	0.30088	257.05
479	0.30222	257.31
480	0.30354	257.45
481	0.30488	257.85
482	0.30621	258.12
483	0.30755	258.39
484	0.30888	258.79
485	0.31022	259.19
486	0.31154	259.6
487	0.31288	260
488	0.31421	260.4
489	0.31555	260.94
490	0.31688	261.34
491	0.31822	261.88
492	0.31955	262.28
493	0.32088	262.82
494	0.32221	263.22
495	0.32355	263.62
496	0.32488	263.89
497	0.32621	264.16
498	0.32755	264.56
499	0.32888	264.97
500	0.33021	265.23

point #	deflection (in)	load (lbs)
501	0.33155	265.5
502	0.33288	265.77
503	0.33421	265.91
504	0.33555	266.17
505	0.33688	266.44
506	0.33821	266.58
507	0.33955	266.84
508	0.34088	267.11
509	0.34221	267.38
510	0.34355	267.78
511	0.34488	268.19
512	0.34622	268.59
513	0.34755	268.99
514	0.34888	269.53
515	0.35021	269.93
516	0.35155	270.2
517	0.35288	270.33
518	0.35422	270.6
519	0.35555	270.87
520	0.35688	271.27
521	0.35821	271.54
522	0.35955	270.6
523	0.36088	270.87
524	0.36222	271.14
525	0.36328	257.45
526	0.36461	257.58
527	0.36595	257.99
528	0.36728	258.66
529	0.36861	259.33
530	0.36995	260
531	0.37128	260.67
532	0.37262	261.34
533	0.37395	262.01
534	0.37527	262.68
535	0.37661	263.36
536	0.37794	263.89
537	0.37928	264.43
538	0.38061	264.97
539	0.38194	265.5
540	0.38328	266.04
541	0.38461	266.58
542	0.38595	266.98
543	0.38728	267.38
544	0.38862	267.78
545	0.38995	268.05
546	0.39128	268.32
547	0.39261	268.72
548	0.39394	268.99
549	0.39528	269.4
550	0.39661	269.66

point #	deflection (in)	load (lbs)
551	0.39794	269.93
552	0.39928	270.07
553	0.40061	270.47
554	0.40195	270.6
555	0.40328	270.74
556	0.40462	270.87
557	0.40595	271.14
558	0.40728	271.27
559	0.40862	271.41
560	0.40995	271.54
561	0.41128	271.54
562	0.41155	271.68
563	0.41288	271.68
564	0.41422	271.54
565	0.41555	271.27
566	0.41661	170.74

In order to evaluate the mechanical properties, a graph of the load versus deflection data is plotted. The straight-line portion of the curve is plotted again with zeroed intercept. This is done by subtracting the initial values of load and deflection from all the subsequent values. The slope of the straight-line portion of the curve gives the value of (P/δ).

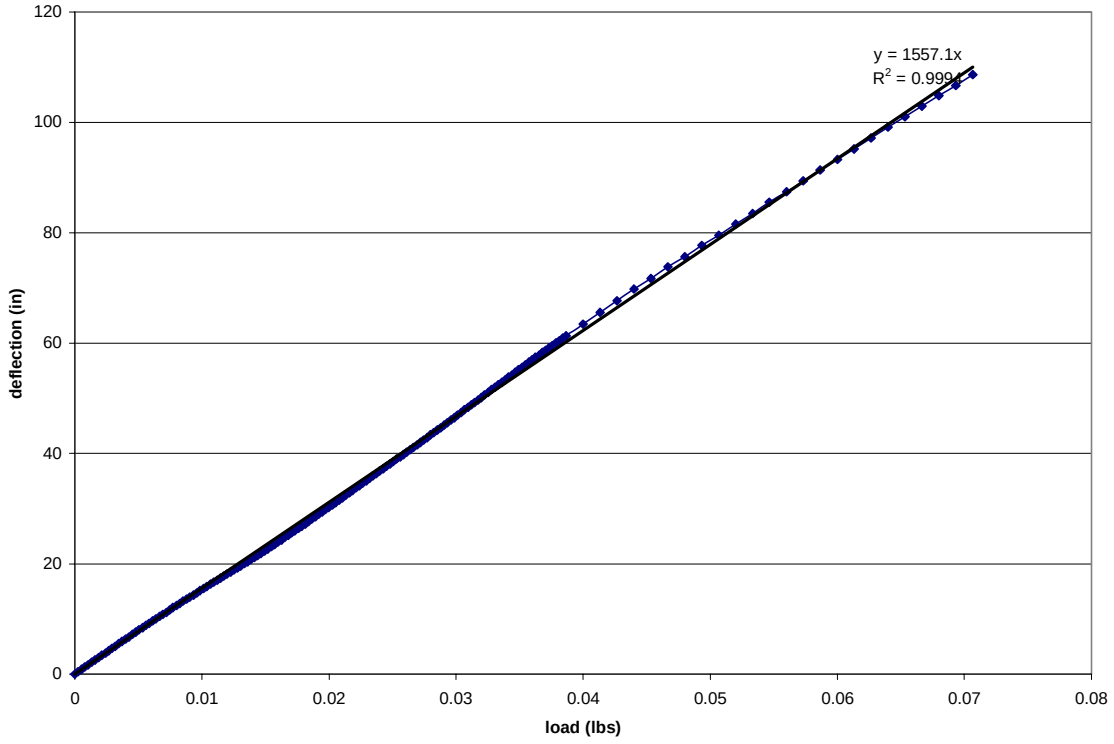

Figure B1: load versus deflection data of wood/HMR/epoxy/glass hybrid with zeroed intercept

Using the graph and the formulae listed, the following data is calculated:

property	**Value**	**Units**
r+t	0.301	inches
L	6	inches
P	271.7	lbs
P/δ	1557.1	lbs/in
I_{wood}	0.0031	in^4
I_{hybrid}	8.38 E-03	in^4
σ	1.46 E+04	psi
E	8.36E+05	psi
EI	7.01 E+03	$lb\text{-}in^2$

Table B1: 6-cycle aging data of wood/HMR/epoxy/glass hybrid samples:

Condition	P (lb)	R (in)	I (in^4)	σ (psi)	P/δ	E (psi)	EI (psi)
Unaged	287.24	0.305	7.76 E-03	1.69E+04	1953.9	1.13E+06	8.8E+03
Cycle 1	221.9	0.305	7.76 E-03	1.31E+04	1556.3	0.90E+06	7.0E+03
Cycle 2	340.54	0.32	9.55 E-03	1.71E+04	2386	1.12E+06	10.7E+03
Cycle 3	254.9	0.295	6.70 E-03	1.68E+04	1615.4	1.08E+06	7.24E+03
Cycle 4	251.4	0.315	8.93 E-03	1.33E+04	1911.3	0.96E+06	8.59E+03
Cycle 6	178.1	0.298	7.01 E-03	1.14E+04	1517.8	0.97E+06	6.86E+03

Table B2: 6-cycle aging data of wood/epoxy/glass hybrid samples:

Condition	P (lb)	R (in)	I (in^4)	σ (psi)	P/δ	E (psi)	EI (psi)
Unaged	299.5	0.292	6.40 E-03	2.05E+04	2552.3	1.79E+06	11.47E+03
Cycle 1	155	0.31	8.33 E-03	8.65E+03	1328.8	0.72E+06	5.98E+03
Cycle 2	123.87	0.289	6.11 E-03	8.78E+03	1213.4	0.89E+06	5.46E+03
Cycle 3	120.38	0.283	5.56 E-03	9.18E+03	891.79	0.72E+06	4.01E+03
Cycle 4	108.9	0.292	6.40 E-03	7.45E+03	744.96	0.52E+06	3.35E+03
Cycle 6	166.5	0.305	7.76 E-03	9.82E+03	1196.6	0.69E+06	5.38E+03

Table B3: 6-cycle aging data of unwrapped wood samples:

Condition	P (lb)	R (in)	I (in^4)	σ (psi)	P/δ	E (psi)	EI (psi)
Unaged	133.25	0.25	3.07E-03	1.63E+04	743.83	1.09E+06	3.35E+03
Cycle 1	147	0.25	3.07E-03	1.80E+04	772.75	1.13E+06	3.48E+03
Cycle 2	164.1	0.25	3.07E-03	2.01E+04	940.88	1.38E+06	4.23E+03
Cycle 3	154.4	0.25	3.07E-03	1.89E+04	917.68	1.35E+06	4.13E+03
Cycle 4	171.8	0.25	3.07E-03	2.10E+04	948.88	1.39E+06	4.27E+03
Cycle 6	160.1	0.25	3.07E-03	1.96E+04	859.63	1.26E+06	3.87E+03

Table B4: Data of wood/HMR/epoxy/glass samples exposed to freeze-thaw cycling in acidic solution of pH 3:

Number of days	P (lb)	r (in)	I (in^4)	σ (psi)	P/δ	E (psi)	EI (psi)
5	271.7	0.301	7.33E-03	1.67E+04	1557.1	0.96E+06	0.70E+04
5	221.2	0.297	6.91E-03	1.43E+04	1847.2	1.21E+06	0.83E+04
				1.55E+04		1.08E+06	0.76E+04
15	148.89	0.295	6.70E-03	9.83E+03	1248.3	0.84E+06	5.62E+03
15	164.4	0.295	6.70E-03	1.09E+04	1407.2	0.94E+06	6.33E+03
				1.03E+04		0.89E+06	5.97E+03
25	145	0.303	7.49E-03	8.79E+03	1212.7	0.73E+06	5.46E+03
25	156.9	0.295	6.70E-03	1.04E+04	1225.5	0.82E+06	5.51E+03
				9.57E+03		0.78E+06	5.49E+03

Table B5: Data of wood/HMR/epoxy/glass samples exposed to freeze-thaw cycling in alkaline solution of pH 13:

Number of days	P (lb)	r (in)	I (in^4)	σ (psi)	P/δ	E (psi)	EI (psi)
5	274.2	0.297	6.91E-03	1.77E+04	1729.6	1.13E+06	7.8E+03
5	257.9	0.297	6.91E-03	1.66E+04	1895.3	1.24E+06	8.5E+03
				1.72E+04		1.18E+06	8.16E+03
15	215.97	0.295	6.70E-03	1.43E+04	1330	0.89E+06	5.99E+03
25	170.5	0.298	6.96E-03	1.09E+04	1530	0.99E+06	6.86E+03
25	193.69	0.299	7.06E-03	1.23E+04	1241.9	0.79E+06	5.59E+03
				1.16E+04		0.89E+06	6.24E+03

Table B6: Data of wood/HMR/epoxy/glass samples exposed to freeze-thaw cycling in neutral solution of pH 7:

Number of days	P (lb)	r (in)	I (in^4)	σ (psi)	P/δ	E (psi)	EI (psi)
5	206	0.297	6.91E-03	1.33E+04	1060.8	0.69E+06	4.78E+03
15	136.59	0.297	6.91E-03	8.81E+03	794.5	0.52E+06	3.58E+03
25	174.12	0.295	6.70E-03	1.15E+04	1310.6	0.88E+06	5.90E+03

Table B7: Data of wood/HMR/epoxy/glass samples exposed to freeze-thaw cycling in 3% salt water solution:

Number of days	P (lb)	r (in)	I (in^4)	σ (psi)	P/δ	E (psi)	EI (psi)
5	266.6	0.301	7.33E-03	1.64E+04	1752.1	1.08E+06	7.88E+03
15	228.7	0.3	7.22E-03	1.43E+04	1653.7	1.03E+06	7.44E+03
25	194.23	0.295	6.70E-03	1.28E+04	1375.5	0.92E+06	6.19E+03

Table B8: Data of wood/epoxy/glass samples exposed to freeze-thaw cycling in neutral solution of pH 7:

Number of days	P (lb)	r (in)	I (in^4)	σ (psi)	P/δ	E (psi)	EI (psi)
5	225.52	0.288	5.98E-03	1.63 E+04	1444.4	1.09E+06	6.47E+03
15	139.76	0.295	6.70E-03	9.22E+03	1007.5	0.67E+06	4.53E+03
25	155.28	0.298	6.96E-03	9.96E+03	1275	0.83E+06	5.74E+03

Table B9: Data of wood/epoxy/glass samples exposed to freeze-thaw cycling in 3% salt water solution:

Number of days	P (lb)	r (in)	I (in^4)	σ (psi)	P/δ	E (psi)	EI (psi)
5	222.1	0.297	6.91E-03	1.43E+04	1489.3	0.97E+06	6.73E+03
15	179.17	0.284	5.70E-03	1.34E+04	1443	1.14E+06	6.47E+03
25	175.57	0.285	5.75E-03	1.31E+04	1217.7	0.96E+06	5.48E+03

Appendix B.3

Sample Calculations for the Generation of a Master Curve from Mechanical Spectroscopy Data

During the frequency/temperature sweep of a hybrid specimen, the storage modulus data over a range of frequency and at different isothermal temperatures is obtained. The following is the data of a wood/HMR/epoxy/glass hybrid subjected to freeze-thaw cycling in water for 25 days.

Data Set A:

Temp = 40C			Temp = 45C			Temp = 50C	
w	G'		w	G'		w	G'
rad/s	dyn/cm.sq.		rad/s	dyn/cm.sq.		rad/s	dyn/cm.sq.
0.1	9.02E+09		0.1	8.48E+09		0.1	8.08E+09
0.158489	8.59E+09		0.158489	8.28E+09		0.158489	7.91E+09
0.25119	8.67E+09	*	0.25119	8.36E+09		0.25119	8E+09
0.398109	8.73E+09		0.398109	8.43E+09		0.398109	8.08E+09
0.630966	8.79E+09		0.630966	8.5E+09		0.630966	8.17E+09
1.00003	8.84E+09		1.00003	8.56E+09		1.00003	8.24E+09
1.58496	8.9E+09		1.58496	8.61E+09		1.58496	8.3E+09
2.51202	8.94E+09		2.51202	8.67E+09	*	2.51202	8.37E+09
3.98132	9E+09		3.98132	8.72E+09		3.98132	8.43E+09
6.31006	9.04E+09		6.31006	8.77E+09		6.31006	8.48E+09
10.0007	9.09E+09		10.0007	8.82E+09		10.0007	8.54E+09
15.8501	9.13E+09		15.8501	8.87E+09		15.8501	8.58E+09
25.1206	9.18E+09		25.1206	8.91E+09		25.1206	8.63E+09
39.8135	9.24E+09		39.8135	8.96E+09		39.8135	8.69E+09
63.1006	9.31E+09		63.1006	9.04E+09		63.1006	8.77E+09
100	9.46E+09		100	9.18E+09		100	8.9E+09

Temp = 50C

w	G'
rad/s	dyn/cm.sq.
0.1	8.08E+09
0.158489	7.91E+09
0.25119	8E+09
0.398109	8.08E+09
0.630966	8.17E+09
1.00003	8.24E+09
1.58496	8.3E+09
2.51202	8.37E+09
3.98132	8.43E+09
6.31006	8.48E+09
10.0007	8.54E+09
15.8501	8.58E+09
25.1206	8.63E+09
39.8135	8.69E+09
63.1006	8.77E+09
100	8.9E+09

Temp = 55C

w	G'
rad/s	dyn/cm.sq.
0.1	7.47E+09
0.158489	7.4E+09
0.25119	7.5E+09
0.398109	7.62E+09
0.630966	7.7E+09
1.00003	7.81E+09
1.58496	7.89E+09
2.51202	7.97E+09
3.98132	8.04E+09
6.31006	8.11E+09
10.0007	8.17E+09
15.8501	8.23E+09
25.1206	8.3E+09
39.8135	8.36E+09
63.1006	8.44E+09
100	8.58E+09

Temp = 60C

w	G'
rad/s	dyn/cm.sq.
0.1	6.43E+09
0.158489	6.42E+09
0.25119	6.6E+09
0.398109	6.76E+09
0.630966	6.92E+09
1.00003	7.06E+09
1.58496	7.2E+09
2.51202	7.31E+09
3.98132	7.41E+09
6.31006	7.52E+09
10.0007	7.62E+09
15.8501	7.71E+09
25.1206	7.8E+09
39.8135	7.88E+09
63.1006	7.99E+09
100	8.14E+09

Temp = 65C

w	G'
rad/s	dyn/cm.sq.
0.1	5.02E+09
0.158489	5.1E+09
0.25119	5.3E+09
0.398109	5.5E+09
0.630966	5.71E+09
1.00003	5.9E+09
1.58496	6.09E+09
2.51202	6.26E+09
3.98132	6.43E+09
6.31006	6.59E+09
10.0007	6.74E+09
15.8501	6.89E+09
25.1206	7.03E+09
39.8135	7.17E+09
63.1006	7.31E+09
100	7.5E+09

Temp = 70C

w	G'
rad/s	dyn/cm.sq.
0.1	3.62E+09
0.158489	3.84E+09
0.25119	4.05E+09
0.398109	4.24E+09
0.630966	4.45E+09
1.00003	4.65E+09
1.58496	4.84E+09
2.51202	5.03E+09
3.98132	5.25E+09
6.31006	5.44E+09
10.0007	5.63E+09
15.8501	5.81E+09
25.1206	5.99E+09
39.8135	6.17E+09
63.1006	6.36E+09
100	6.59E+09

Temp = 75C

w	G'
rad/s	dyn/cm.sq.
0.1	2.73E+09
0.158489	2.91E+09
0.25119	3.03E+09
0.398109	3.19E+09
0.630966	3.35E+09
1.00003	3.54E+09
1.58496	3.71E+09
2.51202	3.89E+09
3.98132	4.07E+09
6.31006	4.26E+09
10.0007	4.46E+09
15.8501	4.67E+09
25.1206	4.88E+09
39.8135	5.09E+09
63.1006	5.31E+09
100	5.56E+09

Temp = 80C

w	G'
rad/s	dyn/cm.sq.
0.1	2.09E+09
0.158489	2.14E+09
0.25119	2.25E+09
0.398109	2.33E+09
0.630966	2.45E+09
1.00003	2.58E+09
1.58496	2.71E+09
2.51202	2.85E+09
3.98132	3.02E+09
6.31006	3.19E+09
10.0007	3.38E+09
15.8501	3.57E+09
25.1206	3.76E+09
39.8135	3.96E+09
63.1006	4.18E+09
100	4.44E+09

Temp = 85C

w	G'
rad/s	dyn/cm.sq.
0.1	1.92E+09
0.158489	1.83E+09
0.25119	1.84E+09
0.398109	1.89E+09
0.630966	1.95E+09
1.00003	2.02E+09
1.58496	2.09E+09
2.51202	2.17E+09
3.98132	2.27E+09
6.31006	2.39E+09
10.0007	2.52E+09
15.8501	2.66E+09
25.1206	2.82E+09
39.8135	2.99E+09
63.1006	3.18E+09
100	3.41E+09

Temp = 90C

w	G'
rad/s	dyn/cm.sq.
0.1	1.82E+09
0.158489	1.69E+09
0.25119	1.69E+09
0.398109	1.74E+09
0.630966	1.76E+09
1.00003	1.78E+09
1.58496	1.81E+09
2.51202	1.86E+09
3.98132	1.9E+09
6.31006	1.96E+09
10.0007	2.03E+09
15.8501	2.11E+09
25.1206	2.2E+09
39.8135	2.32E+09
63.1006	2.45E+09
100	2.62E+09

Temp = 95C

w	G'
rad/s	dyn/cm.sq.
0.1	1.67E+09
0.158489	1.68E+09
0.25119	1.67E+09
0.398109	1.69E+09
0.630966	1.71E+09
1.00003	1.71E+09
1.58496	1.73E+09
2.51202	1.74E+09
3.98132	1.76E+09
6.31006	1.79E+09
10.0007	1.83E+09
15.8501	1.87E+09
25.1206	1.92E+09
39.8135	1.99E+09
63.1006	2.07E+09
100	2.18E+09

Temp = 100C

w	G'
rad/s	dyn/cm.sq.
0.1	1.63E+09
0.158489	1.63E+09
0.25119	1.67E+09
0.398109	1.65E+09
0.630966	1.67E+09
1.00003	1.69E+09
1.58496	1.69E+09
2.51202	1.71E+09
3.98132	1.72E+09
6.31006	1.74E+09
10.0007	1.75E+09
15.8501	1.77E+09
25.1206	1.8E+09
39.8135	1.84E+09
63.1006	1.88E+09
100	1.95E+09

For generation of the master curve, 40^0C is used as the reference temperature. Therefore, all the G' versus ω curves at different temperatures are shifted with respect to 40 ^{0}C. To do this, the value of G′ at 45^0 C (say G'_1) that is closest to the value of G′ at 40^0 C (say G'_2) is chosen. Let ω_1 and ω_2 be the frequency corresponding to G'_1 and G'_2 respectively. The frequency values at 45^0 C are then multiplied by a shift factor of (ω_2/ω_1) without changing the G′ values. This means that the data at 45^0 C is shifted with respect to 40^0C. In the next step, the value of G′ at 50^0 C (say G'_3) that is closest to the value of G′ at 45^0C (say G'_4) is chosen. Let ω_3 and ω_4 be the frequency corresponding to G'_3 and G'_4 respectively. The frequency values at 50^0C are then multiplied by a shift factor of (ω_4/ω_3) without changing the G′ values. This shifts the data at 50^0C to 40^0C. This process is repeated until all the data up to 100^0C is shifted. A plot of the generated G′ versus ω data gives the master curve.

For illustration, the data at 40^0C and 45^0C before and after shifting is shown below.

data at 40C (ref T*)	
À	G'
rad/s	dyn/cm.sq.
0.1	9.02E+09
0.158489	8.59E+09
0.25119	8.67E+09
0.398109	8.73E+09
0.630966	8.79E+09
1.00003	8.84E+09
1.58496	8.9E+09
2.51202	8.94E+09
3.98132	9E+09
6.31006	9.04E+09
10.0007	9.09E+09
15.8501	9.13E+09
25.1206	9.18E+09
39.8135	9.24E+09
63.1006	9.31E+09
100	9.46E+09

data at 45C before shift	
w	**G'**
rad/s	**dyn/cm.sq.**
0.1	8.48E+09
0.158489	8.28E+09
0.25119	8.36E+09
0.398109	8.43E+09
0.630966	8.5E+09
1.00003	8.56E+09
1.58496	8.61E+09
2.51202	8.67E+09
3.98132	8.72E+09
6.31006	8.77E+09
10.0007	8.82E+09
15.8501	8.87E+09
25.1206	8.91E+09
39.8135	8.96E+09
63.1006	9.04E+09
100	9.18E+09

data at 45C after shift	
À	G'
rad/s	dyn/cm.sq.
0.01	8.48E+09
0.015848	8.28E+09
0.025118	8.36E+09
0.039809	8.43E+09
0.063094	8.5E+09
0.099998	8.56E+09
0.158488	8.61E+09
0.25119	8.67E+09
0.398113	8.72E+09
0.630976	8.77E+09
1.000022	8.82E+09
1.584934	8.87E+09
2.51194	8.91E+09
3.98116	8.96E+09
6.309759	9.04E+09
9.999522	9.18E+09

ref T* = reference temperature

The entire data shifted with respect to 40^0C is given in data set B.

Data Set B:

data at 40C (ref T*)	
À	G'
rad/s	dyn/cm.sq.
0.1	9.02E+09
0.158489	8.59E+09
0.25119	8.67E+09
0.398109	8.73E+09
0.630966	8.79E+09
1.00003	8.84E+09
1.58496	8.9E+09
2.51202	8.94E+09
3.98132	9E+09
6.31006	9.04E+09
10.0007	9.09E+09
15.8501	9.13E+09
25.1206	9.18E+09
39.8135	9.24E+09
63.1006	9.31E+09
100	9.46E+09

data at 45C	
À	G'
rad/s	dyn/cm.sq.
0.01	8.48E+09
0.015848	8.28E+09
0.025118	8.36E+09
0.039809	8.43E+09
0.063094	8.5E+09
0.099998	8.56E+09
0.158488	8.61E+09
0.25119	8.67E+09
0.398113	8.72E+09
0.630976	8.77E+09
1.000022	8.82E+09
1.584934	8.87E+09
2.51194	8.91E+09
3.98116	8.96E+09
6.309759	9.04E+09
9.999522	9.18E+09

data at 50C	
À	G'
rad/s	dyn/cm.sq
0.001	8.08E+09
0.001585	7.91E+09
0.002512	8E+09
0.003982	8.08E+09
0.006311	8.17E+09
0.010003	8.24E+09
0.015853	8.3E+09
0.025126	8.37E+09
0.039822	8.43E+09
0.063115	8.48E+09
0.10003	8.54E+09
0.158537	8.58E+09
0.251263	8.63E+09
0.398225	8.69E+09
0.631149	8.77E+09
1.000226	8.9E+09

data at 55C

À	G'
rad/s	dyn/cm.sq.
6.31E-05	7.47E+09
0.0001	7.4E+09
0.000159	7.5E+09
0.000251	7.62E+09
0.000398	7.7E+09
0.000631	7.81E+09
0.001	7.89E+09
0.001585	7.97E+09
0.002512	8.04E+09
0.003982	8.11E+09
0.006311	8.17E+09
0.010002	8.23E+09
0.015853	8.3E+09
0.025125	8.36E+09
0.03982	8.44E+09
0.063106	8.58E+09

data at 60C

À	G'
rad/s	dyn/cm.sq.
2.51E-06	6.43E+09
3.98E-06	6.42E+09
6.3E-06	6.6E+09
9.99E-06	6.76E+09
1.58E-05	6.92E+09
2.51E-05	7.06E+09
3.98E-05	7.2E+09
6.3E-05	7.31E+09
9.99E-05	7.41E+09
0.000158	7.52E+09
0.000251	7.62E+09
0.000398	7.71E+09
0.00063	7.8E+09
0.000999	7.88E+09
0.001584	7.99E+09
0.00251	8.14E+09

data at 65C R54

À	G'
rad/s	dyn/cm.sq
9.99E-08	5.02E+09
1.58E-07	5.1E+09
2.51E-07	5.3E+09
3.98E-07	5.5E+09
6.3E-07	5.71E+09
9.99E-07	5.9E+09
1.58E-06	6.09E+09
2.51E-06	6.26E+09
3.98E-06	6.43E+09
6.3E-06	6.59E+09
9.99E-06	6.74E+09
1.58E-05	6.89E+09
2.51E-05	7.03E+09
3.98E-05	7.17E+09
6.3E-05	7.31E+09
9.99E-05	7.5E+09

data at 70C

À	G'
rad/s	dyn/cm.sq.
6.3E-09	3.62E+09
9.99E-09	3.84E+09
1.58E-08	4.05E+09
2.51E-08	4.24E+09
3.98E-08	4.45E+09
6.3E-08	4.65E+09
9.99E-08	4.84E+09
1.58E-07	5.03E+09
2.51E-07	5.25E+09
3.98E-07	5.44E+09
6.31E-07	5.63E+09
9.99E-07	5.81E+09
1.58E-06	5.99E+09
2.51E-06	6.17E+09
3.98E-06	6.36E+09
6.3E-06	6.59E+09

data at 75C

À	G'
rad/s	dyn/cm.sq.
3.98E-10	2.73E+09
6.3E-10	2.91E+09
9.99E-10	3.03E+09
1.58E-09	3.19E+09
2.51E-09	3.35E+09
3.98E-09	3.54E+09
6.3E-09	3.71E+09
9.99E-09	3.89E+09
1.58E-08	4.07E+09
2.51E-08	4.26E+09
3.98E-08	4.46E+09
6.3E-08	4.67E+09
9.99E-08	4.88E+09
1.58E-07	5.09E+09
2.51E-07	5.31E+09
3.98E-07	5.56E+09

data at 80C

À	G'
rad/s	dyn/cm.sq
2.51E-11	2.09E+09
3.98E-11	2.14E+09
6.3E-11	2.25E+09
9.99E-11	2.33E+09
1.58E-10	2.45E+09
2.51E-10	2.58E+09
3.98E-10	2.71E+09
6.3E-10	2.85E+09
9.99E-10	3.02E+09
1.58E-09	3.19E+09
2.51E-09	3.38E+09
3.98E-09	3.57E+09
6.3E-09	3.76E+09
9.99E-09	3.96E+09
1.58E-08	4.18E+09
2.51E-08	4.44E+09

data at 85C

À	G'
rad/s	dyn/cm.sq.
1.58E-12	1.92E+09
2.51E-12	1.83E+09
3.98E-12	1.84E+09
6.3E-12	1.89E+09
9.99E-12	1.95E+09
1.58E-11	2.02E+09
2.51E-11	2.09E+09
3.98E-11	2.17E+09
6.3E-11	2.27E+09
9.99E-11	2.39E+09
1.58E-10	2.52E+09
2.51E-10	2.66E+09
3.98E-10	2.82E+09
6.3E-10	2.99E+09
9.99E-10	3.18E+09
1.58E-09	3.41E+09

data at 90C

À	G'
rad/s	dyn/cm.sq.
1.58E-13	1.82E+09
2.51E-13	1.69E+09
3.98E-13	1.69E+09
6.3E-13	1.74E+09
9.99E-13	1.76E+09
1.58E-12	1.78E+09
2.51E-12	1.81E+09
3.98E-12	1.86E+09
6.3E-12	1.9E+09
9.99E-12	1.96E+09
1.58E-11	2.03E+09
2.51E-11	2.11E+09
3.98E-11	2.2E+09
6.3E-11	2.32E+09
9.99E-11	2.45E+09
1.58E-10	2.62E+09

data at 95C

À	G'
rad/s	dyn/cm.sq
2.51E-14	1.67E+09
3.98E-14	1.68E+09
6.3E-14	1.67E+09
9.99E-14	1.69E+09
1.58E-13	1.71E+09
2.51E-13	1.71E+09
3.98E-13	1.73E+09
6.3E-13	1.74E+09
9.99E-13	1.76E+09
1.58E-12	1.79E+09
2.51E-12	1.83E+09
3.98E-12	1.87E+09
6.3E-12	1.92E+09
9.99E-12	1.99E+09
1.58E-11	2.07E+09
2.51E-11	2.18E+09

data at 100C

À	G'
rad/s	dyn/cm.sq
6.3E-15	1.63E+09
9.99E-15	1.63E+09
1.58E-14	1.67E+09
2.51E-14	1.65E+09
3.98E-14	1.67E+09
6.3E-14	1.69E+09
9.99E-14	1.69E+09
1.58E-13	1.71E+09
2.51E-13	1.72E+09
3.98E-13	1.74E+09
6.3E-13	1.75E+09
9.99E-13	1.77E+09
1.58E-12	1.8E+09
2.51E-12	1.84E+09
3.98E-12	1.88E+09
6.3E-12	1.95E+09

A graph of G′ versus w (or A) of data set B gives the master curve as shown in figure B2:

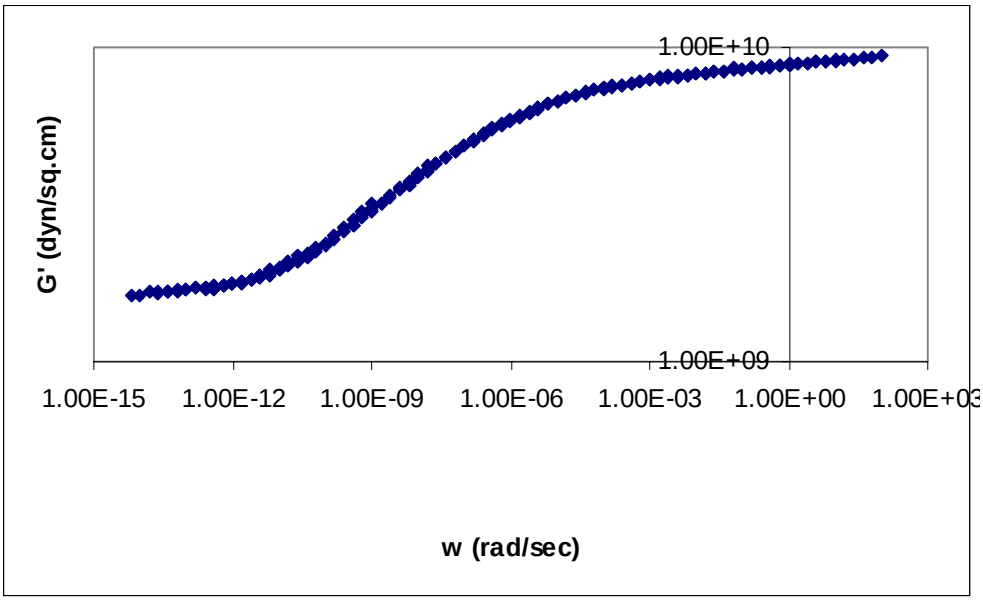

Figure B2: Master curve of wood/HMR/epoxy/glass hybrid subjected to freeze-thaw cycling in water for 25 days

APPENDIX C

Dynamic Spectra of Wood and Wood/HMR/Epoxy/Glass Hybrid Samples Under Unaged and Aged Conditions

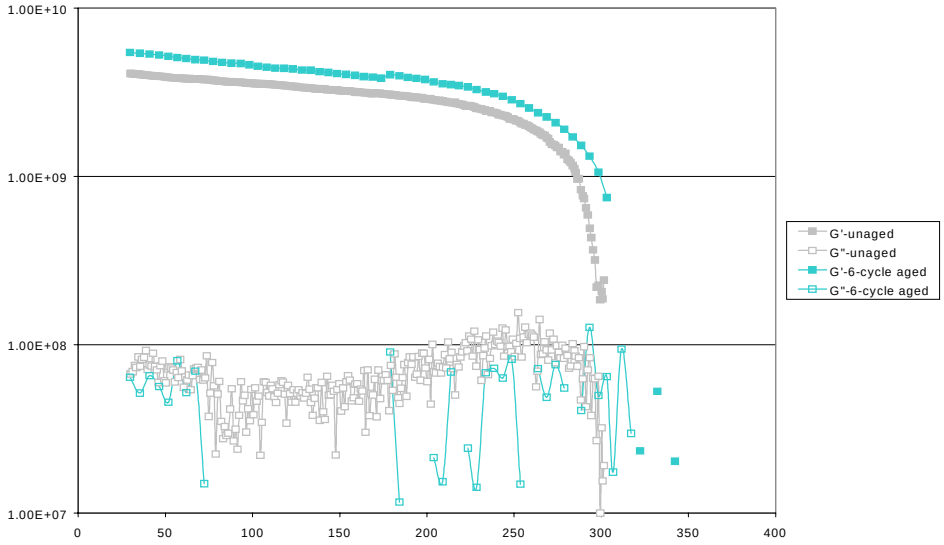

Figure C1: Dynamic properties of wood under unaged and 6-cycle aged conditions

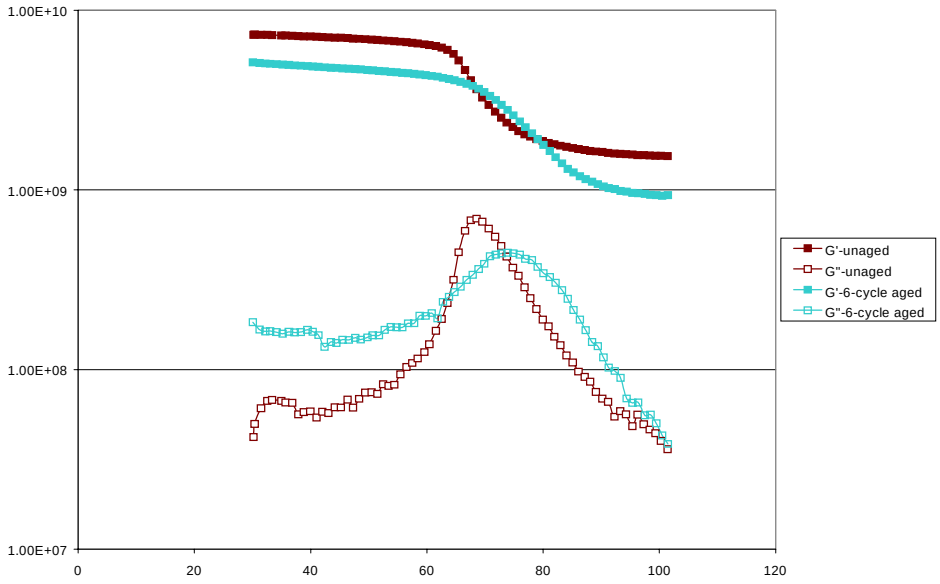

Figure C2: Dynamic properties of wood/HMR/epoxy/glass hybrid under unaged and 6-cycle aged conditions

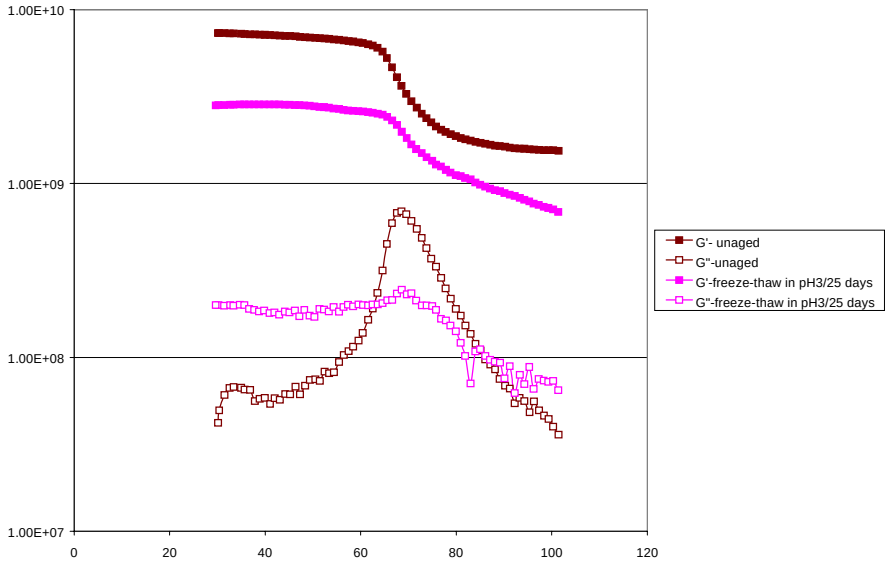

Figure C3: Dynamic properties of wood/HMR/epoxy/glass hybrid under unaged and acidic conditions

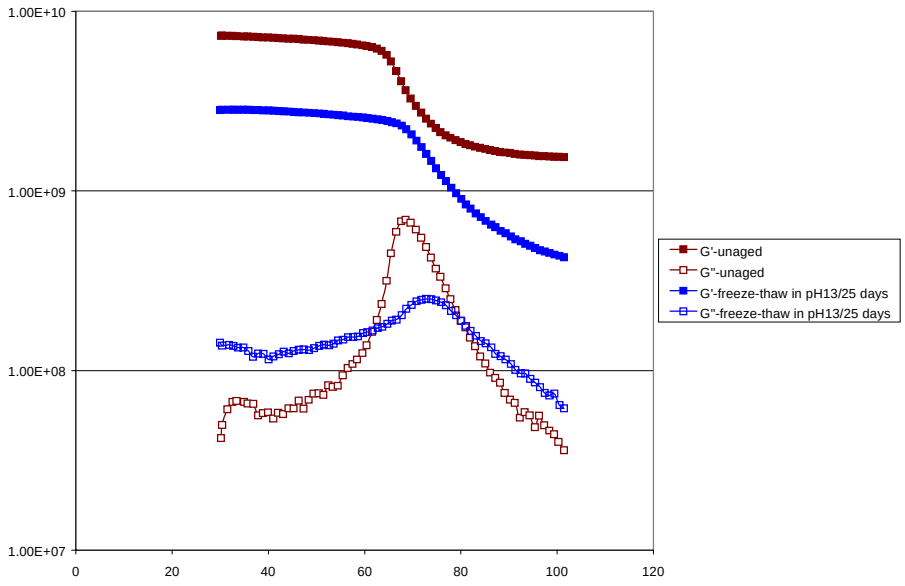

Figure C4: Dynamic properties of wood/HMR/epoxy/glass hybrid under unaged and alkaline conditions

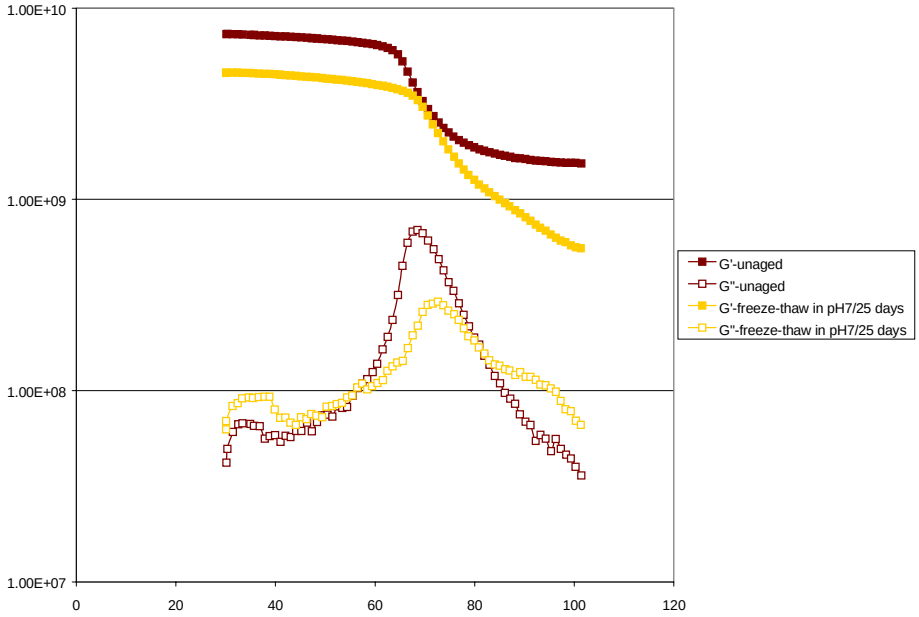

Figure C5: Dynamic properties of wood/HMR/epoxy/glass hybrid under unaged and neutral conditions

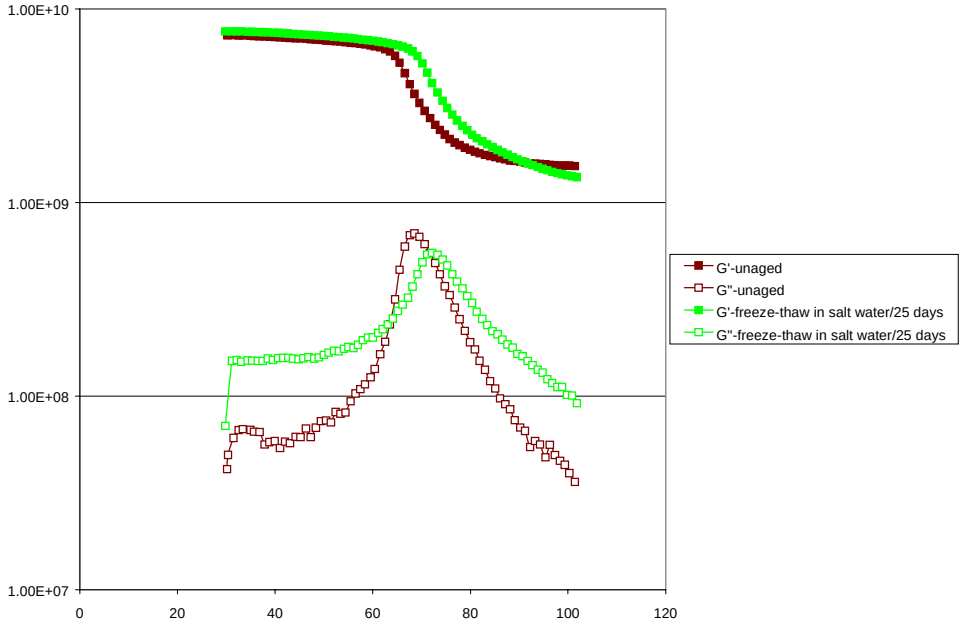

Figure C6: Dynamic properties of wood/HMR/epoxy/glass hybrid under unaged and salt water conditions